Contract No:

This document was prepared in conjunction with work accomplished under Contract No. DE-AC09-08SR22470 with the U.S. Department of Energy (DOE) Office of Environmental Management (EM).

We put science to work.™

Savannah River
National Laboratory™

OPERATED BY SAVANNAH RIVER NUCLEAR SOLUTIONS

A U.S. DEPARTMENT OF ENERGY NATIONAL LABORATORY • SAVANNAH RIVER SITE • AIKEN, SC

Liquid Secondary Waste: Waste Form Formulation and Qualification

A. D. Cozzi
K. L. Dixon
K. A. Hill
W. D. King
R. L. Nichols

March 2016
SRNL-STI-2015-00685, Revision 0

SRNL.DOE.GOV

DISCLAIMER

Printed in the United States of America

Prepared for
U.S. Department of Energy

SRNL-STI-2015-00685
Revision 0

Keywords: *Hanford*
Liquid Secondary Waste
Waste Form

Retention: *Permanent*

Liquid Secondary Waste: Waste Form Formulation and Qualification

A. D. Cozzi
K. L. Dixon
K. A. Hill
W. D. King
R. L. Nichols

March 2016

Prepared for the U.S. Department of Energy under contract number DE-AC09-08SR22470.

Savannah River National Laboratory™
OPERATED BY SAVANNAH RIVER NUCLEAR SOLUTIONS

REVIEWS AND APPROVALS

AUTHORS:

____

A. D. Cozzi, Hanford Mission Programs Date

____

K. L. Dixon, Geosciences Date

____

K. A. Hill, Engineering Process Development Date

____

W. D. King, Advanced Characterization and Processing Date

____

R. L. Nichols, Geosciences Date

TECHNICAL REVIEW:

____

D. L. McClane, Engineering Process Development, Reviewed per E7 2.60 Date

APPROVAL:

____

C. C. Herman, Manager Date
Hanford Mission Programs

____

D. J. Swanberg, Manager Date
Washington River Protection Solutions

EXECUTIVE SUMMARY

The Hanford Site Effluent Treatment Facility (ETF) currently treats aqueous waste streams generated during Site cleanup activities. When the Hanford Tank Waste Treatment and Immobilization Plant (WTP) begins operations, a liquid secondary waste (LSW) stream from the WTP will need to be treated. The volume of effluent for treatment at the ETF will increase significantly.

Washington River Protection Solutions is implementing a Secondary Liquid Waste Immobilization Technology Development Plan to address the technology needs for a waste form and solidification process to treat the increased volume of waste planned for disposal at the Integrated Disposal Facility IDF). Waste form testing to support this plan is composed of work in the near term to demonstrate the waste form will provide data as input to a performance assessment (PA) for Hanford's IDF.

Three Hanford Liquid Secondary Waste simulants were developed based on existing and projected waste streams. Using these waste simulants, fourteen mixes of Hanford Liquid Secondary Waste were prepared and tested varying the waste simulant, the water to dry materials blend, and the dry materials blend composition. The samples were prepared in the same manner as the samples prepared for the Supplemental Low Activity Waste programs. [1] Additions of a water reducing admix was required to facilitate the incorporation of the dry blend materials into the waste simulant. In this testing, the introduction of the dry blends into the waste simulant resulted in the release of noticeable ammonia odor during sample casting. Air sampling indicated exposure to personnel was below regulatory limits. However, due to the odor and irritant properties of ammonia, it was recommended that sample casting be conducted in a laboratory hood.

The compressive strength of all of the mixes exceeded the target of 3.4 MPa (500 psi) to meet the requirements identified as potential IDF Waste Acceptance Criteria in Table 1 of the Secondary Liquid Waste Immobilization Technology Development Plan. [2] The hydraulic properties of the waste forms tested (hydraulic conductivity and water characteristic curves) were comparable to the properties measured on the SRS Saltstone waste form. X-ray diffraction analysis of samples cured for 4 months showed unreacted cement phases.

Future testing should include efforts to first; 1) determine the rate and amount of ammonia released during each unit operation of the treatment process to determine if additional ammonia management is required, then; 2) reduce the ammonia content of the ETF concentrated brine prior to solidification, making the waste more amenable to grouting, or 2) manage the release of ammonia during production and ongoing release during storage of the waste form, or 3) develop a lower pH process/waste form thereby precluding ammonia release. Testing should also evaluate alternative water reducing additives to reduce the yield stress of the fresh mixes. Formulations including additional water should be tested to achieve waste forms that have sufficient water for hydration and additional samples of future mixes should be archived for testing at cure times greater than 28 days. Additional compressive strength testing dhould be performed prior to the 28 day convention to provide data to aid waste form handing decisions.

TABLE OF CONTENTS

LIST OF TABLES

LIST OF FIGURES

LIST OF ABBREVIATIONS

DFLAW	Direct Feed Low Activity Waste
EMF	Effluent Management Facility
ERDF	Environmental Restoration Disposal Facility
ETF	Effluent Treatment Facility
IC	Ion chromatography
ICP-AES	Inductively coupled plasma-atomic emission spectroscopy
IDF	Integrated Disposal Facility
LSW	Liquid Secondary Waste
PA	Performance Assessment
PNNL	Pacific Northwest National Laboratory
QAP	Quality Assurance Program
SRNL	Savannah River National Laboratory
SRS	Savannah River Site
UPV	Ultrasonic pulse velocity
W/DM	Water to dry materials ratio
WAC	Waste Acceptance Criteria
WRPS	Washington River Protection Solutions
WTP	Hanford Tank Waste Treatment and Immobilization Plant

1.0 Introduction

The Hanford Site Effluent Treatment Facility (ETF) currently treats aqueous waste streams including evaporator condensates from the 242-A Evaporator, Environmental Restoration Disposal Facility (ERDF), and relatively small volumes of laboratory wastes. The concentrated brine from the secondary treatment train within the ETF is currently fed to a thin film dryer, producing a powdered salt waste form for disposal in drums. The ETF is also expected to treat liquid secondary waste (LSW) from Hanford Waste Treatment and Immobilization Plant (WTP) operations, including Direct Feed Low Activity Waste (DFLAW). A stabilized solidified waste form is needed to provide a more leach resistant waste form for disposal in Hanford's Integrated Disposal Facility (IDF).

A Secondary Liquid Waste Immobilization Technology Development Plan was generated to address the technology needs in support of the design and operation of an ETF solidification unit including waste form performance, process development, process design, and process operations.[2] Since then a decision was made to have the waste treated off-site prior to disposal in the IDF. The current focus is on waste form/process development and waste treatment vendor qualification. High priority activities include waste feed envelope definition and simulant development, formulation development, and waste form qualification. A plan was developed to guide the technology development needed to support the IDF Performance Assessment (PA).[3] The waste form qualification activities needed to implement this plan are composed of work to 1) demonstrate that the waste form will meet waste acceptance criteria for the IDF, 2) demonstrate the equivalency of the performance through scale-up of the solidification process and with waste forms prepared with actual radioactive wastes or simulants prepared with radioactive components, and 3) provide long-term waste form performance data and information on degradation and release mechanisms to support the IDF PA.

The ETF liquid secondary waste immobilization waste form will be needed to support DFLAW operations if the program chooses treat the condensate from the Effluent Management Facility (EMF) and the WTP caustic scrubber rather than return these streams to the tank farm. This waste form will need to be included in, and analyzed as part of, the IDF PA being initiated in FY16 or in future PA maintenance activities..

Work on this scope began in FY14 with the Pacific Northwest National Laboratory (PNNL) initiating development of updated simulants based on flowsheet analyses performed by Washington River Protection Solutions (WRPS). Work in FY15 was performed by a consortium of laboratories including Savannah River National Laboratory (SRNL) and PNNL. SRNL was requested to further the development of a waste form for liquid secondary waste.[4] The work was described in a Task Technical and Quality Assurance Plan.[5]

2.0 Experimental Approach

A matrix of formulations was developed to evaluate the effects of mix components on the properties of the LSW waste form. The test parameters and their ranges that were investigated in the screening tests included;

- simulants representing the three primary influents to the ETF—242-A, ERDF, and WTP,
- water-to-dry-materials blend ratio (W/DM)—0.5 and 0.6,
- dry materials blend components—hydrated lime, ordinary portland cement, blast furnace slag, and Class F fly ash,
- dry materials blend ratios—variable, and
- mineral admix—Xypex C-500, added as a 5% substitution into the dry blend.

The fresh properties measured in this testing were gel time, set time , free liquid, grout flow, heat of hydration, density, and rheology. The properties of the cured waste forms measured were compressive strength, porosity, hydraulic conductivity, and the water characteristic curve. The mineralogy of each mix was also investigated.

The three simulants that were evaluated in this study are discussed in Section 3.0. The compositions of the 242-A and WTP brines were based on an internal WRPS memo, Appendix A. The ERDF brine was based on existing characterization data.[6] The 0.5 and 0.6 values of the free-water-to-dry-solids mix ratio were selected based on previous work[7] and scoping tests performed at PNNL.

The dry blend mix ratio and materials were varied to evaluate the effects of both the ratio and cementitious materials blend on the fresh and cured properties listed above. The calcium and aluminum contents (from hydrated lime and blast furnace slag) were adjusted from those used in Reference 7 to exploit the formation of early ettringite to incorporate the sulfate in the waste simulants. The Xypex C-500 mineral admix has been previously shown to improve leach resistance.[8]

3.0 Simulant Development and Validation

Three waste streams were evaluated in this work scope. Currently, the ETF treats condensates from the 242-A evaporator, and leachates from ERDF. Table 3-1 shows the targeted composition of the 242-A brine solution. The 242-A simulant was prepared to target a 10 wt % total solids concentration. Table 3-2 shows the targeted composition of the ERDF leachate simulant. This simulant targeted 12 wt % total solids, slightly greater than the solids expected in Reference 6. When the WTP begins operations, an additional secondary liquid stream, the combined Effluent Management Facility (EMF) off-gas condensate and the caustic scrubber may also be transferred to the ETF for treatment. Table 3-3 shows the targeted composition of the WTP simulant—the EMF off-gas condensate/caustic scrubber solution that would be processed through the ETF. The WTP simulant targeted an 18 wt % total solids concentration. Further descriptions of the origins of these simulants are in Appendix A. This task addresses the scope of work discussed in Section 3.1 of the proposal[9] to Reference 4.

Simulants for testing were prepared to the final wt % solids content discussed above. Each simulant was analyzed for composition using inductively coupled plasma-atomic emission spectroscopy[10] (ICP-AES) and ion chromatography[11] (IC). The density, and solids content[12,13] (total and dissolved in supernate) were also measured for each simulant.

Table 3-1 Target Concentrations and Simulant Make Up for 242-A Brine Simulant

Species	Mole Fraction		Component	g/L
SO_4^{2-}	0.324		Na_2SO_4	7.3
NH^{4+}	0.541		$CaSO_4$	7.3
Na^+	0.075		$(NH_4)_2SO_4$	84
Ca^{2+}	0.023		$MgSO_4 \cdot 7H_2O$	5.2
Cl^-	0.013		NaCl	1.4
SiO_4^{2-}	0.011		KCl	0.5
Mg^{2+}	0.009		$Na_2SiO_3 \cdot 5H_2O$	5.5
K^+	0.003		H_2O	~943
Total	0.999		--	--

Table 3-2 Target Concentration and Simulant Make Up for ERDF Simulant

Species	Mole Fraction		Component	g/L
SO_4^{2-}	0.235		Na_2SO_4	33.0
Na^+	0.222		$CaSO_4$	9.1
Cl^-	0.162		$Ca(NO_3)_2 \cdot 4H_2O$	29.6
NO_3^-	0.117		$CaCl_2$	18.8
Ca^{2+}	0.171		$MgSO_4 \cdot 7H_2O$	47.8
Mg^{2+}	0.092		H_2O	~941
Total	0.999		--	--

Table 3-3 Target Concentration and Simulant Make Up for WTP Simulant from the EMF

Species	Mole Fraction		Component	g/L
SO_4^{2-}	0.250		Na_2SO_4	55
NH^{4+}	0.330		$(NH_4)_2SO_4$	100
Na^+	0.295		NaCl	1.6
Cl^-	0.006		NaF	0.2
NO_3^-	0.117		$NaNO_3$	45
NO_2^-	0.001		$NaNO_2$	0.3
F^-	0.001		H_2O	~923
Total	1.000		--	--

Liquid Secondary Waste Stream simulants were prepared following the recipes reported in the tables above. Recipes used for the preparation of these simulants are provided in Appendix B. The measured density, weight percent solids, and pH data are provided in Table 3-4 for each simulant. These results were in good agreement with the simulants prepared at PNNL.[14]

Table 3-4. Measured Densities, Weight Percent Solids and pH Data for the LSW Simulants.

Waste Simulant	Density (mg/L)	Wt % Total Solids	Wt % Insoluble Solids	pH
242-A	1.059	9.9	0.4	8.6
WTP	1.126	18.0	0.1	6.3
ERDF	1.087	11.2	4.7	6.8

During the preparation of the 242-A simulant, insoluble solids were observed upon the addition of magnesium sulfate reagent. The final reagent added, calcium sulfate, was visually observed to be largely insoluble. A separate small-scale simulant preparation was conducted in which the sodium meta-silicate reagent was omitted. In that test, no precipitation was visually observed upon addition of the magnesium reagent. ICP-AES analysis of filtered liquid from the full simulant preparation revealed that only 70% of the added magnesium and 8% of the silicon were soluble, Table 3-5. These observations are indicative of a chemical interaction between magnesium and silicon which promotes partial precipitation of these elements from solution. ICP-AES also confirmed visual observations that only a portion (28%) of the calcium sulfate solids dissolved. Precipitation or insolubility of these species has a small impact on the weight percent (total and insoluble) solids (9.9% measured total solids content versus the target of 10%), since these are minor simulant components. Soluble concentrations of sodium, ammonium, potassium, chloride, and sulfate were all within 15% of the values expected based on reagent additions. Calcium sulfate insolubility has a negligible impact on the total soluble sulfate concentration. Based on visual observations, dilution of the 242-A waste simulant in water at a ratio of 1:10 (simulant to final solution) resulted in the dissolution of almost all of the insoluble solids. This behavior indicates the solids were formed from saturated solution rather than from a precipitation reaction.

Significant insoluble solids (4.7 wt%) were visually observed in the ERDF simulant which are believed to be primarily calcium sulfate solids based on the analytical data. Only 4% of the added calcium and 25% of the added sulfate were observed in the liquid phase. Concentrations of sodium, magnesium, and chloride in the filtered liquid were within 15% of the values expected based on reagent additions. The measured nitrate concentration was 32% higher than the expected concentration. The measured total weight percent solids value was slightly below the target value of 12% and the insoluble solids approached 5 wt %, which was consistent with visual observations of significant solids.

Essentially all the reagents added to the WTP simulant were soluble, based on visual observations and analytical data indicating 0.1 wt% insoluble solids. Soluble sodium, ammonium, sulfate, nitrate, and chloride concentrations were within 15% of the values expected based on reagent additions, Table 3-5. The minor components fluoride and nitrite were within 30% of the expected values. The wt % total solids concentration was near the target value (18%).

Table 3-5. Percentage of Soluble Components Versus Reagent Amounts in Simulants.

	% Soluble		
Component	242-A	WTP	ERDF
NH_4^+	93	90	---
Na^+	98	87	106
K^+	99	---	---
Mg^{2+}	70	---	113
Ca^{2+}	28	---	4
Si	8	---	---
SO_4^{2-}	87	100	25
NO_3^-	---	88	132
NO_2^-	---	123	---
Cl^-	89	101	86
F^-	---	127	---

4.0 Liquid Secondary Waste Formulation Development

Waste form samples were made using the formulations shown in Table 4-1. The brine waste simulant compositions that were used to prepare the simulated waste forms are shown in Table 3-1, Table 3-2, and Table 3-3, which are represented in terms of mole fraction. The dry blend materials were; hydrated lime (HL),[*] ordinary portland cement (OPC)[15], blast furnace slag (BFS),[16] and Class F fly ash (FA).[17] The mineral admix, Xypex C-500,[†] was tested as reported in Reference 8, and is included in select formulations. A Type A/Type F[18] full range water reducer[‡] targeted an addition rate of 0.6 ml/100 g dry materials.

---

[*] Graymont- Rivergate Terminal, Portland, OR
[†] Xypex Chemical Corporation, Xypex Admix C-500
[‡] BASF MasterGlenium 3030

Table 4-1 Matrix of Formulations for this Study

Test ID	Simulant	W/DM	HL/OPC/BFS/FA Blend	Mineral Admix
1	242-A	0.5	20/35/45/0	None
2[a]	ERDF	0.5	20/35/45/0	None
3	WTP	0.5	20/35/45/0	None
4	242-A	0.6	20/35/45/0	None
5	ERDF	0.6	20/35/45/0	None
6[b]	WTP	0.6	20/35/45/0	None
7[a]	ERDF	0.5	20/35/45/0	None
8[b]	WTP	0.6	20/35/45/0	None
9	242-A	0.5	20/10/70/0	None
10	WTP	0.5	20/10/70/0	None
11	WTP	0.6	0/20/45/35	Xypex
12	242-A	0.6	0/20/45/35	Xypex
13	WTP	0.6	0/8/45/47	None
14	242-A + ERDF	0.5	0/20/45/35	None

[a] Replicate mixes
[b] Replicate mixes

Grout mixes were prepared using the setup shown in Figure 4-1. The initial agitator speed was 200 rpm and the initial temperature of the waste simulant was recorded. As the dry blend was added, the agitator speed was increased to incorporate the dry blends. The water reducing admixture (WRA) was added as need to maintain a vortex. Scoping work performed at PNNL identified the need for a rheological modifier to fully incorporate the dry materials into the waste simulants. In some formulations, less water reducer than originally planned was used in mixes where sufficient mixing was achieved with less than the maximum admixture. After the dry blend was incorporated, the temperature of the slurry was recorded. Mixing continued for a total of 10 minutes. At the conclusion of mixing, the temperature of the slurry was recorded and the fresh properties of the grout mixture were measured. During pouring and handling of the grout mixture, monitoring by Industrial Hygiene noted that although the ammonia concentration was below regulatory limits, sufficient ammonia was present as a respiratory irritant, and that all mixing and handling of grout slurries should be performed in a chemical hood. The MasterGlenium 3030 WRA dosage used, and the temperatures measured during mixing for each of the mixes are shown in Table 4-2. The demand for WRA was reduced with increasing W/DM. This effect is expected as additional water associated with the waste would assist in incorporating the dry blend into the mix. Mixes made without hydrated lime also required less WRA to maintain a vortex during mixing. The percentage WRA in Table 4-2 refers to the reduced amount of WRA used relative to the target dosage of 0.6 ml/100 grams dry blend. The temperature rise during mixing is influenced by the water to dry blend ratio and the addition of the mineral admix Xypex C-500 and the WRA MasterGlenium 3030. The additional liquid associated with higher W/DM (e.g. the mass fraction water in Mix 1 was 0.3217 while the mass fraction water in Mix 2 was 0.3604) provides a greater heat sink for the energy created, reducing the final temperature. The porosity modifying mineral admix, Xypex C-500, contains pulverized cement and silica fume, both highly reactive components, potentially increasing the final temperature.

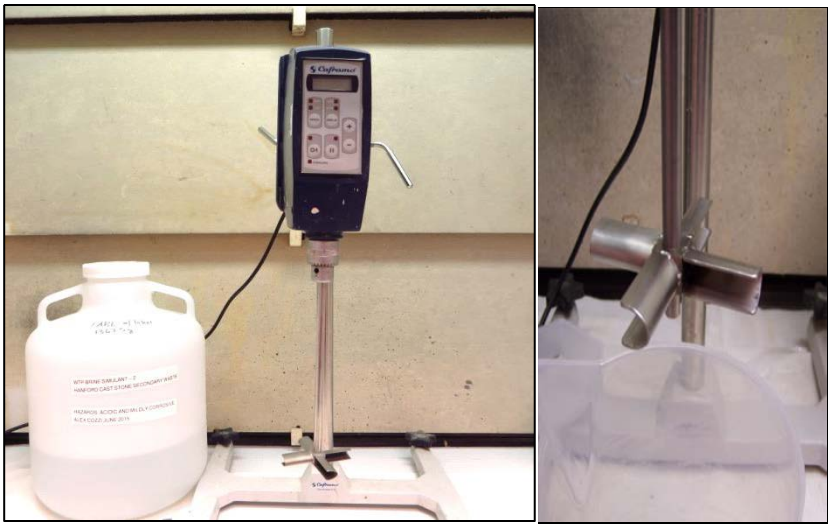

Figure 4-1. Mixer/impeller used to prepare LSW mixes.

Table 4-2. Water Reducing Additive Dosage and Temperatures Measured During Mixing.

Test ID	Simulant	W/DM	HL/OPC/BFS/FA Blend	Mineral Admix	% WRA	Mix Temperature (°C)			
						T_{init}	T_{mid}	T_{fin}	ΔT
1	242-A	0.5	20/35/45/0	None	100	22.5	28.8	29.8	7.3
2[a]	ERDF	0.5	20/35/45/0	None	100	23.3	25.9	27.3	4.0
3	WTP	0.5	20/35/45/0	None	100	23.5	28.3	30.5	7.0
4	242-A	0.6	20/35/45/0	None	100	23.3	28.9	28.3	5.0
5	ERDF	0.6	20/35/45/0	None	62.2	23.1	25.7	26.1	3.0
6[b]	WTP	0.6	20/35/45/0	None	70.5	24.0	29.0	29.2	5.2
7[a]	ERDF	0.5	20/35/45/0	None	100	24.1	27.5	28.2	4.1
8[b]	WTP	0.6	20/35/45/0	None	80.3	24.1	27.9	28.9	4.8
9	242-A	0.5	20/10/70/0	None	100	22.8	27.3	28.5	5.7
10	WTP	0.5	20/10/70/0	None	100	23.8	28.2	29.2	5.4
11	WTP	0.6	0/20/45/35	Xypex	77.3	23.2	31.0	30.2	7.0
12	242-A	0.6	0/20/45/35	Xypex	29.4	21.5	29.2	28.4	6.9
13	WTP	0.6	0/8/45/47	None	19.0	23.2	28.9	29.0	6.8
14	242-A + ERDF	0.5	0/20/45/35	None	100	23.0	27.5	28.7	5.7

5.0 Processing and Curing Properties

5.1 Fresh Properties

After preparation of the mixes, properties of the freshly prepared waste form slurries were measured. The properties measured and the methods used are listed in Table 5-1.

Table 5-1 Measurement Methods for Fresh Properties

Property	Method
Gel time	Static Cup[19]
Set time (initial, final)	Vicat[20] and Ultrasonic Pulse Velocity[21]
Free or Standing Water / Liquid	Direct Measure[19]
Grout Flow	SRNL Modified ASTM D 6103-97[19,22]
Heat of Hydration	Isothermal Calorimetry[23]
Density	SRNL Modified ASTM D 1475-13[24]
Rheology	Flow Curve[25, 26]

5.1.1 Gel Time

Gel time is a subjective method of determining duration of grout flowability. In a continuous process, the gel time is an indication of the time after an interruption in the grout making process that is available to restart the process before it becomes necessary to perform a clean-up/shut down sequence. Gel time is also an indication of how long the placed grout (in a waste container) can maintain flowability. Gel time was measured by filling five ~100 ml containers with fresh grout. A timer was started as the first cylinder was filled. The cylinders are sequentially opened and tipped over a second container, each after an increasing amount of time. The grout is deemed gelled when the grout will no longer pour from a cylinder under its own weight. An example gel test is illustrated in Figure 5-1. In this example, the slurry poured from the first three cylinders when tipped into the second container. The slurry would not pour from the fourth container after resting for a period of 40 minutes after filling. Gel time is therefore approximately 40 minutes for this slurry.

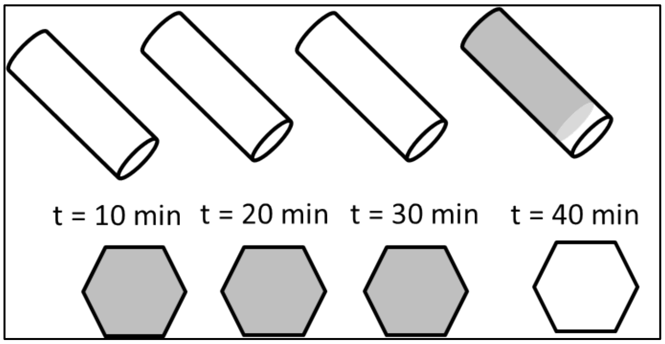

Figure 5-1. Illustration of gel time determination.

The results for the gel times for each of the mixes processed are shown in Table 5-2. Gel times measured for this set of mixes ranged from 90 seconds to greater than 40 minutes. The gel time was affected by both the waste simulant and the blend ratio of the dry materials. In addition to the gel time being a subjective measurement, there is also inherent uncertainty in the test. Mix 2 and mix 7 are replicate tests. The WRA dose was maintained for both mixes, however, mix 2 had a gel time of 17:30, whereas the gel time for mix 7 was 25:00, a difference of almost 50%. Mixes reported in Reference 19 had replicate variability of ~ 30%. The mixes reported in Reference 19 were prepared with a wholly different waste simulant and dry materials blend. In mixes 1, 2, and 3, the waste simulant was the only variable. In these tests, mix 2, the mix using the ERDF simulant, exhibited a significantly greater gel time than the mixes with the 242-A and WTP simulants, which were indistinguishable. The effect of W/DM is demonstrated in mixes for each of the waste simulants. In all of the instances, mixes 1 and 4, mixes 2 and 5, and mixes 3 and 6, the gel time was increased by additional water in the mix. In the case of mixes 2 and 5, the gel time for the higher W/DM was greater even though the WRA was reduced during preparation of mix 5. Effects on the gel time by the amount of WRA added and the dry blend composition were less pronounced. It appeared that replacing hydrated lime with fly ash in the mix increased gel time. This observation is consistent with both the formation of gypsum and ettringite during mixing when hydrated lime is included in the dry materials blend and the relatively slow hydration rate of Class F fly ash. It was also noted that <20% of the WRA target dosage was needed during mixing when the dry materials blend from the LAW testing was used, mix 13. The effect of Xypex on gel time was not isolated in these tests as it had been demonstrated to extend gel time in previous testing.[27]

Table 5-2. Gel Times for each of the Mixes Tested.

Test ID	Simulant	W/DM	HL/OPC/BFS/FA Blend	Mineral Admix	% WRA	Gel Time (min)
1	242-A	0.5	20/35/45/0	None	100	01:30
2[a]	ERDF	0.5	20/35/45/0	None	100	17:30
3	WTP	0.5	20/35/45/0	None	100	02:00
4	242-A	0.6	20/35/45/0	None	100	11:00
5	ERDF	0.6	20/35/45/0	None	62.2	22:50
6[b]	WTP	0.6	20/35/45/0	None	70.5	>15:00
7[a]	ERDF	0.5	20/35/45/0	None	100	25:00
8[b]	WTP	0.6	20/35/45/0	None	80.3	15:00
9	242-A	0.5	20/10/70/0	None	100	10:00
10	WTP	0.5	20/10/70/0	None	100	02:00
11	WTP	0.6	0/20/45/35	Xypex	77.3	>40:00
12	242-A	0.6	0/20/45/35	Xypex	29.4	20:00
13	WTP	0.6	0/8/45/47	None	19.0	16:00
14	242-A + ERDF	0.5	0/20/45/35	None	100	07:00

[a] Replicate mixes
[b] Replicate mixes

5.1.2 *Set Time*

Set time was measured using ASTM C 191-13.[20] For this testing, the final set described in the ASTM procedure was modified to allow for up to 2 mm of penetration. The modification from the ASTM is derived from the utilization of the data. The ASTM method is often used to determine when a pour can be walked on by the average worker. For waste form testing, the 2 mm set is an indication that sufficient structure was developed such that an additional lift could be placed without development of additional hydraulic head. The time unit for measurement is in hours, or fractions thereof. Simultaneously, the time of flight of an ultrasonic pulse (ultrasonic pulse velocity (UPV)) through a sample was measured to determine whether the sound velocity that correlates to set measured by the ASTM Vicat method is a fixed value, or is dependent on mix parameters. Set time corresponds to the development of structure from hydration and may be used as a process control point for the transport of waste packages.

The initial velocity of sound through the freshly prepared LSW mixes was significantly higher than the velocity of mixes prepared for Supplemental Waste grout testing.[28] This behavior may be attributed to the solids formed, and in turn, the heat produced, during mixing. Or, the increased velocity may be due to less entrained air. Entrained air in fresh mixes has been shown to attenuate the ultrasonic pulse.[29] Most of the mixes in this study set within 24 hours, Table 5-3. The longer set time reported for Mix 11 may be greater than the true set as there were no measurements made between 48 hours and the final set at almost 90 hours. The early setting nature of these mixes made it difficult to relate the UPV response to the Vicat results as the overnight set did not allow tracking of the development of the structure. The WRA admix used is formulated to promote faster setting times. In the UPV, there was little change in the velocity during set relative to responses obtained in reference 28. In some mixes, air gaps developed between the transducer and receiver, resulting in a sharp decrease in measured velocity. This was the case during the final set measurements in Mixes 2 and 9. The velocity in parentheses for these mixes is the maximum velocity recorded during the test. Figure 5-2 shows two UPV curves representative of the responses for all of the mixes in this study. The plots are annotated with the Vicat results. All of the plots are included in Appendix C.

Table 5-3. Set time Measured by Vicat and Corresponding Sound Velocity for each Mix.

Test ID	Simulant	W/DM	HL/OPC/BFS/FA Blend	Mineral Admix	Vicat (h)	UPV (m/s)
1	242-A	0.5	20/35/45/0	None	16:13	2187
2[a]	ERDF	0.5	20/35/45/0	None	20:23	1088*(2027)
3	WTP	0.5	20/35/45/0	None	21:25	2061
4	242-A	0.6	20/35/45/0	None	20:01	1555
5	ERDF	0.6	20/35/45/0	None	20:51	1531
6[b]	WTP	0.6	20/35/45/0	None	21:19	2140
7[a]	ERDF	0.5	20/35/45/0	None	16:25	2246
8[b]	WTP	0.6	20/35/45/0	None	18:00	2095
9	242-A	0.5	20/10/70/0	None	18:15	1477*(1745)
10	WTP	0.5	20/10/70/0	None	18:25	1855
11	WTP	0.6	0/20/45/35	Xypex	89:42	2581
12	242-A	0.6	0/20/45/35	Xypex	19:00	1769
13	WTP	0.6	0/8/45/47	None	21:04	1979
14	242-A + ERDF	0.5	0/20/45/35	None	16:00	2287

[a]Replicate mixes
[b]Replicate mixes
*Velocity when Vicat set was collected, actual velocity was higher.

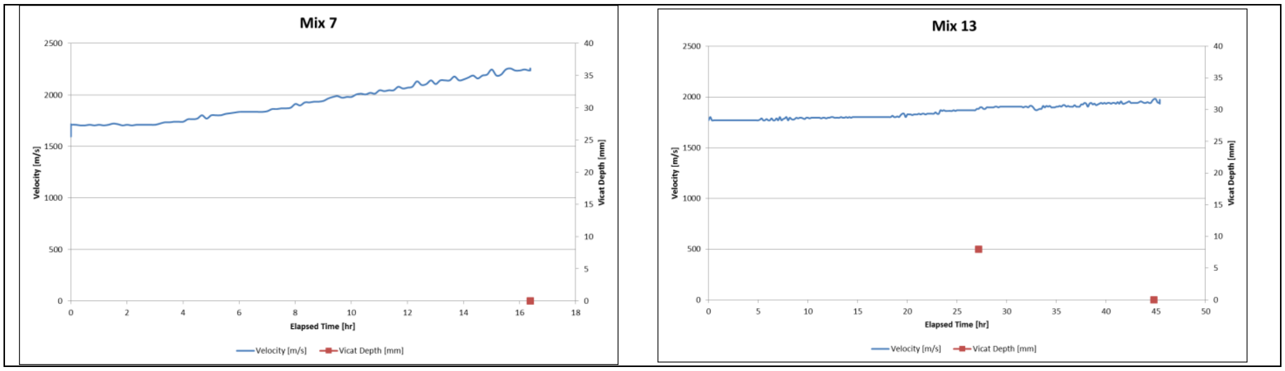

Figure 5-2. UPV response representative of the mixes in this study.

5.1.3 Free Liquids/Standing Water

Standing water was determined by measuring the residual liquid remaining after 24 hours and an additional time after that (typically 3 days ± 1 day). The volume of the residual liquid was measured as mass. The density of the liquid is assumed to be the same as the waste simulant salt solution used to prepare the mix. Although the formation of ettringite during mixing changes the composition of the pore solution, sampling of the pore solution for the porosity testing in Section 5.2.2 revealed a density of the extracted pore solution similar to the starting waste simulant. The standing water calculation is reported as the volume of fluid collected over the volume of hardened grout. Standing water present in the sample is a preliminary indication that settling may have occurred. This may or may not be an indication of preferential settling (segregation). Residual water may also be reabsorbed with time. If free liquids were present after the first measurement, a second measurement was made to determine if the excess liquid would be reabsorbed or persist. Three of the mixes exhibited free liquid after one day, and two mixes had free liquid persist to the second analysis. As can be seen in Table 5-4, free liquids were present in formulations made without hydrated lime and a W/DM of 0.6. Samples are stored in a zip top bag with a moist towel to maintain a humid environment to mitigate any potential losses from evaporation.

Table 5-4. Volume Percent Free Liquids Associated with Mixes.

Test ID	Simulant	W/DM	HL/OPC/BFS/FA Blend	Mineral Admix	%WRA	Free Liquid (Vol %)			
						Day 1		Day 2 or 4	
11	WTP	0.6	0/20/45/35	Xypex	77.3	5.5	5	2.3 (4)	2.1(4)
12	242-A	0.6	0/20/45/35	Xypex	29.4	1.9	2.1	0.6 (2)	0.7 (2)
13	WTP	0.6	0/8/45/47	None	19.0	0.4	0.6	0 (4)	0 (4)

5.1.4 Grout Flow

The grout flowability was measured by a modified ASTM D 6103-97 as described in Reference 19. A cylinder of smaller proportions than those specified by the ASTM method was used (77 mm height × 43 mm inside diameter [ID] rather than the 150 mm × 76 mm specified in the method). This was done based on historical data indicating that some of the mixes tested would flow a distance that could not be easily measured or contained when the larger cylinders were used. This method provides an indication of the ability of the grout slurry to flow after a period of stasis. The grout flow method differs from the gel test in that the extent of flow is measured rather than a flow/no flow condition. An open-ended cylinder was placed on a flat, level surface and filled with fresh grout. The cylinder was raised so the grout would flow into a circular patty to attain symmetry. The diameter of the resulting patty was measured in perpendicular and the results averaged to account for asymmetric samples.

The average diameters of replicate mixes were within 10%. The extent of flows in this sample set were dependent upon the waste simulant, the W/DM, and the water reducing additive, Table 5-5. The flow diameter of mixes made with the 242-A and WTP waste simulants were similar (within the replicate variability), however, duplicate Mixes 2 and 7 made with the ERDF waste simulant exhibited greater flow. With an increased W/DM, the average flow diameter was increased as well. The effect of the WRA can be seen between Mix 2 and Mix 5, where the W/DM is increased and less WRA was added, resulting in a similar average flow diameter.

A representative flow result is shown in Figure 5-3. The steel plate used is unfinished and has texture associated with it. Therefore, results are relative to flow tests within a study. The cylinder used for the test is shown in the upper right corner of the figure.

Table 5-5. Average Flow Diameters of Mixes.

Test ID	Simulant	W/DM	HL/OPC/BFS/FA Blend	Mineral Admix	% WRA	Flow Diameter (mm)
1	242-A	0.5	20/35/45/0	None	100	127.8
2[a]	ERDF	0.5	20/35/45/0	None	100	186.4
3	WTP	0.5	20/35/45/0	None	100	119.6
4	242-A	0.6	20/35/45/0	None	100	150.9
5	ERDF	0.6	20/35/45/0	None	62.2	185.8
6[b]	WTP	0.6	20/35/45/0	None	70.5	150.8
7[a]	ERDF	0.5	20/35/45/0	None	100	173.7
8[b]	WTP	0.6	20/35/45/0	None	80.3	164.6
9	242-A	0.5	20/10/70/0	None	100	149.5
10	WTP	0.5	20/10/70/0	None	100	121.6
11	WTP	0.6	0/20/45/35	Xypex	77.3	210.8
12	242-A	0.6	0/20/45/35	Xypex	29.4	174.5
13	WTP	0.6	0/8/45/47	None	19.0	147.7
14	242-A + ERDF	0.5	0/20/45/35	None	100	145.0

[a] Replicate mixes
[b] Replicate mixes

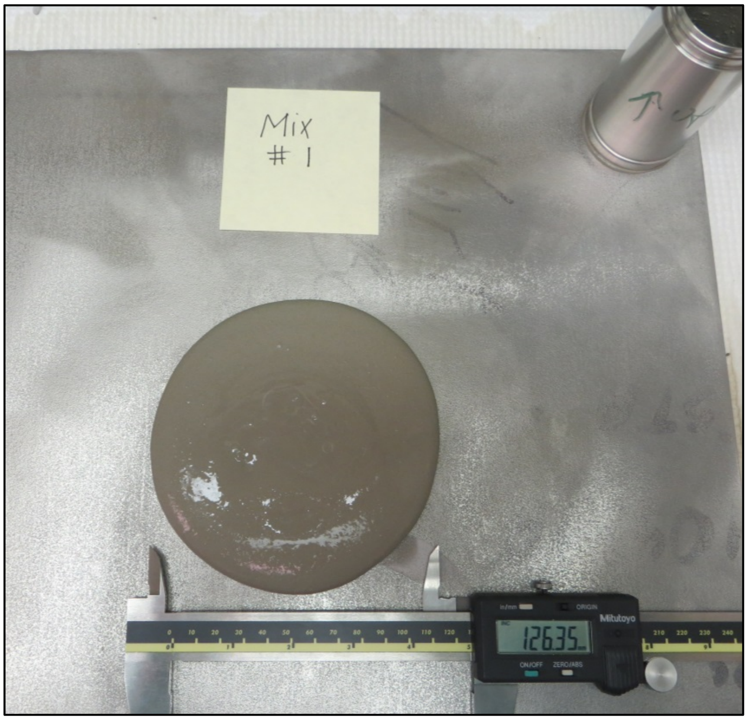

Figure 5-3. Patty formed during the flow test for Mix 1.

5.1.5 Heat of Hydration

The heat of hydration was measured by isothermal calorimetry at 25 °C in two, eight-channel isothermal calorimeters.[23] Samples were prepared using the formulation in Table 4-1. The simulant waste solution was placed in a vial and the requisite amount of the preblended dry materials was added. The total material mixed was 13.0 grams using the same ratio of materials to prepare the mixes in Table 4-1. The vial was inserted into a Resodyn acoustic mixer and mixed using a force of ~20-30 g for approximately one minute. The sample was then inserted into the isothermal calorimeter and the test initiated. A mass of quartz sand corresponding to the heat capacity of cement (similar to these mixes) was placed in a vial in the reference position of the calorimeter. Hydration continues almost indefinitely. In these tests, the data were collected for at least fourteen days. The total heat evolved and instantaneous power were normalized to the amount of dry blend materials in the sample.

The heat-of-hydration results include the total heat generated over 300 hours of testing, the maximum heat flow, and the elapsed time to reach the maximum heat flow, Table 5-6. Reaction kinetics between the dry blend components and waste simulants in this study have not yet been thoroughly evaluated. Referring to the temperature rise during mixing noted in Table 4-2, reactions associated with the addition of hydrated lime—rise in pH and formation of gypsum and ettringite—it can be speculated that a not insignificant amount of heat is generated during the mixing process. The early generation of heat in the plots is substantiated by the “Time to Peak” column in Table 5-6, where all but one of the mixes containing hydrated lime peaked within 20 minutes of initiating the test. This is in contrast to the mixes prepared without hydrated lime that reached peak heat flow after greater elapsed times, similar to the Supplemental LAW waste forms tested in Reference 28. Mix 14 was the exception to the mixes without hydrated lime in that the waste simulant, ERDF, contained calcium nitrate, introducing a soluble calcium source for early heat generation. The heat generated after 300 hours was not strongly influenced by any of the parameters in this study. Mix 13 had a much greater heat flow at peak than the other mixes. This may be an artifact of the amount of WRA added. Mix 13 only required 13% of the WRA to make a pourable mix. Although formulated by the manufacturer as a set accelerator, in these formulations, the WRA is also a set retarder, both delaying and dampening the heat generation peak. The total heat generated from cement and water is greater than 450 J/g. The generated heat captured in this task are similar but somewhat lower than the values in Reference 28. This shortfall can be attributed to the heat generated during mixing.

Table 5-6. Total Heat, Heat Flow, and Time to Maximum Heat Flow for Mixes at 25 °C.

Test ID	Simulant	W/DM	HL/OPC/BFS/FA Blend	% WRA	Heat @ 300 hr (J/g)	Heat Flow at Peak (mW/g)	Time to Peak (hh:mm)
1	242-A	0.5	20/35/45/0	100	325	31.9	00:02
2[a]	ERDF	0.5	20/35/45/0	100	341	18.0	00:02
3	WTP	0.5	20/35/45/0	100	336	19.7	00:02
4	242-A	0.6	20/35/45/0	100	321	1.75	06:58
5	ERDF	0.6	20/35/45/0	62.2	377	2.97	04:12
6[b]	WTP	0.6	20/35/45/0	70.5	380	1.91	06:49
7[a]	ERDF	0.5	20/35/45/0	100	311	2.61	03:50
8[b]	WTP	0.6	20/35/45/0	80.3	377	2.00	06:45
9	242-A	0.5	20/10/70/0	100	248	1.29	15:46
10	WTP	0.5	20/10/70/0	100	296	1.29	19:38
11	WTP	0.6	0/20/45/35	77.3	283	1.45	63:00
12	242-A	0.6	0/20/45/35	29.4	265	1.95	53:00
13	WTP	0.6	0/8/45/47	19.0	281	37.2	00:02
14	242-A + ERDF	0.5	0/20/45/35	100	310	2.06	05:17

[a] Replicate mixes
[b] Replicate mixes

5.1.6 Density

The density of freshly prepared grout waste form slurries was measured using a cup of known volume as described in Reference 24, with the exception that the cup volume is checked, but not calibrated per the procedure. Prior to testing, the volume of the sample cup was verified with ASTM Type I water at room temperature following the calibration steps in the ASTM D1475 method. After the initial calibration check, only the tare weight of the cup was recorded assuming that the volume of the stainless steel cup remained constant throughout the testing period. To measure the fresh density, the sample cup was filled with fresh slurry to form a meniscus. The container was capped and the excess material expressed from the overflow was wiped away. The sample cup was wiped to remove any material from the outer surfaces and then was placed on a balance to obtain the mass of the sample. The fresh density is calculated from the mass of the sample divided by the known volume of the sample cup.

The cured density of each monolith was measured geometrically. The diameter of each cylinder was measured near the top, middle, and bottom. The length or each cylinder was then measured three times, rotating the cylinder ~ 120° between measurements. The average value of the diameter measurements and the average value of the overall length measurements were used to determine the volume of the monolith. Each monolith was weighed to determine its mass. The mass of the monolith was divided by the determined volume to calculate the cured density.

The calculated density of each mix was determined using the density and ratio of the waste simulant and the dry materials blend for each formulation. The densities of the waste simulants were taken from Table 3-4. The density of each of the dry material blends was calculated from the densities of the individual components, Table 5-7. The grout density was calculated using the rule of mixtures, using the weighted mean of each component to predict the property.

Table 5-7. Density of the Individual Dry Materials.

Component	Density (g/cm^3)
Blast furnace slag	2.881
Class F fly ash	2.588
Ordinary portland cement	3.204
Hydrated lime	2.211
Xypex C-500	2.800

The density of each formulation determined by the three methods described above is shown in Table 5-8. The results indicate fairly good agreement among the methods for each mix. The results indicate that the fresh density can have variability introduced by the air entrained in the mix that reduces the density, and the test method that can be affected by the rheological properties of the fresh mix—higher yield strength and plastic viscosity increase the variability of the measurement. In these tests, where gypsum and ettringite are formed from the reaction between the waste simulant and the dry materials, the calculated density may not be as accurate as those calculated for the LAW grout waste forms. The addition of Xypex did not affect the measured density. It is apparent from the data that the density of the mixes is primarily dependent on the W/DM, exhibiting higher densities for lower W/DM.

Table 5-8. Density of the Mixes Measured Fresh, Cured, and Calculated.

Test ID	Simulant	W/DM	HL/OPC/BFS/FA Blend	Fresh (g/cm^3)	Cured (g/cm^3)	Calculated (g/cm^3)
1	242-A	0.5	20/35/45/0	1.76	1.78	1.78
2[a]	ERDF	0.5	20/35/45/0	1.80	1.82	1.77
3	WTP	0.5	20/35/45/0	1.87	1.76	1.79
4	242-A	0.6	20/35/45/0	1.75	1.70	1.70
5	ERDF	0.6	20/35/45/0	1.70	1.71	1.69
6[b]	WTP	0.6	20/35/45/0	1.77	1.73	1.72
7[a]	ERDF	0.5	20/35/45/0	1.78	1.78	1.77
8[b]	WTP	0.6	20/35/45/0	1.76	1.73	1.72
9	242-A	0.5	20/10/70/0	1.81	1.74	1.77
10	WTP	0.5	20/10/70/0	1.80	1.75	1.78
11	WTP	0.6	0/20/45/35	1.75	1.74	1.72
12	242-A	0.6	0/20/45/35	1.73	1.74	1.70
13	WTP	0.6	0/8/45/47	1.72	1.72	1.71
14	242-A + ERDF	0.5	0/20/45/35	1.78	1.77	1.78

[a] Replicate mixes
[b] Replicate mixes

5.1.7 Rheology

The flow curve used to measure the yield stress and plastic viscosity of the grout slurry mixture is a linear ramp for five minutes to 300 s^{-1}; a 30 second hold; and a linear ramp for five minutes to 0 s^{-1}. It is assumed that during the flow curve measurements in this task, time dependent issues that could be associated with the grout slurries (e.g. chemical reactions) do not affect the measurement. The most common rheological model used to describe the flow of concrete, mortars, and cement is the Bingham Plastic model.[30,31] Previous studies have also interpreted Saltstone slurries rheological data as Bingham Plastic fluids.[32,33] The rheological properties of the fresh grout waste form slurry were measured using a bob and cup method described in Reference 26. Figure 5-4 is a flow curve for the N35 standard oil (viscosity ~55 cP @ 25 °C) generated using the rheology method developed for grout mixtures.

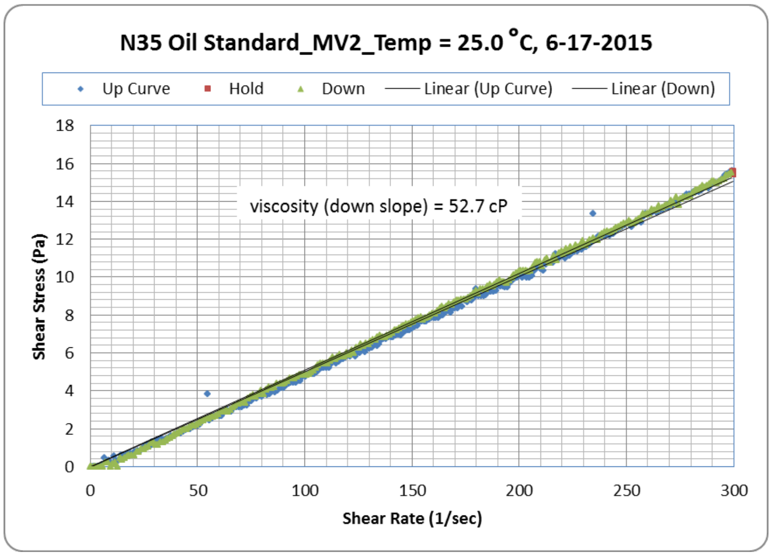

Figure 5-4. A flow curve for the N35 standard oil used to verify rheometer response.

All the flow curves were obtained with a rotoviscometer (Haake RS6000, ThermoFisher, Waltham, MA), using the MV2 cylindrical rotor and cup configuration. The MV2 bob was selected given its range of measurement and design (e.g., the only shearing surface is the cylinder itself). The rheological measurements were obtained at the temperature of the slurry (i.e., the temperature as measured at the end of the mixing activities). Thixotropic response was expected, given that some of the slurries start developing structure when shearing (mixing) stops. Table 5-9 shows the yield stress and plastic viscosity determined by applying the Bingham Plastic model. In this study, all the down flow curves were analyzed as Bingham Plastic fluids. The rheograms for all of the mixes evaluated in this study are located in Appendix D.

Table 5-9. Yield Stress and Plastic Viscosity Determined by Fitting Rheograms to a Bingham Plastic Model.

Test ID	Simulant	W/DM	HL/OPC/BFS/FA Blend	% WRA	Plastic Viscosity (cP)	Yield Stress (Pa)
1	242-A	0.5	20/35/45/0	100	45.1	416
2[a]	ERDF	0.5	20/35/45/0	100	4.9	398
3	WTP	0.5	20/35/45/0	100	72.5	361
4	242-A	0.6	20/35/45/0	100	18.5	194
5	ERDF	0.6	20/35/45/0	62.2	12.4	230
6[b]	WTP	0.6	20/35/45/0	70.5	30.5	215
7[a]	ERDF	0.5	20/35/45/0	100	10.8	456
8[b]	WTP	0.6	20/35/45/0	80.3	31.7	193
9	242-A	0.5	20/10/70/0	100	23.8	345
10	WTP	0.5	20/10/70/0	100	54.4	288
11	WTP	0.6	0/20/45/35	77.3	8.8	143
12	242-A	0.6	0/20/45/35	29.4	11.9	127
13	WTP	0.6	0/8/45/47	19.0	26.6	211
14	242-A + ERDF	0.5	0/20/45/35	100	37.9	315

[a] Replicate mixes
[b] Replicate mixes

The plastic viscosities for the mixes ranged from 4.2 – 72.5 cP. The variability among these values was decreased by the use of the WRA in the preparation of the mixes. The WRA additions were made with the goal of attaining mixability, therefore it would be expected that the measured viscosities would not vary as widely as might be expected. The yield stress for the mixes in this study ranged from 127 – 456 Pa. All of the yield stresses measured for these mixes were greater than the yield stresses in previous work, Reference 28. The higher yield stresses can be attributed to the formation of solids during mixing, increasing the overall solids content of the mixes. The WRA used in this study, MasterGlenium 3030 is formulated to preserve slump characteristics of a cement mix. It is likely then, that the WRA did not affect the yield strength as it did the plastic viscosity.

5.2 Cured Properties

Samples of the grout slurries that were cast into molds and cured as described in Section 4.0 were analyzed for properties identified in Table 5-10.

Table 5-10 Cured Properties Analytical Methods

Property	Method
Compressive Strength	Uniaxial compression ASTM C 39/39M-15a[34,35]
Porosity	Mass loss[36]
Hydraulic Conductivity	Permeameter ASTM D 5084-10[37]
Water Characteristic Curve	Soil Water Characteristic Curve ASTM D 6836-02[38]
Mineralogy	XRD L16.1 ADS 1120[39]

5.2.1 Compressive Strength

Compressive strength is commonly used as an indication of the overall quality (mix design and preparation) of the sample. After curing for 28 days, 2 in diameter x 4 in height cylindrical samples were demolded and tested for compressive strength in triplicate using unbonded caps.[34,33] The demolded samples were inspected for parallel surfaces. If an end of a sample showed a clear deviation from flatness, the excess material was removed. If the imperfection was a small nodule, coarse grit sandpaper was used to true the surface. For larger imperfections, the sample surface was trimmed using a miter saw. The resulting cylinder was measured as described in Section 5.1.6, capped, and tested. Compressive strength testing was conducted using a hydraulic compression tester.[*] The compressive load was applied until the load indicated by the equipment was reduced to 75% of the maximum load applied to the specimen. The loading rate was set at approximately 0.25 MPa/s (29.4 kN/min) as specified by Reference 34. It should be noted that a noticeable ammonia odor was emitted from samples after compression testing.

The compressive strength target is a minimum of 3.4 MPa (500 psi) to meet the requirements identified in Reference 2. All of the mixes tested exceeded 17.2 MPa (2500 psi), Table 5-11. As was determined in the compression testing in Reference 28, the W/DM affected the compressive strength with the mixes prepared with a W/DM of 0.5 having a consistently higher compressive strength than samples prepared with a W/DM of 0.6. Mixes made without hydrated lime and including fly ash (Mix 11 and Mix 12) had lower compressive strength than the corresponding mixes that included hydrated lime (Mix 3 and Mix 4). As discussed above, the addition of hydrated lime promotes the formation of gypsum and ettringite, which both can contribute to early strength (28 days). Class F fly ash is slower to react and can take several more weeks to fully develop strength. The different waste simulants tested did not significantly affect the compressive strength.

---

[*] Humboldt Manufacturing, Schiller Park, IL, model #HCM-0300 with Test Mark Industries, LXI data acquisition system

Table 5-11. Compressive Strength of Triplicate Cylinders of each Mix.

Test ID	Simulant	W/DM	HL/OPC/BFS/FA Blend	Mineral Admix	Compressive Strength (psi)			
					-1	-2	-3	Avg
1	242-A	0.5	20/35/45/0	None	6383	6389	6361	6378
2[a]	ERDF	0.5	20/35/45/0	None	7387	7659	7163	7403
3	WTP	0.5	20/35/45/0	None	6587	6362	6556	6502
4	242-A	0.6	20/35/45/0	None	4893	4884	NM	4889
5	ERDF	0.6	20/35/45/0	None	5885	5775	5394	5685
6[b]	WTP	0.6	20/35/45/0	None	5636	5546	5629	5604
7[a]	ERDF	0.5	20/35/45/0	None	6855	7564	7175	7198
8[b]	WTP	0.6	20/35/45/0	None	5287	2364	5269	4307
9	242-A	0.5	20/10/70/0	None	4641	4880	4781	4767
10	WTP	0.5	20/10/70/0	None	5506	5406	5491	5468
11	WTP	0.6	0/20/45/35	Xypex	2253	2732	2680	2555
12	242-A	0.6	0/20/45/35	Xypex	3515	3480	3546	3514
13	WTP	0.6	0/8/45/47	None	5824	5099	5359	5427
14	242-A + ERDF	0.5	0/20/45/35	None	6479	7538	6498	6838

[a] Replicate mixes
[b] Replicate mixes

5.2.2 Porosity

The porosity was measured on remnants of samples tested for compressive strength. Portions of the compressive strength samples were collected from internal pieces of the primary sample to limit the extent of drying (maintain original saturation). The porosity was measured by the method described in Reference 36. The samples were heated at ~105 °C overnight. The mass was measured daily until the mass change on consecutive days was <5%. The total porosity is defined here as the percentage of total volume occupied by the pore solution for a saturated sample. In previous work, it was assumed that the density of the pore solution is equivalent to the density of the salt solution from which the sample was prepared. In this study, the reactions that occur when hydrated lime is added to the waste simulant preclude this assumption. To determine the density of the pore solution, a portion of Mix 6 was cured for five days. The sample was then centrifuged until sufficient pore solution was expressed that a compositional analysis and a density measurement could be performed, Table 5-12. The porosity was then calculated by dividing the volume of the pore solution by the overall volume of the sample. The volume of the pore solution is determined by assuming the mass loss is due entirely to water and dividing by the density of the pore solution and the volume fraction of water in the pore solution. The difference in calculated porosities between using the densities of the starting waste simulant rather than the density of the pore solution extracted from Mix 6 was <4%. Mix 6 was the only mix tested where pore solution was extractable.

The porosity across all of the mixes ranged from 48.72% (Mix 2) to 58.00% (Mix 13). In general, the porosity trended lower for mixes prepared with a W/DM of 0.5 compared to mixes with a W/DM of 0.6. The porosity did not vary noticeably across the different waste simulants. The mixes prepared without hydrated lime tended to have greater porosity. This may be attributed to the reaction of hydrated lime with the waste solution to form additional solids in the waste form.

Table 5-12. Comparison of WTP Waste Simulant and Pore Solution Expressed from Mix 6 Prepared using the WTP Waste Simulant.

	Mol Fraction	
Species	WTP*	Mix 6 Pore Solution
SO_4^{2-}	0.250	0.131
PO_4^{2-}	0.000	0.003
NH^{4+}	0.330	0.260
Na^+	0.295	0.427
K^+	0.000	0.016
Cl^-	0.006	0.012
NO_3^-	0.117	0.114
NO_2^-	0.001	0.004
F^-	0.001	0.000
OH^-	0.000	0.032
Total	1.000	0.999
Density (g/cm^3)	1.126	1.071
pH	6.3	13.3

*from Table 3-4.

Table 5-13. Porosity Calculated using Method from Reference 36 and Measurements from Table 5-12.

Test ID	Simulant	W/DM	HL/OPC/BFS/FA Blend	Porosity (%)
1	242-A	0.5	20/35/45/0	49.82
2[a]	ERDF	0.5	20/35/45/0	47.77
3	WTP	0.5	20/35/45/0	54.82
4	242-A	0.6	20/35/45/0	54.96
5	ERDF	0.6	20/35/45/0	51.78
6[b]	WTP	0.6	20/35/45/0	58.61
7[a]	ERDF	0.5	20/35/45/0	48.56
8[b]	WTP	0.6	20/35/45/0	58.80
9	242-A	0.5	20/10/70/0	53.13
10	WTP	0.5	20/10/70/0	46.72
11	WTP	0.6	0/20/45/35	60.07
12	242-A	0.6	0/20/45/35	57.29
13	WTP	0.6	0/8/45/47	60.24
14	242-A + ERDF	0.5	0/20/45/35	48.94

[a] Replicate mixes
[b] Replicate mixes

5.2.3 Hydraulic Conductivity

Hydraulic conductivity (K) is the coefficient used to express the ease with which a fluid passes through a porous matrix. K therefore depends both on degree of saturation as well as matrix and fluid properties. The relevant fluid properties are density and viscosity. The relevant properties of the solid matrix are saturation and factors effecting pore geometry such as grain size distribution, grain shape, tortuosity, porosity etc. Numerical models of fluid flow in porous matrices such as Saltstone and Cast Stone typically use saturated K (Ksat) and a correlation between K and saturation determine the K for calculations of fluid flow and contaminant transport. These models have been successfully used to simulate fluid flow and contaminant transport through porous waste forms and can be used to model the transport of water through the LSW waste form.

Select samples from the screening test matrix in Table 4-1 were analyzed to determine the saturated hydraulic conductivity. Mixes were selected to evaluate the effect of W/DM and the dry blend ratio on the hydraulic conductivity. As with the samples for compressive strength, 2 x 4 inch cylindrical samples were demolded. The samples were trimmed to have parallel faces and a height of approximately 2 inches—a sample aspect ratio of 1. After being trimmed, the samples were submerged in water and placed under vacuum to displace air and saturate the samples. Following vacuum saturation, the samples were tested in a flexible wall permeameter using Method C in Reference 37 for determining hydraulic conductivity of saturated materials. The samples were loaded into a tri-axial cell with a glass fiber filter, porous stainless steel disk and cap on both ends with a surrounding rubber membrane held in place with O-rings. Once the samples were placed in the permeameter, saturation was completed on the samples using back pressure to remove any residual gas bubbles. The permeation was started by increasing the influent pressure while keeping the effluent pressure constant to maintain the back-pressure. Testing was deemed complete when at least four values of steady hydraulic conductivity were obtained.

Performance of the test involves measurement of the inflow and outflow of permeant. For low permeability samples the flow can be as low as tenths of a mL per day, and the method allows the ratio of inflow and outflow to vary between 0.75 and 1.25. Cumulative inflow exceeded outflow in each of the four samples with low permeability. The excess inflow may have been consumed by additional hydration or other processes that ultimately lead to a reduction in K.

The measured initial K and final K values are reported in Table 5-14. No water permeated Mix 5 during the saturation period, therefore, the hydraulic conductivity reported was the detection limit of this test setup, $<1\times10^{-9}$ cm/s. Following the determination of the initial K, testing was continued to investigate if any temporal trends in K existed. Four of the six samples exhibited a trend of decreasing K with curing time. Figure 5-5 shows the temporal variability of hydraulic conductivity with curing time (days since samples were mixed and cast into monoliths). Mix 10 had a relatively large K and, as a result, the test could not be run continuously. The sample was placed in a stand-by condition with no pressure gradient across the sample between measurements. The inherent variability in the method for samples with hydraulic conductivities in the 10^{-8}-10^{-9} cm/s range makes it difficult to resolve effects on the measurement. For Mix 10, the Test Time is the number of days the sample was in the test cell.

To mitigate the potential effect on the hydraulic conductivity by the osmotic pressure of the pore solution, the permeant is chosen to match the osmotic pressure of the pore solution, typically a simplified version of the waste simulant. In this study, the reaction during mixing of the waste simulant and the dry blend materials changed the composition of the pore solution, Table 5-12, thus the composition of the pore simulant was not yet determined at the initiation of the experiments. Therefore water was used as the permanent with the knowledge that there may be osmotic pressure effects.

Table 5-14. Initial and Final Hydraulic Conductivities Measured on Select Sample from the Test Matrix in Table 4-1.

Test ID	Simulant	W/DM	HL/OPC/BFS/FA Blend	Permeant		Test Time (d)	Hydraulic Conductivity	
				V_{in} (ml)	V_{out} (ml)		Initial (cm/s)	Final (cm/s)
3	WTP	0.5	20/35/45/0	16.4	15.2	18.9	$2.4x10^{-8}$	$2.6x10^{-9}$
5	ERDF	0.6	20/35/45/0	0.0	0.0	--	$<1x10^{-9}$	$<1x10^{-9}$
6[b]	WTP	0.6	20/35/45/0	19.0	17.3	20.1	$1.5x10^{-8}$	$3.9x10^{-9}$
8[b]	WTP	0.6	20/35/45/0	38.9	40	49.1	$1.1x10^{-9}$	$<1x10^{-9}$
10	WTP	0.5	20/10/70/0	872	883	11.7	$8.9x10^{-6}$	$7.1x10^{-6}$
11	WTP	0.6	0/20/45/35	10.2	8.7	41.8	$9.8x10^{-9}$	$1.54x10^{-9}$

[b]Replicate mixes

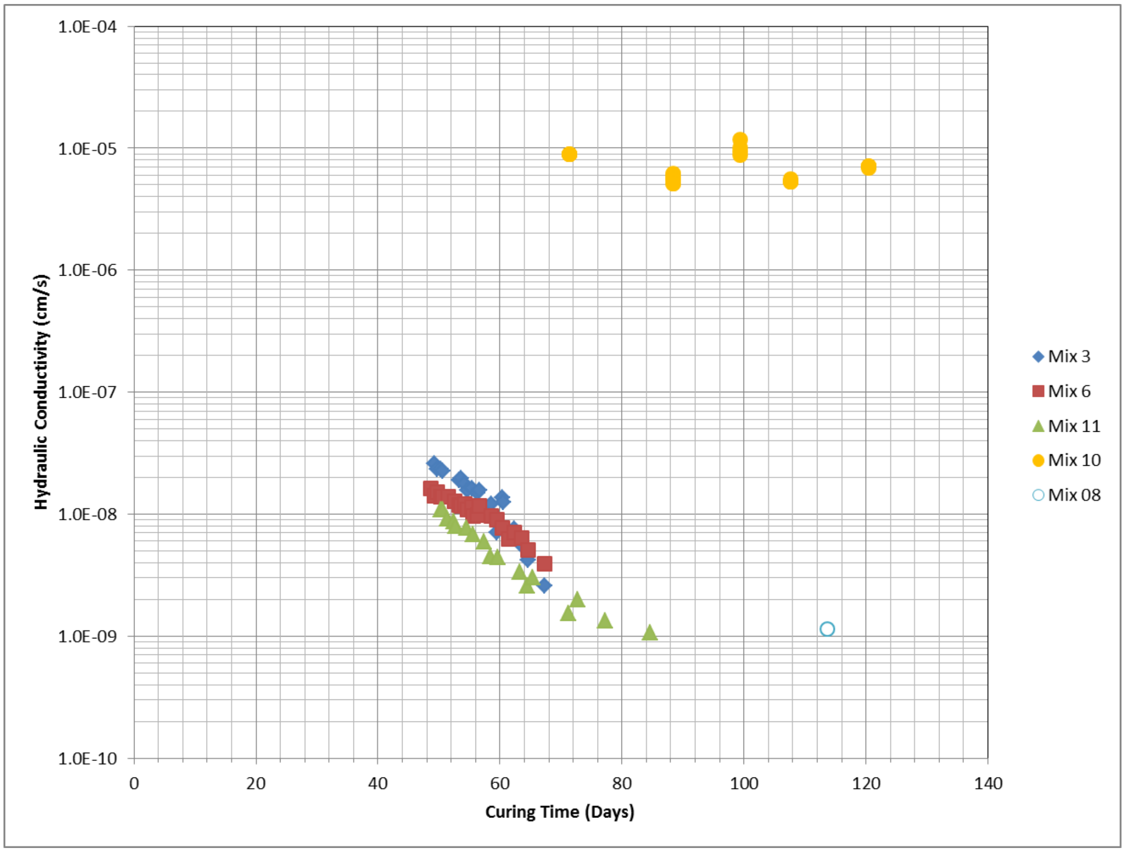

Figure 5-5. Hydraulic conductivity as a function of time for the mixes tested.

5.2.4 Water Characteristic Curve

The water characteristic curve, describes the desorption potential of a sample. When the curve is generated by the methods from Reference 38, the results, saturation as a function of suction, are in the terms of matric suction. Dependent upon the conceptual model selected to calculate the transport of contaminants in the IDF, results may be used to model transport in unsaturated flow conditions.

The moisture retention properties of three formulations—Mixes 3, 6, and 11—of Liquid Secondary Waste were analyzed to determine the van Genuchten parameters commonly used in unsaturated flow models.[40] Hydraulic and physical properties of the three formulations are provided in Table 5-15. Cured samples of all three formulations were tested using a pressure plate apparatus and using a measured vapor pressure method (chilled mirror hygrometer).

Table 5-15. Physical and Hydraulic Properties from Table 5-13 and Table 5-14.

Test ID	Dry Bulk Density (g/cm^3)	Porosity (cm^3/cm^3)	Particle Density[a] (g/cm^3)	Hydraulic Conductivity (cm/s)
Mix 3	1.31	0.5279	2.77	$2.60\text{x}10^{-9}$
Mix 6	1.20	0.5644	2.75	$3.93\text{x}10^{-9}$
Mix 11	1.19	0.5784	2.82	$1.54\text{x}10^{-9}$

a Particle density calculated as $\rho_s = \rho_b/(1-\eta)$ where ρ_b is dry bulk density and η is porosity.

Testing of samples using the pressure plate apparatus generally followed Reference 38, Method C. Thin wafers of each formulation were vacuum saturated in the waste simulant prior to the onset of testing. Once saturated, the samples were placed in the pressure plate apparatus and an initial pressure of 0.1 bar was applied. Samples were periodically removed from the pressure plate apparatus, weighed, and placed back into the pressure plate apparatus. Applied pressures were increased incrementally over time ultimately reaching a maximum pressure of 4.0 bar. When this type of test is applied to soils, capillary drainage is typically observed due to the applied pressure. The resulting dataset is used to establish a drainage curve as a function of applied pressure. However, for all three formulations tested, no drainage was observed over the applied pressure range, that is, the air-entry pressure exceeded 4.0 bar. In fact, at each pressure increment, the samples actually gained weight. This was attributed to the osmotic gradient between the porous ceramic plate (saturated with tap water) and the secondary waste samples (saturated with waste simulant). This may also be attributed to the samples containing unreacted cementitious components. As a result, no useful data was obtained from the pressure plate apparatus and testing was terminated in favor of the measured vapor pressure method, which enables testing at higher pressures.

Measured vapor pressure method testing was performed using a chilled mirror hygrometer Reference 38, Method D. The chilled mirror hygrometer[*] uses the chilled mirror dew point technique to measure the total moisture potential of porous materials.[41,42] Total moisture potential is the sum of osmotic and matric potential—neglecting hydrostatic pressure and gravitational effects. Generally, osmotic potential is negligible and the total potential is assumed to be equal to the matric potential. However, in the case of the secondary liquid waste formulations, there is an osmotic component due to the high salinity of the simulants used—relative to groundwater. Therefore, the total potential measurements include the osmotic potential due to the salt content of the simulant and the matric potential due to capillarity and adsorptive forces binding moisture to the saltstone particles.

Samples from each of the secondary waste formulations cured for a minimum of 28 days were prepared for testing by crushing the grout samples with a mortar and pestle. The crushed grout was sieved to produce bulk powder with a particle size of 2 mm or less. The chilled mirror measures the absorptive forces binding water to individual particles. Capillary contributions, and thus particle size, become negligible for matric potential values near the dry end.[43] The bulk powder from each formulation was oven dried at ~105 °C to eliminate volatile compounds that could potentially interfere with the controlled vapor pressure measurements. The bulk material was subsequently rewetted with deionized water for testing in the WP4C. Samples were tested starting at, or near, saturation. After the initial moisture potential measurement, each sample was oven dried to achieve a lower moisture potential (drier condition). The samples were allowed to equilibrate (balance the air-water interface) for several hours between moisture potential measurements. Data from these measurements were used to establish a drying (desorption) moisture characteristic curve, and at the conclusion of the drying tests, samples were

---

[*] Decagon Devices Model WP4C

sequentially rewetted with deionized water to create a wetting (adsorption) moisture characteristic curve. This data is tabulated in Appendix E.

The moisture retention data from both the drying and wetting measured vapor equilibrium tests were analyzed using RETC[44] to estimate the parameters α, n and m in the van Genuchten functional form[40]

$$S_e = \frac{1}{[1+(\alpha\psi)^n]^m} \tag{1}$$

Where α is related to the inverse of the air entry suction and, *n* is a measure of the pore-size distribution, and where effective saturation is defined by

$$S_e \equiv \frac{\theta - \theta_r}{\theta_s - \theta_r} = \frac{S - S_r}{1 - S_r} \tag{2}$$

The subscripts for θ, water content, refer to saturated (s) and residual (r) conditions. Using S_e the relative hydraulic conductivity K was calculated at incremental pressure heads using the Mualem-van Genuchten type function

$$K = S_e^L \left[1 - \left(1 - S_e^{1/m}\right)^m\right]^2 \tag{3}$$

where *L* is an empirical pore-connectivity parameter and assumed to be 0.5. Datasets from each formulation were analyzed individually and combined. Due to the similarity of the results across the three formulations, only the results of the combined analysis are presented here. The combination results for Mixes 3, 6, and 11 will be referred to as Secondary Waste. For each dataset, θ_s was set equal to the average measured porosity for the three formulations in Table 5-15. The RETC program was allowed to fit θ_r, α, and *n*. The parameter *m* was calculated from *n* using the standard assumption $m = 1\text{-}1/n$.[45] The van Genuchten transport parameters for the drying and wetting datasets are presented in Table 5. Additionally, an analysis was conducted on the combined wetting and drying datasets and the results are presented in Table 5. In this case, both θ_s and θ_r were fixed to provide the best fit to the measured data. θ_s was set equal to the average porosity as previously discussed and θ_r was set to 0.06 which is essentially the same as calculated for the individual datasets. For comparison purposes, the van Genuchten parameters currently used for saltstone[46] are included in Table 5-16. The transport parameters determined from the combined drying and wetting datasets compares very favorably to the saltstone parameters reproduced in the table from Reference 46. Confidence limits (95%) for the van Genuchten parameters estimated from the secondary waste datasets are provided in Table 5-17.

Table 5-16. Van Genuchten Transport Parameters Data. Analyzed using Mualem Relationship between n and m where m = 1 – 1/n.

Material	θ_s[a] (cm^3/cm^3)	θ_r (cm^3/cm^3)	α[b] (1/cm)	n	m	r^2
Secondary Waste - Drying	0.5569	0.06375	3.26E-06	1.94086	0.48476	0.978
Secondary Waste – Wetting	0.5569	0.06097	7.45E-06	1.79683	0.44346	0.965
Secondary Waste - Combined	0.5569	0.06000	6.03E-06	1.64883	0.39351	0.848
Saltstone PA	0.5800	0.00000	1.008E-05	1.67131	0.40167	0.986

[a] set equal to the average measured porosity in Table 5-15.

[b] α calculated from RETC output using van Genuchten empirical relationship for moisture retention data.

Table 5-17. Confidence Limits (95%) for Van Genuchten Transport Parameters.

Material	θ_s[a] (cm^3/cm^3)		θ_r (cm^3/cm^3)		α[b] (1/cm)		n	
	Lower	Upper	Lower	Upper	Lower	Upper	Lower	Upper
Secondary Waste – Wetting	-	-	0.0000	0.2480	-	-	1.2227	2.3709
Secondary Waste - Drying	-	-	0.0000	0.1460	-	-	1.5880	2.2937
Secondary Waste - Combined	-	-	-	-	-	-	1.4946	1.8030

[a] set equal to the average measured porosity in Table 5-15.

[b] RETC output precision for α insufficient to provide confidence limits.

Figure 5-6 through Figure 5-8 provide the characteristic curves for Hanford secondary waste. For comparison purposes, the characteristic curves for saltstone are included in these figures. Good agreement is noted between the observed moisture retention data and the fitted characteristic curves for all datasets. Furthermore, the general shape of the secondary waste curves compare favorably to the saltstone curves. Figure 5-9 and Figure 5-10 show the relative permeability function and hydraulic conductivity function for Hanford secondary waste as compared to saltstone. Differences noted in Figure 5-10 between saltstone and secondary waste, are due to the higher average saturated hydraulic conductivity of saltstone ($6.4x10^{-9}$ cm/sec compared to $2.69 x10^{-9}$ cm/sec).

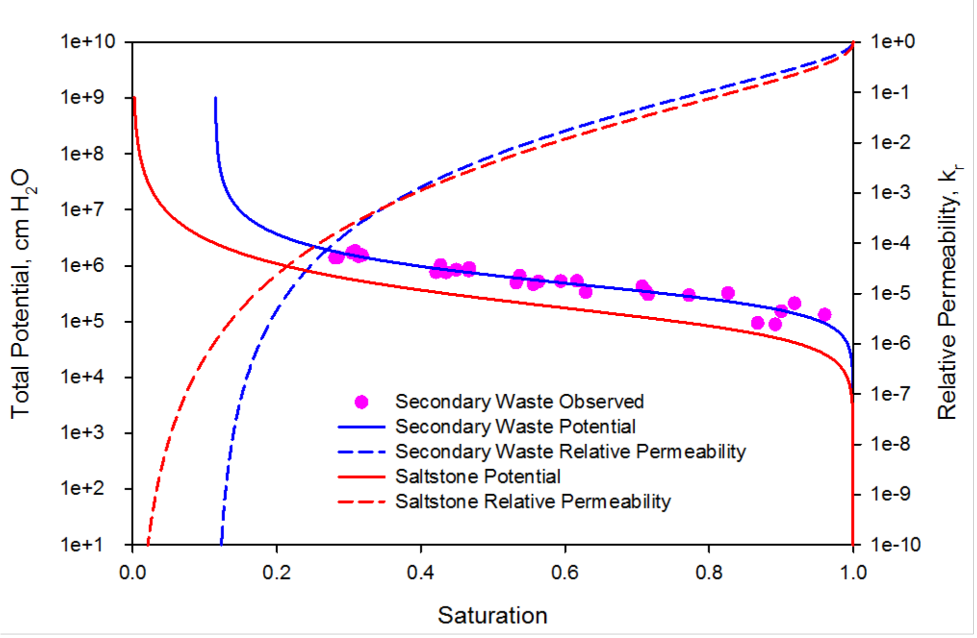

Figure 5-6. Characteristic curves for Mixes 3, 6, and 11 combined - Drying.

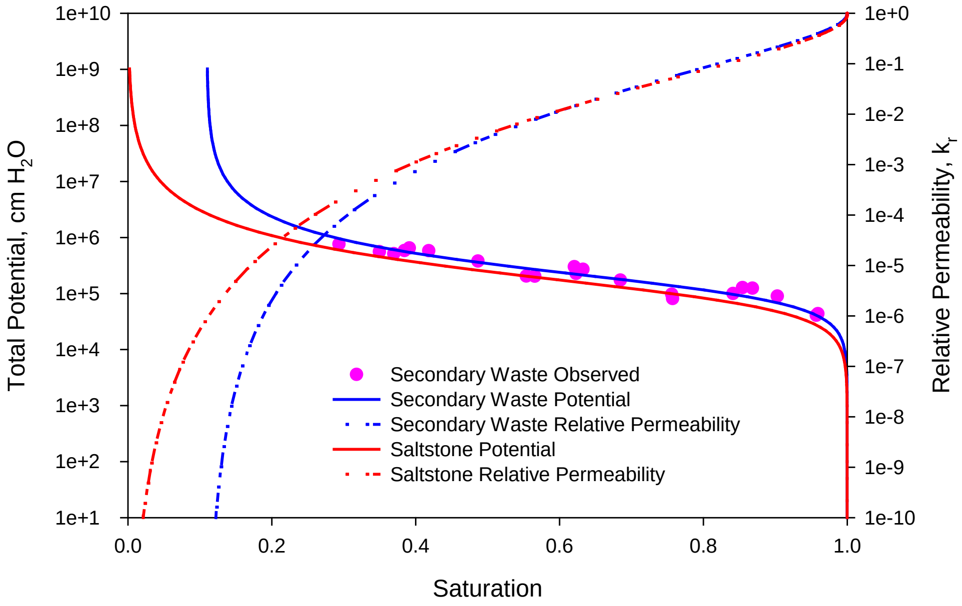

Figure 5-7. Characteristic curves for Mixes 3, 6, and 11 combined - Wetting.

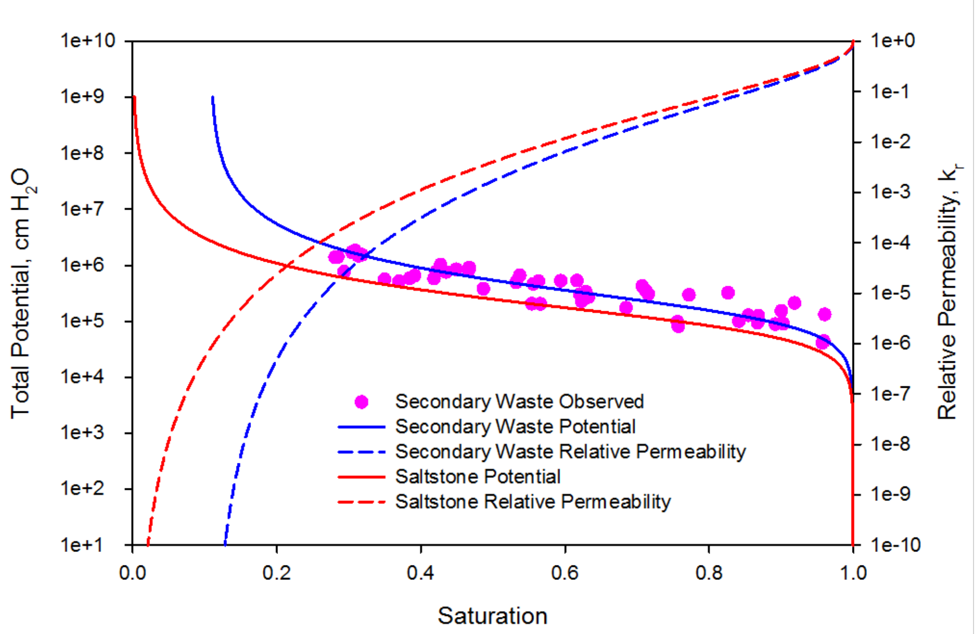

Figure 5-8. Characteristic curves for Mixes 3, 6, and 11 combined – Drying and Wetting.

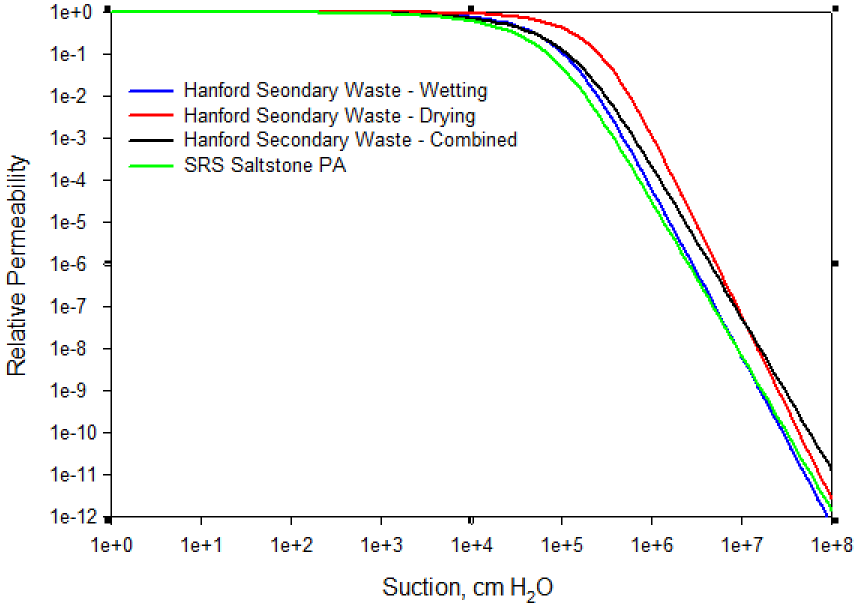

Figure 5-9. Comparison of relative permeability curves for LSW and Saltstone (based on Saltstone PA model).

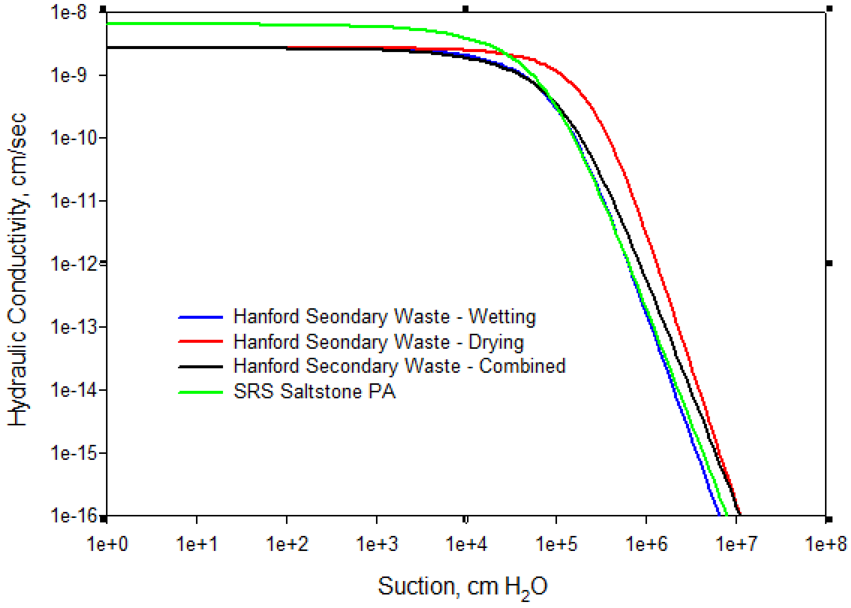

Figure 5-10. Comparison of hydraulic conductivity curves for LSW and Saltstone (based on Saltstone PA model).

5.2.5 Mineralogy

The mineralogical makeup of each mix was determined from samples collected from compression testing. X-ray diffraction data were collected on a Bruker D8 X-ray diffractometer by step scanning over the 2 Θ ranges of 5-70° with a step size of 0.02° and a dwell time of 1 second. Search-match identification of all the phases was performed using Jade software (Version 9.0) from Materials Data Inc. combined with the ICDD's PDF-4 database. Quantification of the crystalline and amorphous phases were omitted from this study as selection of an appropriate internal standard that does not overlap any of the peaks associated with the multiple phases present and the difficulty in deconvoluting mixtures of substituted mineral phases with significant amorphous phases provide subjective results.[47]

Ettringite and calcite were present in each diffractogram of the mixes. Each of the diffractograms contained an amorphous hump associated with CSH gel. The mineralogy did not vary noticeably among the waste simulants. Unreacted alite was identified in the mixes made with 20% hydrated lime and 35% OPC. Many of the mixes also contained unreacted belite. These cement phases are present in the diffractogram of the cement used in the dry blend, Figure 5-11. Mixes made with fly ash all contained quartz. The diffractograms for the mixes are presented in Appendix F.

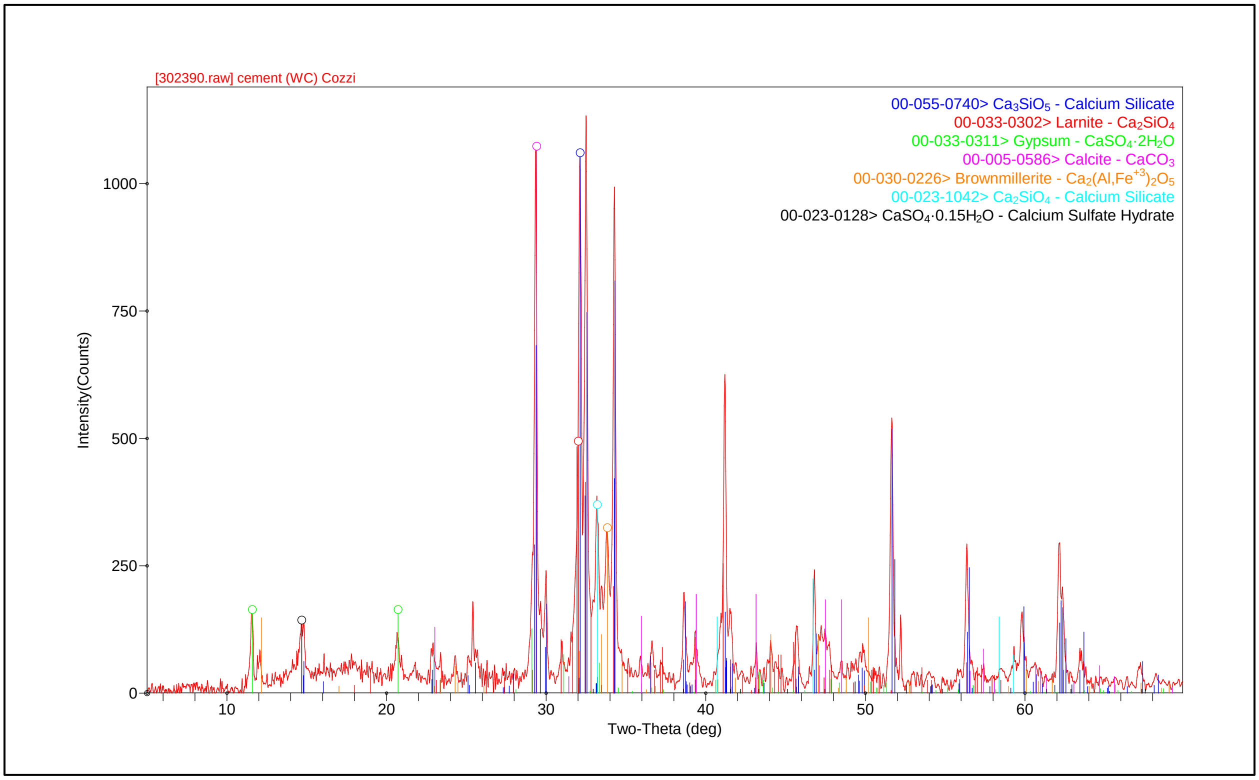

Figure 5-11. Diffractogram of cement used in the dry blend mixtures.

5.3 Quality Assurance

The work scope was performed in accordance with a Quality Assurance Program (QAP) that meets the Quality Assurance criteria specified in DOE Order 414.1D, Quality Assurance; 10 CFR 830, "Nuclear Safety Management," Subpart A, "Quality Assurance Requirements," paragraph 830.122; and also meets the requirements of ASME NQA-1-2004, Quality Assurance Requirements for Nuclear Facility Applications, including NQA-1a-2005 and NQA-1b-2007 Addenda, or later version. The work scope was performed in accordance with Savannah River Site Manual 1Q, QAP 2-3 (Control of Research and Development Activities). Requirements for performing reviews of technical reports and the extent of review are established in manual E7 2.60. SRNL documents the extent and type of review using the SRNL Technical Report Design Checklist.[48]

6.0 Conclusions

Three Hanford Liquid Secondary Waste simulants were developed based on existing and projected waste streams. Using these waste simulants, fourteen mixes were prepared and tested varying the waste simulant, the water to dry materials blend, and the dry materials blend composition.

During mixing, the introduction of the dry blends into the waste simulant resulted in noticeable quantities of ammonia from the waste simulant being released. The dry blend materials were not readily incorporated into the waste simulants and required the use of an admix to modify rheological properties. Prior scoping work selected MasterGlenium 3030, a full range water reducing admixture formulated for slump retention. Additions of the admix facilitated the incorporation of the dry blend materials into the waste simulant. The gel times for the mixes ranged from 90 seconds to > 40 minutes. The structure developed in the mixes with gel times shorter than 20 minutes do not affect waste form properties, but can introduce operational challenges in a facility to recover from interruptions in processing. All but one of the formulations set fully in less than 24 hours. The WRA is formulated to provide a faster setting time, however, the manufacturer intends this product to be used in a concrete mix with water, rather than the dry blends used in this study with a waste simulant as the hydration source. The formulations that contained fly ash, Mixes 11, 12, and 13, that were prepared using a W/DM of 0.6, contained free liquids after 24 hours. Mixes 11 and 12 retained free liquids after 72 hours. The free liquid associated with Mix 13 were reabsorbed into the waste form. Fly ash is slower to hydrate than the other dry material blend components in these tests. The neutral pH of the waste simulants do not accelerate the hydration of the blast furnace slag in the same way as caustic waste simulants. The presence of free liquids is an indication of settling. The amount of free liquids is less meaningful as the repeatability of measurement varies.[19] The grout flow was moderately affected by the waste simulant and the amount of WRA used, however, at this time, no clear waste simulant component or property could be identified to explain the effect on flow. The yield stress of the mixes tested, 127-456 Pa, were higher than the yield stresses measured in the low activity waste simulant testing in Reference 28. A mix with a high yield stress will not affect cured properties, but may require additional consideration for routine waste treatment operations.

Results from the isothermal calorimetry testing, along with the heat rise measured during mixing, indicated that the reactions that occurred during mixing and the early stages of curing generated the majority of the heat created in these formulations. Because the waste simulants are near neutral, a portion of the heat generated may be attributed to the heat of reaction of the hydrated lime with the waste solution, rather than solely caused by heat of hydration. The total heat generated in these tests were generally less than the heat measured in prior testing with low activity waste simulants. This may be caused by the test method not capturing the early heat generated during mixing and, insufficient water to complete hydration.

The compressive strength of all of the mixes exceeded the target of 3.4 MPa (500 psi) to meet the requirements identified in Reference 2. The compressive strength was dependent primarily on the W/DM ratio, with samples made using a W/DM of 0.5 have a greater compressive strength than samples prepared with a W/DM of 0.6. The mixes with the lowest compressive strength measured after 28 days of curing were mixes made containing fly ash as one of the dry blend components.

The hydraulic conductivities of select mixes were measured using a flexible wall permeameter. Testing in all but the most permeable sample, Mix 11, took weeks to attain equilibrium flow. The decrease in hydraulic conductivity with time for several mixes as shown in Figure 5-5 is an indication that there may have been additional reactions occurring in the samples during saturation and testing. Thus, the hydraulic conductivity data may not fully represent the formulations in the matrix as the samples may not have been mature enough for testing, particularly in the early stages of testing. However, the final condition may be representative of a more mature, saturated waste form. This supposition is supported by the columns of flows in Table 5-14 that demonstrate more water entered the samples than exited. Similar behavior was noted in the measurement of the water characteristic curves. Although the response of the mixes tested were comparable to the properties measured for the SRS Saltstone waste form,[49] testing using the pressure plate method did not achieve any flow through the samples.

The x-ray diffraction analysis of each of the mixes detected notable amounts of ettringite in addition to unreacted dry blend components. The changes in dry blend components affected the mineralogical make up, whereas mixes with different waste simulants and similar dry blends showed similar mineralogy.

7.0 Recommendations

- Alternative water reducing additives should be evaluated to reduce the yield stress of the fresh mixes. Although the yield stresses of the mixes in this study were addressed at bench-scale, alternative additives should be investigated.
- Methods to reduce the ammonia content of the ETF concentrate prior to solidification should be evaluated .

- Formulations including additional water should be tested to achieve waste forms that have sufficient water for hydration. X-ray diffraction analysis showed excess calcium available to react with additional sulfate associated with the addition of greater amounts of was simulant. Tracking of the ettringite formed over several months of aging is recommended.

- Additional samples should be produced to evaluate strength development at times shorted than 28 days to permit reduced hold times prior to final disposal.

- Additional samples of future mixes should be archived for leach testing at cure times greater than 28 days. The 28 day cure time is adopted from the concrete industry where strength is the primary concern and develops in concrete samples in a well-known manner such that strength measurements at short cure times—14 or 28 days—are indicative of behavior at longer times.

8.0 References

[1] Westsik, Jr., J. H., Piepel, G. F., Lindberg. M. J., Heasler, P. G., Mercier, T. M., Russell, R. L., Cozzi, A. D., Daniel, W. E., Eibling, R. E., Hansen, E. K., and Reigel, M. M., Supplemental Immobilization of Hanford Low-Activity Waste: Cast Stone Screening Tests, RPP-RPT-55960, Revision 0, Washington River protection Solutions, Richland, Washington, September 2013.

[2] Ramsey, A.A. Secondary Liquid Waste Treatment Cast Stone Technology Development Plan, RPP-51790, Revision 0, Washington River Protection Solutions, Richland, Washington, July 2012.

[3] Brown, E.E., Kelly, S. E., and Swanberg, D. J. Hanford Integrated Disposal Facility Performance Assessment Technology Support Program Plan, RPP-PLAN-60520, Revision 0, Washington River Protection Solutions, Richland, Washington, August 2015.

[4] Swanberg, D. R., Secondary Waste Cast Stone Formulation and Waste Form Qualification, Request for Proposal #273608, Washington River Protection Solutions, Richland, Washington, January, 2015.

[5] Cozzi, A. D., Crawford, C. L., and Roberts, K. A., Task Technical and Quality Assurance Plan for the Secondary Waste Cast Stone Formulation and Waste Form Qualification, SRNL-RP-2015-00235 Revision 0, Savannah River National Laboratory, Aiken, South Carolina, June 2015.

[6] Halgren, D. L., 200 Area Effluent Treatment Facility Basin 43 2012 Campaign Process Control Plan, CHPRC-01871, Revision 1, CH2M HILL Plateau Remediation Company, December 2012.

[7] Cooke, G. A., Lockrem, L. L., Avila, M., and Westberg, R. A., Effluent Treatment Facility Waste Stream Monolith Testing Phase II, RPP-RPT-31077, Revision 0, CH2M HILL Hanford Group, Inc., Hanford, Washington, September 2006.

[8] Cozzi. A. D., Fox, K. M., Hansen, E. K., and Roberts, K. A., Supplemental Immobilization of Hanford Low-Activity Waste: Cast Stone Augmented Formulation Matrix Tests, SRNL-STI-2014-00619, Revision 0, Savannah River National Laboratory, Aiken, South Carolina, July 2015.

[9] Cozzi, A. D., SRNL Scope and Cost Estimate in Response to : Secondary Waste Cast Stone Formulation and Waste Form Qualification Statement of Work Requisition #:273608 Revision 1, SRNL-L3100-2015-00005, Revision 0, Savannah River National Laboratory, Aiken, South Carolina, January 2015.

[10] Inductively Coupled Plasma-Atomic Emission Spectrometer Agilent 730 ES, L29 ITS-0079.

[11] Anion Analysis Using the Dionex DX-500 and ICS-5000 Ion Chromatograph, L29 ITS-0027.

[12] Weight Percent Solids Determination Using a Furnace or Oven, L29 ITS-0078.

[13] Operation of Mettler Toledo Hr73 Halogen Moisture Analyzer, L29 ITS-0007.

[14] Russell. R L., Westsik, Jr., J. H., Rinehart, D. E. Swanberg, D. J., and Mahoney, J. L., Secondary Waste Simulant Development for Cast Stone Formulation Testing, PNNL-24195, RPT-SWCS-003 Rev 0, Washington River protection Solutions, Richland, Washington, April 2015.

[15] Standard Specification for Portland Cement, ASTM, West Conshohocken, PA, C 150/150M – 12.

[16] Standard Specification for Slag Cement for Use in Concrete and Mortars, ASTM, West Conshohocken, PA, C989/989M-14.

[17] Standard Specification for Coal Fly Ash and Raw or Calcined Natural Pozzolan for Use in Concrete, ASTM, West Conshohocken, PA, C618-12a

[18] Standard Specification for Chemical Admixtures for Concrete, ASTM, West Conshohocken, PA, C494/494M-13.

[19] Harbour, J.R., Edwards, T.B., Hansen, E.K., and Williams, V.J., Variability Study for Saltstone, WSRC-TR-2005-00447, Revision 0, Savannah River National Laboratory, Aiken, South Carolina, October 2005.

[20] Standard Test Method for Time of Setting of Hydraulic Cement by Vicat Needle, ASTM, West Conshohocken, PA, ASTM C 191-13.

[21] Monitoring Set Time of Grout Using Ultrasonic Pulse Velocity (UPV) System, ITS-WI-0044.

[22] Standard Test Method for Flow Consistency of Controlled Low Strength Material (CLSM), ASTM, West Conshohocken, PA, D 6103 – 04.

[23] Standard Practice for Measuring Hydration Kinetics of Hydraulic Cementitious Mixtures Using Isothermal Calorimetry, ASTM, West Conshohocken, PA, C 1679-09.

[24] Standard Test Method for Density of Liquid Coatings, Inks, and Related Products, ASTM, West Conshohocken, PA, D 1475-13.

[25] Hansen, E.K. and Langton, C.A., Physical Characterization of FY2004 Saltstone Simulant Studies, WSRC-TR-2005-00365 Savannah River National Laboratory, Aiken, South Carolina, Decemer 2005.

[26] Haake RheoStress (RS) Rheometers, L29 ITS-0073.

[27] Cozzi, A. D., Fox, K. M., Hansen, E. K., and Roberts, K. A. Supplemental Immobilization of Hanford Low-Activity Waste: Cast Stone Augmented Formulation Matrix Tests, SRNL-STI-2014-00619, Revision 0, Savannah River National Laboratory, Aiken, South Carolina July, 2015.

[28] Westsik, Jr., J. H., Piepel, G. F., Lindberg. M. J., Heasler, P. G., Mercier, T. M., Russell, R. L., Cozzi, A. D., Daniel, W. E., Eibling, R. E., Hansen, E. K., and Reigel, M. M., Supplemental Immobilization of Hanford Low-Activity Waste: Cast Stone Screening Tests, PNNL-22747, SRNL-STI-2013-00465, Revision 0, Pacific Northwest National Laboratory, Richland, Washington, Savannah River National Laboratory, Aiken, South Carolina, September 2013.

[29] Cozzi A. D., Daniel, W. E., and Hansen, E. K., Sonic Velocities and other Properties of Fresh SRS Saltstone Grout SRNL-L3100-2013-00062, Revision 0, Savannah River National Laboratory, Aiken, South Carolina April, 2013.

[30] Ferraris, C. F., Obla, K. H., and Hill, R., The influence of mineral admixtures on the rheology of cement paste and concrete, Cement and Concrete Research, Volume 31, pp 245-255, 2001

[31] Banfill, P. F. G., The Rheology of Fresh Cement and Concrete – A Review, Proc 11th Cement Chemistry Congress, May 2003

[32] Langton, C. A. and Wilhite, E. L., Trip Report Slurry Property Evaluation at Halliburton February, 1985, DP-ST-85-469, April 1985.

[33] Langton, C. A. and Wilhite, E. L., Trip Report Slurry Property collected by Halliburton for Full-Scale Mixing and Pumping Test, DP-ST-85-498, April 1985.

[34] "Standard Test Method for Compressive Strength of Cylindrical Concrete Specimens," ASTM, West Conshohocken, PA, C39/C39M – 15a.

[35] "Standard Practice for Use of Unbonded Caps in Determination of Compressive Strength of Hardened Concrete Cylinders," ASTM, West Conshohocken, PA, C1231/C1231M – 14.

[36] Harbour, J.R., Williams, V.J., Edwards, T.B., Eibling, R.E., Schumacher, R.F., "Saltstone Variability Study – Measurement of Porosity," WSRC-STI-2007-00352 Revision 0, .

[37] "Standard Test Methods for Measurement of Hydraulic Conductivity of Saturated Porous Materials Using a Flexible Wall Permeameter," ASTM, West Conshohocken, PA, D5084-10.

[38] "Standard Test Methods for Determination of the Soil Water Characteristic Curve for Desorption Using Hanging Column, Pressure Extractor, Chilled Mirror Hygrometer, or Centrifuge," ASTM, West Conshohocken, PA, D 6836– 02 (Reapproved 2008).

[39] Panalytical X'pert Pro 3040 X-Ray Diffraction System, L16.1 ADS-1120.

[40] Van Genuchten, M. Th., A Closed-form Equation for Predicting the Hydraulic Conductivity of Unsaturated Soils, Soil Science Society of America Journal, v44, 892-898. 1980.

[41] Nimmo, J. R. and Winfield, K. A., Water Retention and Storage: Miscellaneous Methods. p 710-711. In J. H. Dane and G. C. Topp (ed.), Methods of Soil Analysis, Part 4, Physical Methods, Soil Science Society of America. 2002.

[42] Gee, G. W., Campbell, M. D., Campbell, G. S., and Campbell, J. H., Rapid Measurement of Low Soil Water Potentials using a Water Activity Meter. Soil Science Society of America Journal, v56, 1068-1070. 1992.

[43] Or, D., and Tuller, M., Liquid retention and interfacial area in variably saturated porous media: Upscaling from single-pore to sample-scale model, Water Resour. Res., 35(12), 3591-3606. 1999.

[44] Van Genuchten, M. Th., Leij, F. J. , and Yates, S. R., The RETC Code for Qualifying the Hydraulic Functions of Unsaturated Soils, Version 1.0, EPA Report 600/2-91/065, U.S. Salinity Laboratory, USDA, ARS, Riverside, California. 1991.

[45] Mualem, Y., A New Model for Predicting the Hydraulic Conductivity of Unsaturated Porous Media, Water Resources Research, v12 n3, pp 513–522. doi:10.1029/WR012i003. 1976.

[46] Flach, G. P. and Smith, III, F. G., Degradation Of Cementitious Materials Associated with Saltstone Disposal Units, SRNL-STI-2013-00118, Revision 2, Savannah River National Laboratory, Aiken, South Carolina, September 2014.

[47] Jenkins, R. and Snyder, R. L., Quantitative Analysis. *Introduction to X-ray Powder Diffractometry*, 1st ed. Chemical Analysis; Volume 138; John Wiley & Sons, Inc. New York, 1996, pp370-376.

[48] Butcher, B. T., Savannah River National Laboratory Technical Report Design Check Guidelines, WRSC-IM-2002-00011, Revision 2, Savannah River National Laboratory, Aiken, South Carolina, August 2004.

[49] Dixon, K. L., Harbour, J. R., and Phifer, M. A., Hydraulic and Physical Properties of Saltstone Grouts and Vault Concretes, SRNL-STI-2008-00421, Revision 0, Savannah River National Laboratory, Aiken, South Carolina, November 2008.

Appendix A. Origin of Simulant Brine Compositions

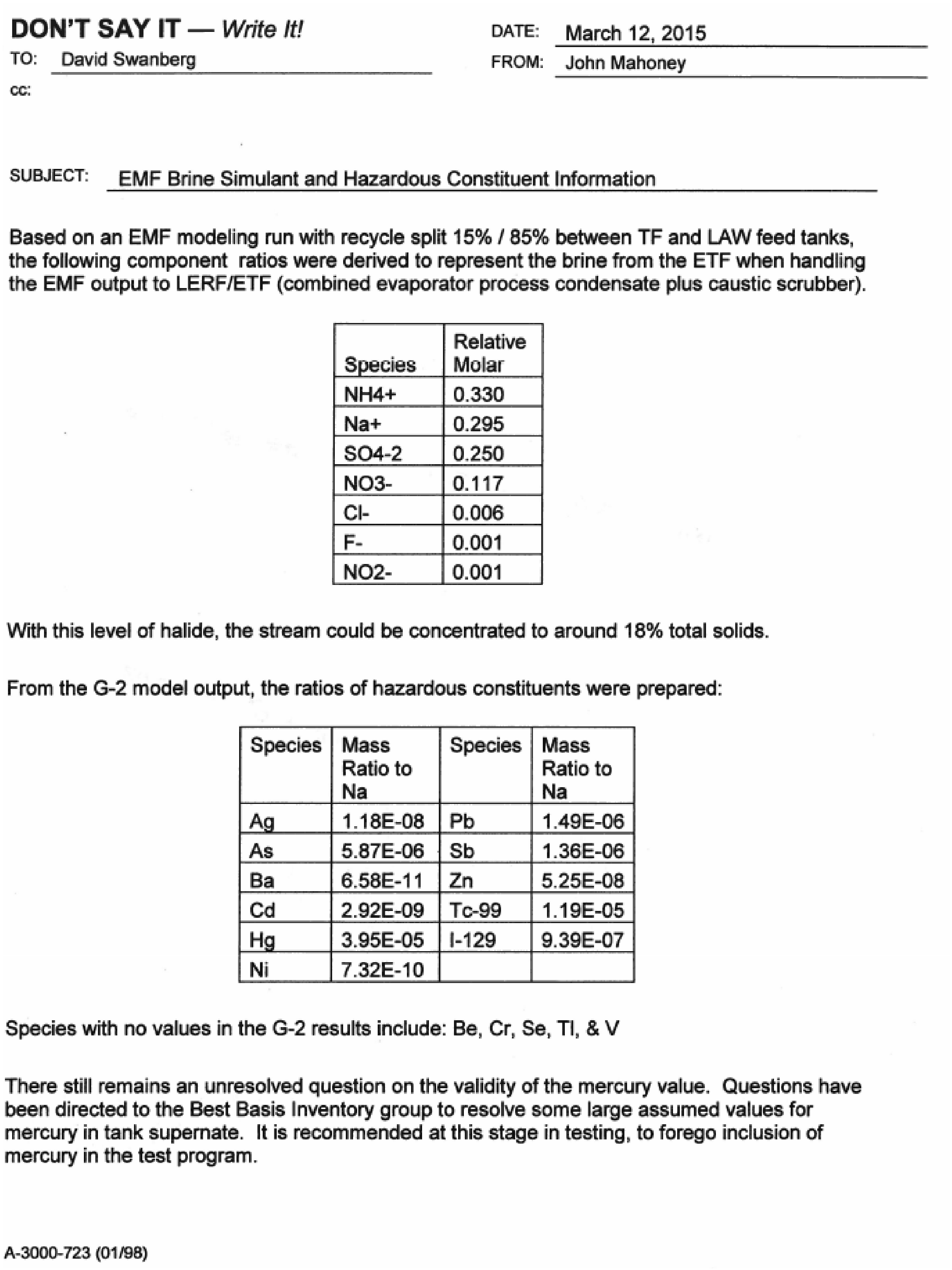

DON'T SAY IT — *Write It!*

DATE: March 12, 2015
TO: David Swanberg
FROM: John Mahoney
cc:

SUBJECT: EMF Brine Simulant and Hazardous Constituent Information

Based on an EMF modeling run with recycle split 15% / 85% between TF and LAW feed tanks, the following component ratios were derived to represent the brine from the ETF when handling the EMF output to LERF/ETF (combined evaporator process condensate plus caustic scrubber).

Species	Relative Molar
NH4+	0.330
Na+	0.295
SO4-2	0.250
NO3-	0.117
Cl-	0.006
F-	0.001
NO2-	0.001

With this level of halide, the stream could be concentrated to around 18% total solids.

From the G-2 model output, the ratios of hazardous constituents were prepared:

Species	Mass Ratio to Na	Species	Mass Ratio to Na
Ag	1.18E-08	Pb	1.49E-06
As	5.87E-06	Sb	1.36E-06
Ba	6.58E-11	Zn	5.25E-08
Cd	2.92E-09	Tc-99	1.19E-05
Hg	3.95E-05	I-129	9.39E-07
Ni	7.32E-10		

Species with no values in the G-2 results include: Be, Cr, Se, Tl, & V

There still remains an unresolved question on the validity of the mercury value. Questions have been directed to the Best Basis Inventory group to resolve some large assumed values for mercury in tank supernate. It is recommended at this stage in testing, to forego inclusion of mercury in the test program.

A-3000-723 (01/98)

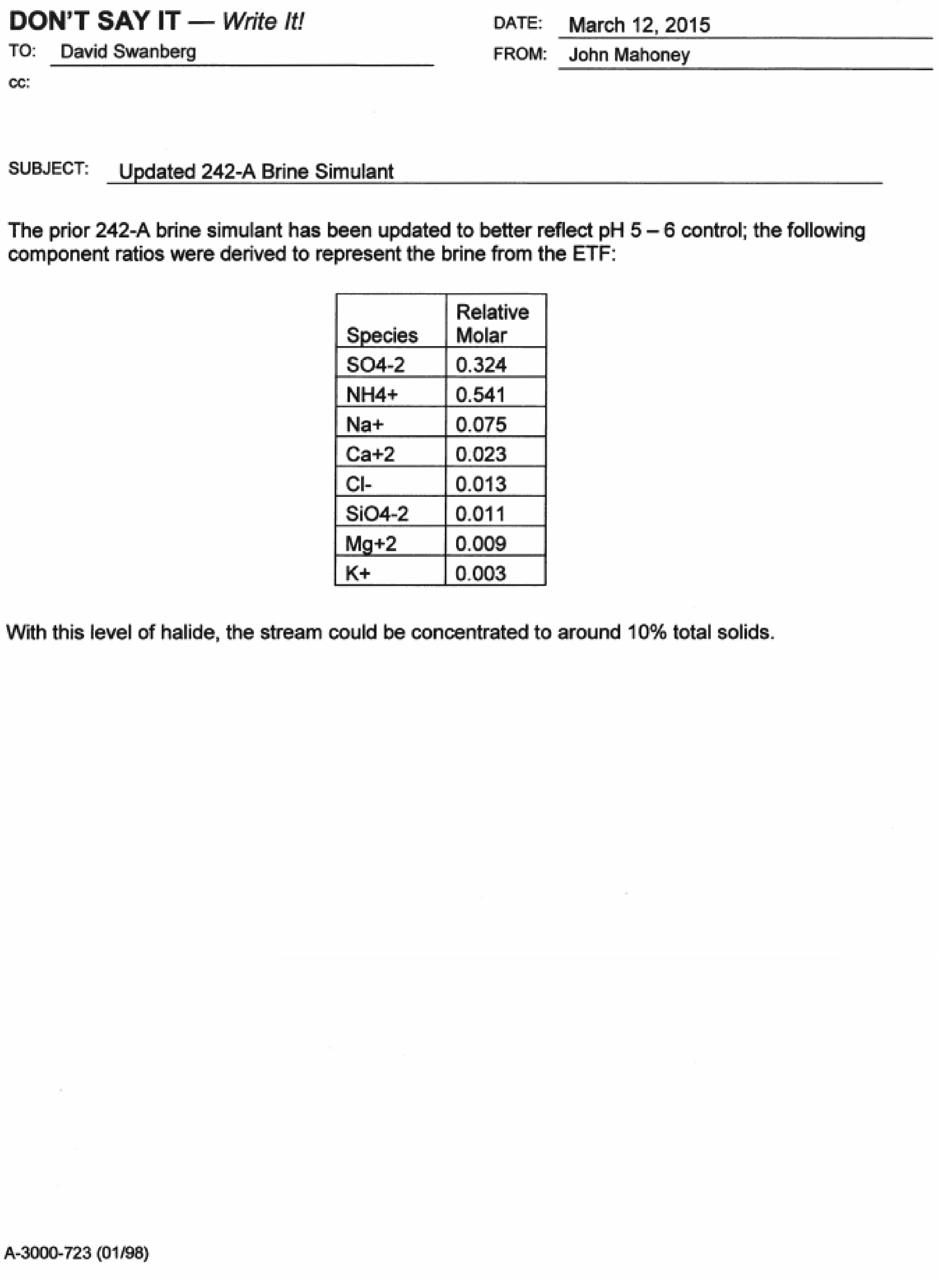

DON'T SAY IT — *Write It!*

DATE: March 12, 2015

TO: David Swanberg

FROM: John Mahoney

cc:

SUBJECT: Updated 242-A Brine Simulant

The prior 242-A brine simulant has been updated to better reflect pH 5 – 6 control; the following component ratios were derived to represent the brine from the ETF:

Species	Relative Molar
SO4-2	0.324
NH4+	0.541
Na+	0.075
Ca+2	0.023
Cl-	0.013
SiO4-2	0.011
Mg+2	0.009
K+	0.003

With this level of halide, the stream could be concentrated to around 10% total solids.

A-3000-723 (01/98)

Appendix B. Recipes for Liquid Secondary Waste Simulants

242 Brine Simulant

Volume of Feed 10000 mL

Obtain a Simulant Container larger than 10 L

Record mass of Simulant Container ______________ grams

Total Mass of Simulant to be prepared 10532.00 grams

To the bottle add the following in the order indicated with mixing

Compounds	Formula	Mass Needed (g)	Actual Mass (g)
Water	H_2O	7500	
Sodium Metasilicate Pentahydrate	Na_2SiO_3 $5H_2O$	54.5	
Sodium Chloride	NaCl	13.7	
Potassium Chloride	KCl	5.2	
Sodium Sulfate	Na_2SO_4	73.0	
Magnesium Sulfate Heptahydrate	$MgSO_4$ $7H_2O$	51.9	
Water for rinsing	H_2O	500	

solids may be observed upon addition of magnesium sulfate

To the same bottle add the following with mixing

Add	Formula	Mass Needed (g)	Actual Mass (g)
Ammonium Sulfate	$(NH_4)2SO_4$	835	
Caclium Sulfate	$CaSO_4$	73.2	
Water for rinsing	H_2O	1425	

Mix thoroughly. All of the solids will not dissolve.
Continue mixing for several hours.

Record Final Gross Weight ______________ grams

Measure the Density ______________ g/mL

Measure the pH ______________

Solution Labeling

242 Brine Simulant
Hanford Cast Stone Secondary Waste

HAZARDS: basic and mildly corrosive
A. Cozzi June 2015

Technician or Researcher ______________ Date

Balance #'s ______________

ERDF Simulant 6/1/2015
08CQL3C04Y

Volume of Simulant 8000 mL 8 L

Obtain a Simulant Container larger than 8000 mL 8 L

Record mass of Simulant Container ☐ grams

Total Mass of Simulant to be prepared 8360 grams

To the container add the following in the order indicated with mixing

Compounds	Formula	Mass Needed (g)	Actual Mass (g)
Water	H2O	6129	
Calcium Nitrate Hydrate	$Ca(NO_3)_2\,4H_2O$	236.6	
Calcium Chloride	$CaCl_2$	150.5	
Magnesium Sulfate Hydrate	$MgSO_4\,7H_2O$	382.3	
Sodium Sulfate	Na_2SO_4	264.3	
Calcium Sulfate	Ca_5O_4	73.0	
Water for rinsing	H_2O	1395	

Mix thoroughly. All of the solids will not dissolve.

Continue mixing for several hours.

Record Final Gross Weight ☐ grams

Measure the Density ☐ g/mL

Measure the pH ☐

Measure wt% solids ______ dissolved

(total and dissolved) ______ total

Solution Labeling

ERDF Simulant
Hanford Cast Stone Secondary Waste

HAZARDS: acidic and mildly corrosive
A. Cozzi June 2015

Technician or Researcher ☐

Balance # ☐

Date ☐

WTP Brine Simulant

08CQL3C04Y

Volume of Simulant	4000	mL	4	L
Obtain a Simulant Container larger than	4000	mL	4	L
Record mass of Simulant Container		grams		
Total Mass of Simulant to be prepared	4500.00	grams		

To the bottle add the following in the order indicated with mixing

Compounds	Formula	Mass Needed (g)	Actual Mass (g)
Water	H_2O	3200	
Sodium Chloride	NaCl	6.4	
Sodium Fluoride	NaF	0.8	
Sodium Sulfate	Na_2SO_4	221	
Sodium Nitrate	$NaNO_3$	182	
Sodium Nitrite	$NaNO_2$	1.3	
Sodium Iodide	NaI	0.47	
Ammonium Sulfate	$(NH_4)_2SO_4$	399	
Water for rinsing	H_2O	490	

Mix thoroughly until all of the solids dissolve.

Continue mixing for several hours.

Record Final Gross Weight		grams
Measure the Density		g/mL
Measure the pH		

Solution Labeling

WTP Brine Simulant
Hanford Cast Stone Secondary Waste

HAZARDS: acidic and mildly corrosive
A. Cozzi June 2015

Technician or Researcher	
Balance #	
Date	

Appendix C. UPV Plots for All Mixes Tested

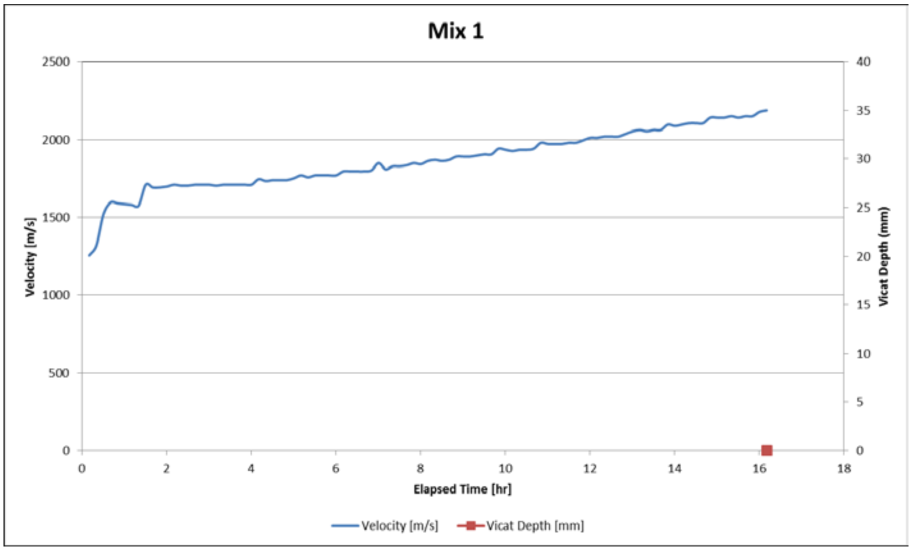
Mix 1
Velocity [m/s]
2500
2000
1500
1000
500
0
Vicat Depth (mm)
40
35
30
25
20
15
10
5
0
Elapsed Time [hr]
0
2
4
6
8
10
12
14
16
18
Velocity [m/s]
Vicat Depth [mm]

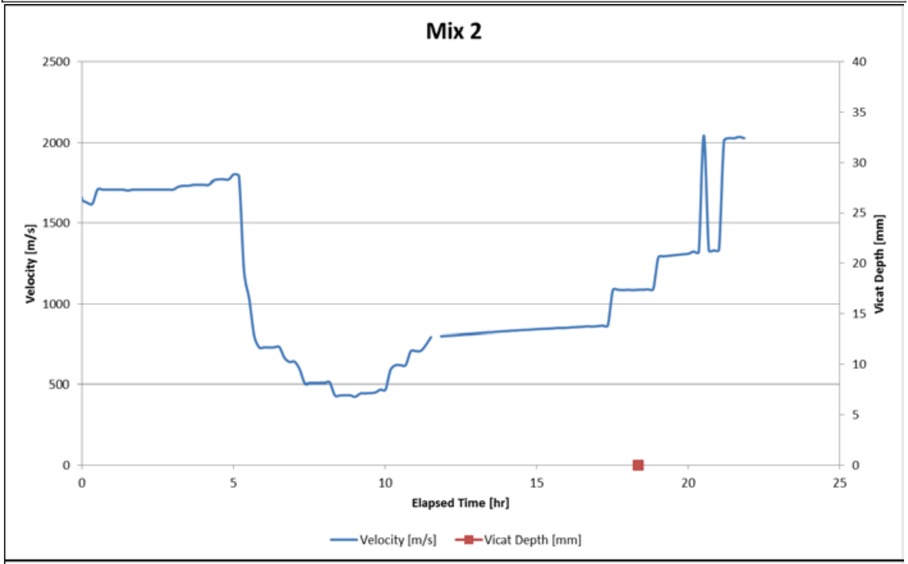
Mix 2
Velocity [m/s]
2500
2000
1500
1000
500
0
Vicat Depth [mm]
40
35
30
25
20
15
10
5
0
Elapsed Time [hr]
0
5
10
15
20
25
Velocity [m/s]
Vicat Depth [mm]

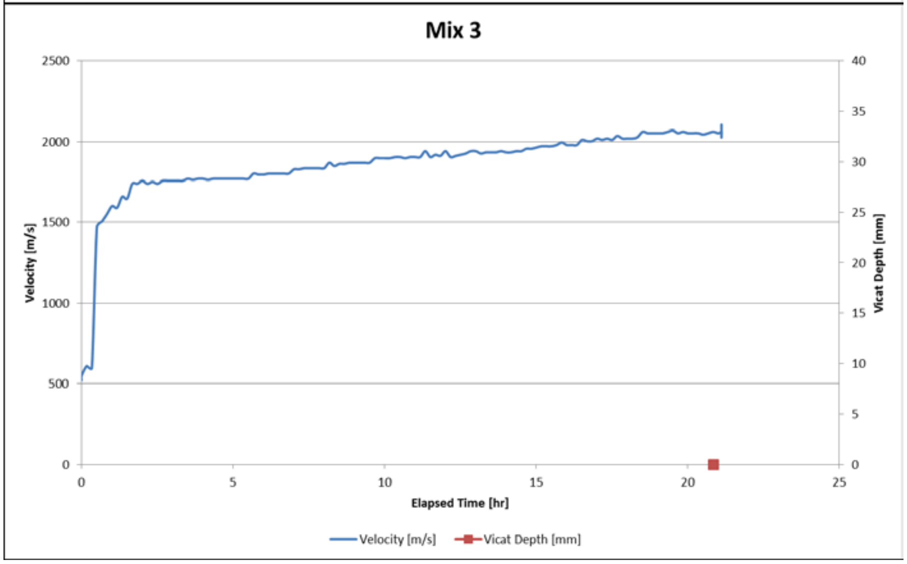
Mix 3
Velocity [m/s]
2500
2000
1500
1000
500
0
Vicat Depth (mm)
40
35
30
25
20
15
10
5
0
Elapsed Time [hr]
0
5
10
15
20
25
Velocity [m/s]
Vicat Depth [mm]

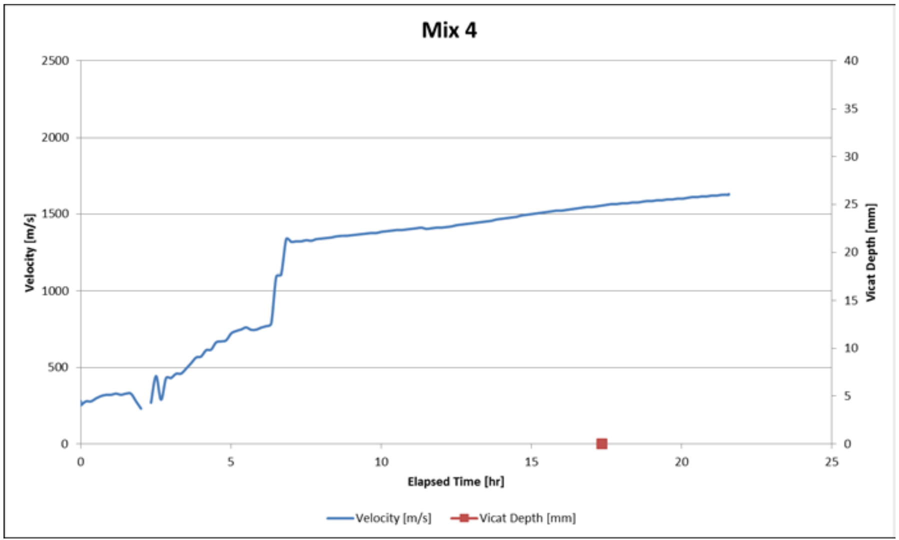
Mix 4
2500
2000
1500
1000
500
0
Velocity [m/s]
40
35
30
25
20
15
10
5
0
Vicat Depth [mm]
0
5
10
15
20
25
Elapsed Time [hr]
Velocity [m/s]
Vicat Depth [mm]

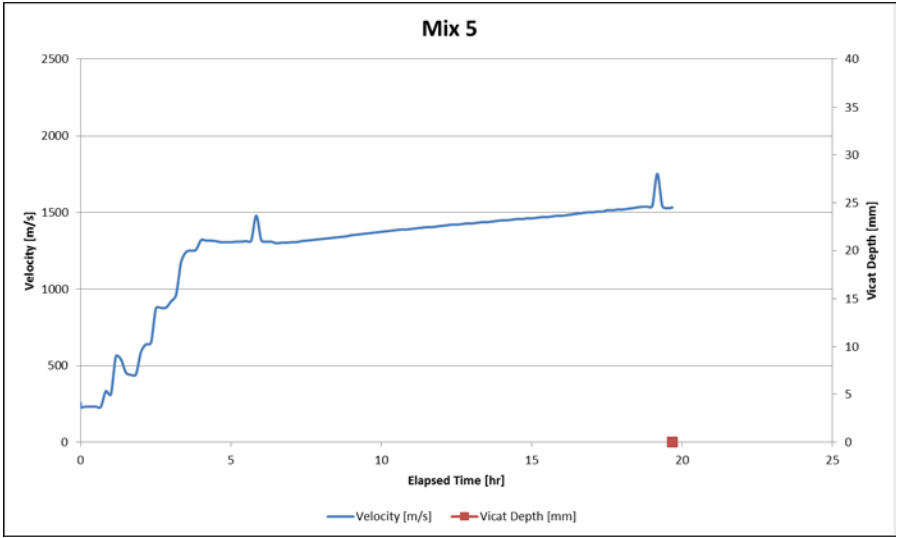
Mix 5
2500
2000
1500
1000
500
0
Velocity [m/s]
40
35
30
25
20
15
10
5
0
Vicat Depth [mm]
0
5
10
15
20
25
Elapsed Time [hr]
Velocity [m/s]
Vicat Depth [mm]

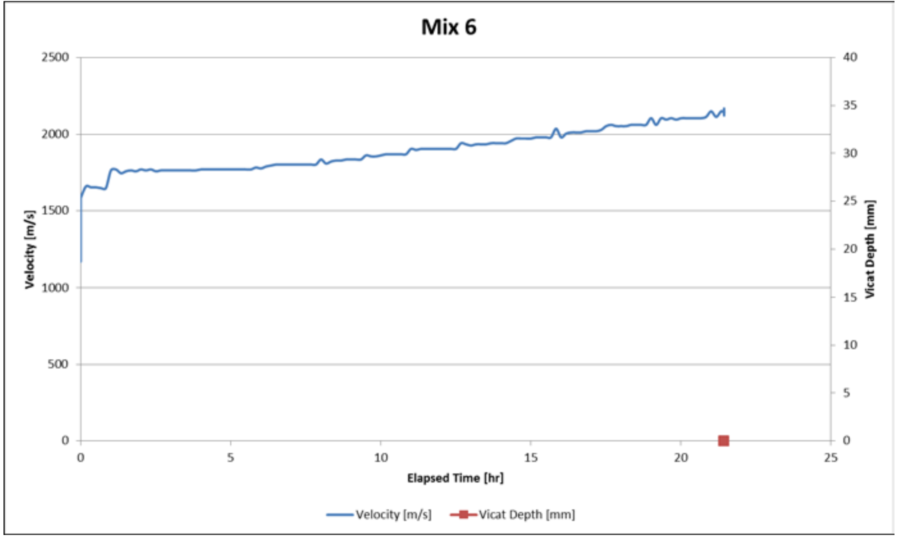
Mix 6
2500
2000
1500
1000
500
0
Velocity [m/s]
40
35
30
25
20
15
10
5
0
Vicat Depth [mm]
0
5
10
15
20
25
Elapsed Time [hr]
Velocity [m/s]
Vicat Depth [mm]

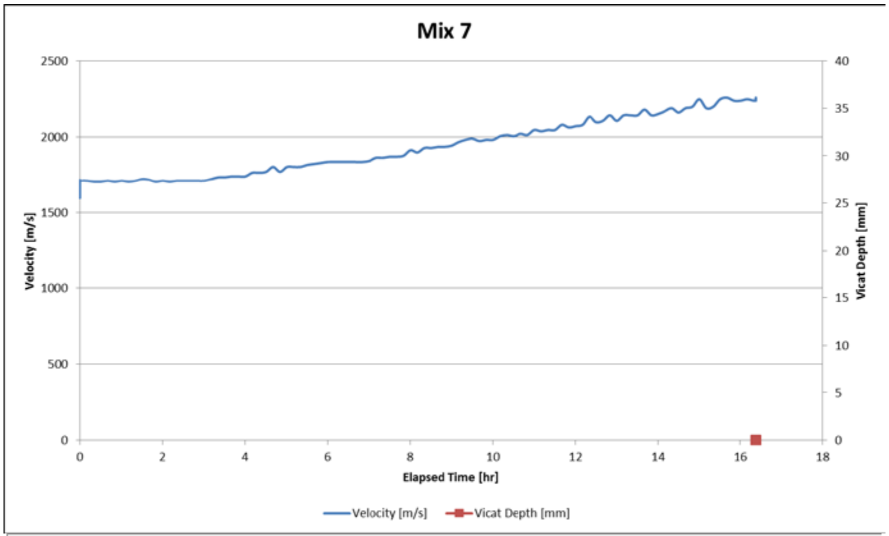
Mix 7
Velocity [m/s]
Vicat Depth [mm]
Elapsed Time [hr]
0
500
1000
1500
2000
2500
0
5
10
15
20
25
30
35
40
0
2
4
6
8
10
12
14
16
18
Velocity [m/s]
Vicat Depth [mm]

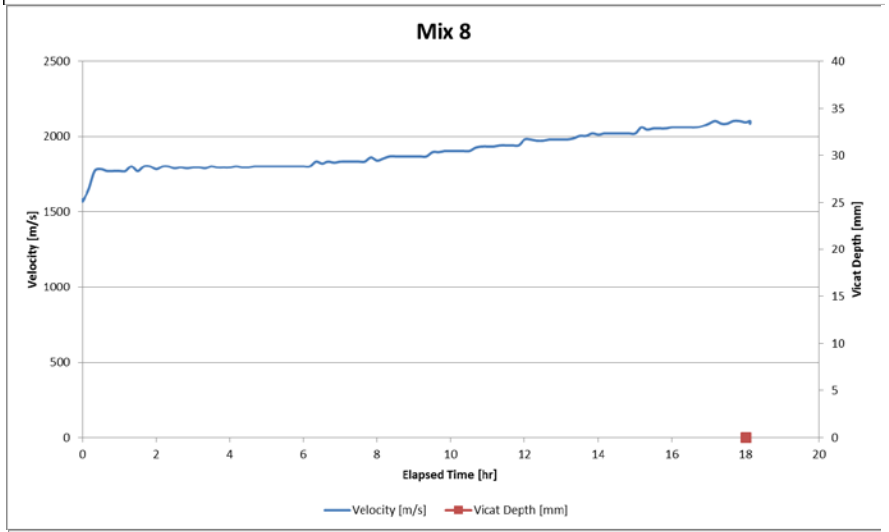
Mix 8
Velocity [m/s]
Vicat Depth [mm]
Elapsed Time [hr]
0
500
1000
1500
2000
2500
0
5
10
15
20
25
30
35
40
0
2
4
6
8
10
12
14
16
18
20
Velocity [m/s]
Vicat Depth [mm]

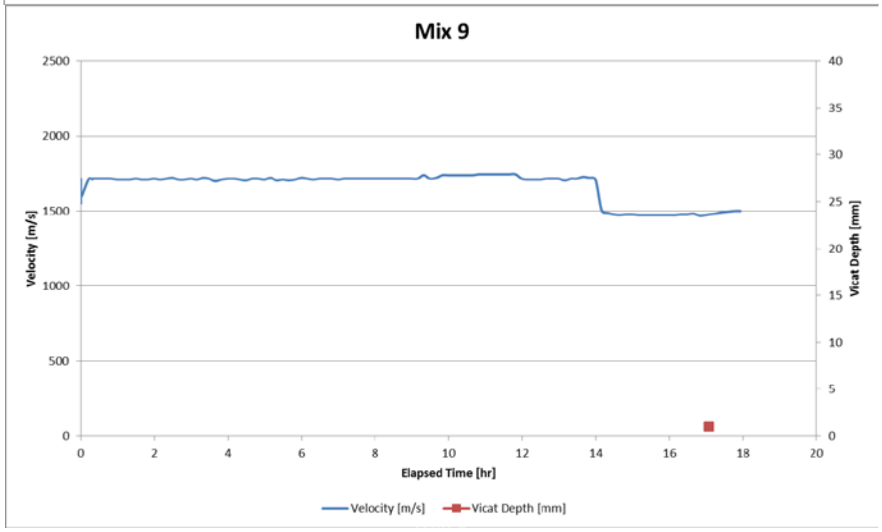
Mix 9
Velocity [m/s]
Vicat Depth [mm]
Elapsed Time [hr]
0
500
1000
1500
2000
2500
0
5
10
15
20
25
30
35
40
0
2
4
6
8
10
12
14
16
18
20
Velocity [m/s]
Vicat Depth [mm]

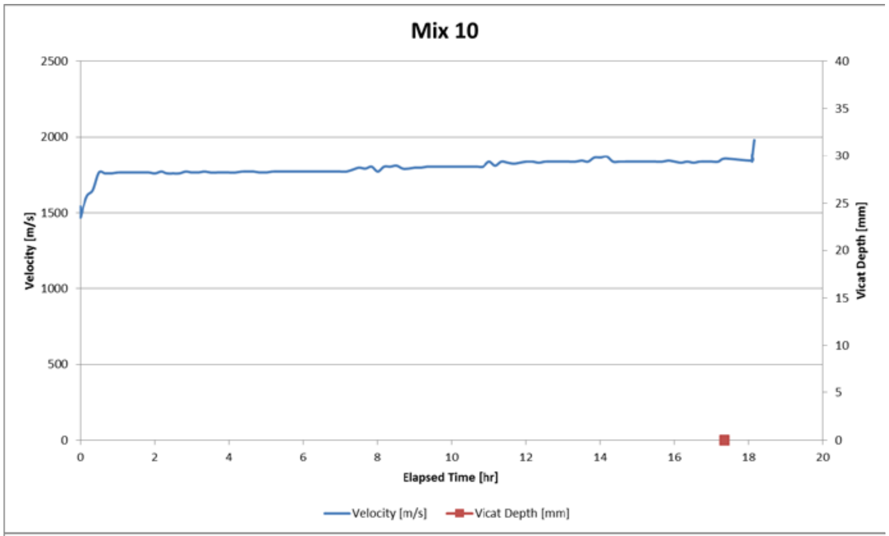
Mix 10
Velocity [m/s]
Vicat Depth [mm]
Elapsed Time [hr]
0
500
1000
1500
2000
2500
0
5
10
15
20
25
30
35
40
0
2
4
6
8
10
12
14
16
18
20
Velocity [m/s]
Vicat Depth [mm]

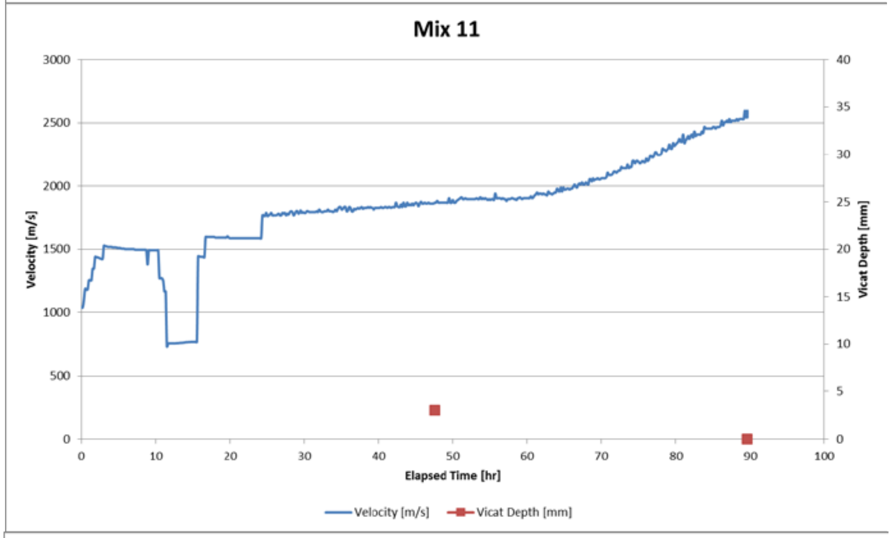
Mix 11
Velocity [m/s]
Vicat Depth [mm]
Elapsed Time [hr]
0
500
1000
1500
2000
2500
3000
0
5
10
15
20
25
30
35
40
0
10
20
30
40
50
60
70
80
90
100
Velocity [m/s]
Vicat Depth [mm]

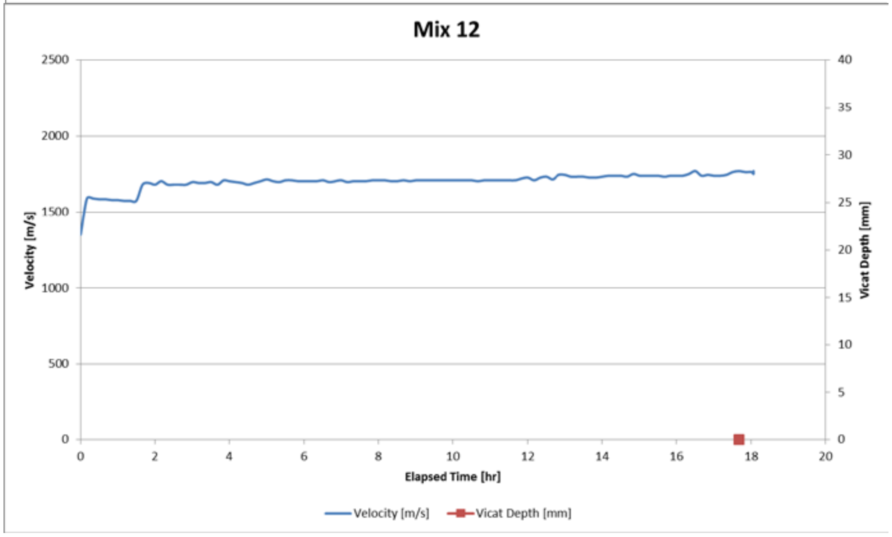
Mix 12
Velocity [m/s]
Vicat Depth [mm]
Elapsed Time [hr]
0
500
1000
1500
2000
2500
0
5
10
15
20
25
30
35
40
0
2
4
6
8
10
12
14
16
18
20
Velocity [m/s]
Vicat Depth [mm]

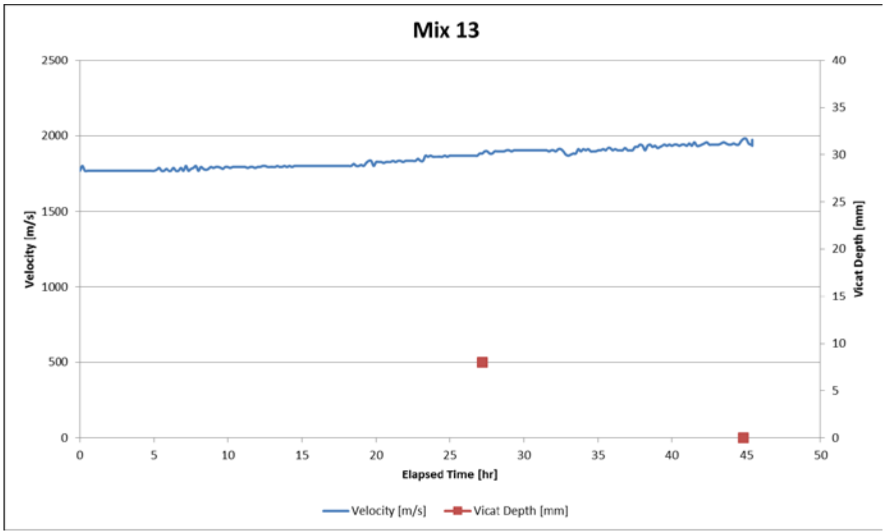
Mix 13
Velocity [m/s]
2500
2000
1500
1000
500
0
Vicat Depth [mm]
40
35
30
25
20
15
10
5
0
Elapsed Time [hr]
0
5
10
15
20
25
30
35
40
45
50
Velocity [m/s]
Vicat Depth [mm]

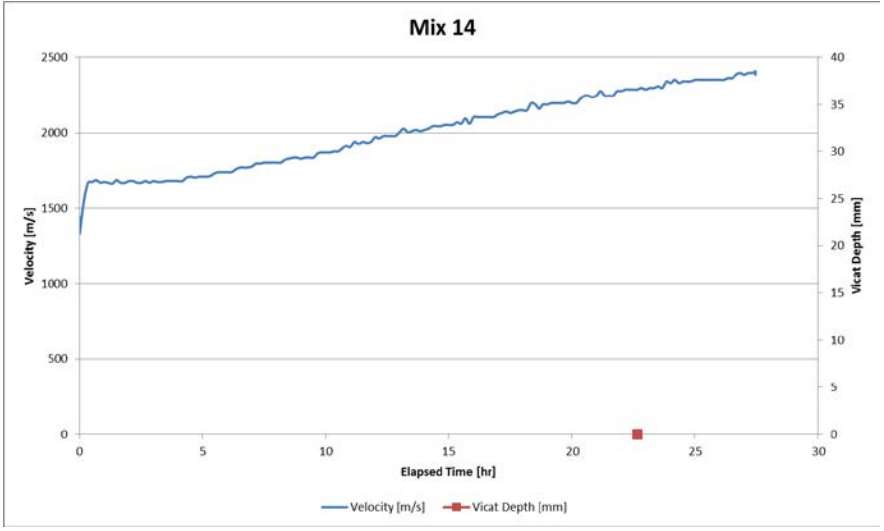
Mix 14
Velocity [m/s]
2500
2000
1500
1000
500
0
Vicat Depth [mm]
40
35
30
25
20
15
10
5
0
Elapsed Time [hr]
0
5
10
15
20
25
30
Velocity [m/s]
Vicat Depth [mm]

Appendix D. Rheograms for All Mixes Tested.

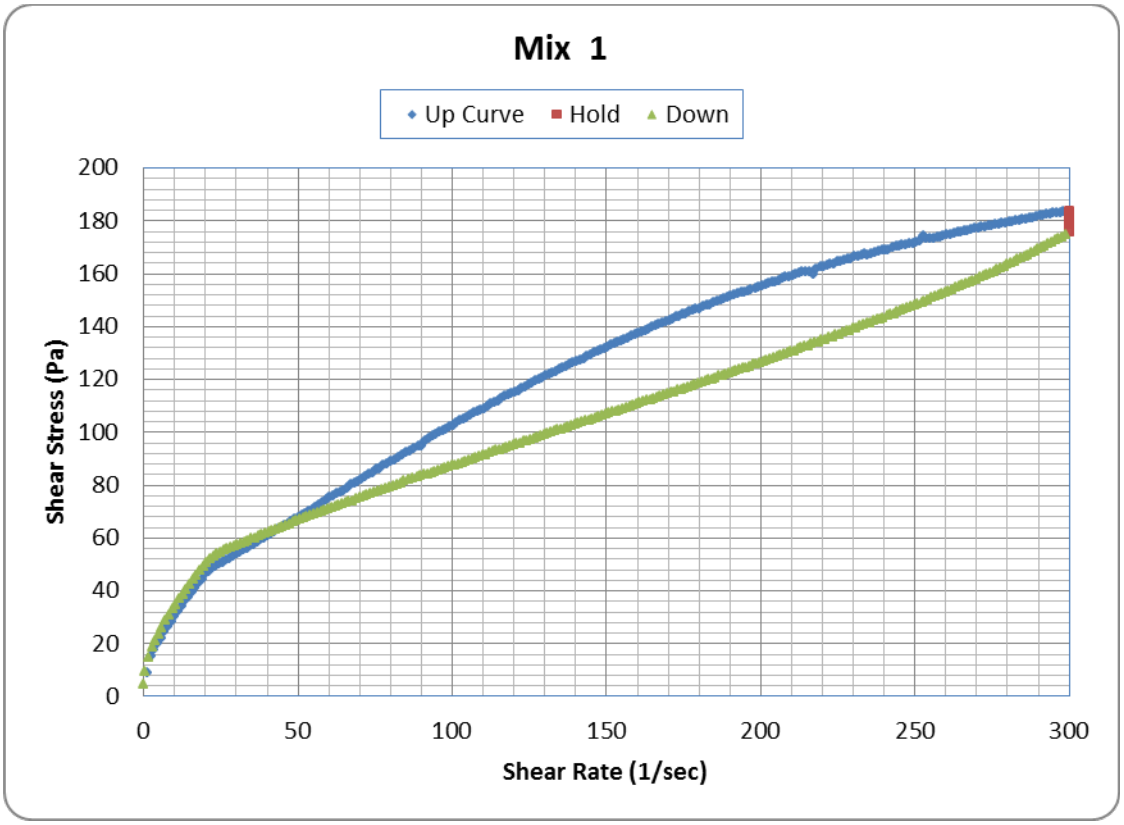
Mix 1
Up Curve
Hold
Down
Shear Stress (Pa)
0
20
40
60
80
100
120
140
160
180
200
0
50
100
150
200
250
300
Shear Rate (1/sec)

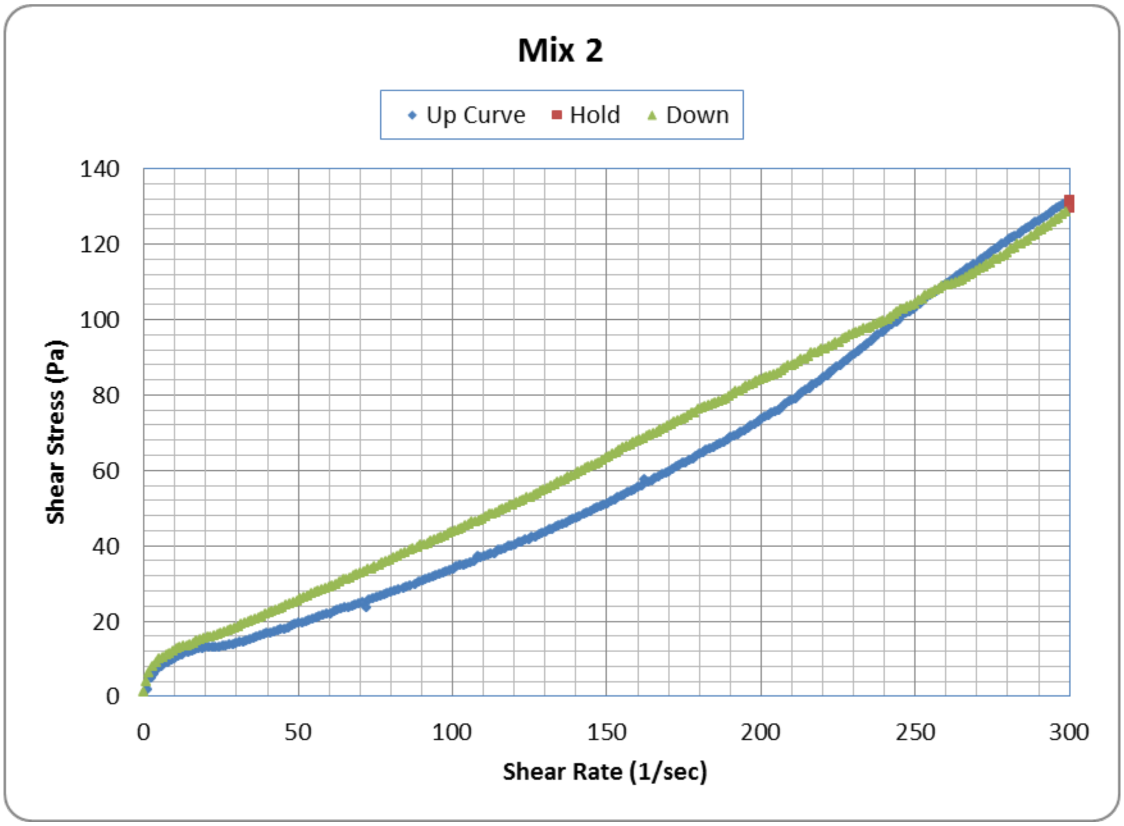
Mix 2
Up Curve
Hold
Down
Shear Stress (Pa)
0
20
40
60
80
100
120
140
0
50
100
150
200
250
300
Shear Rate (1/sec)

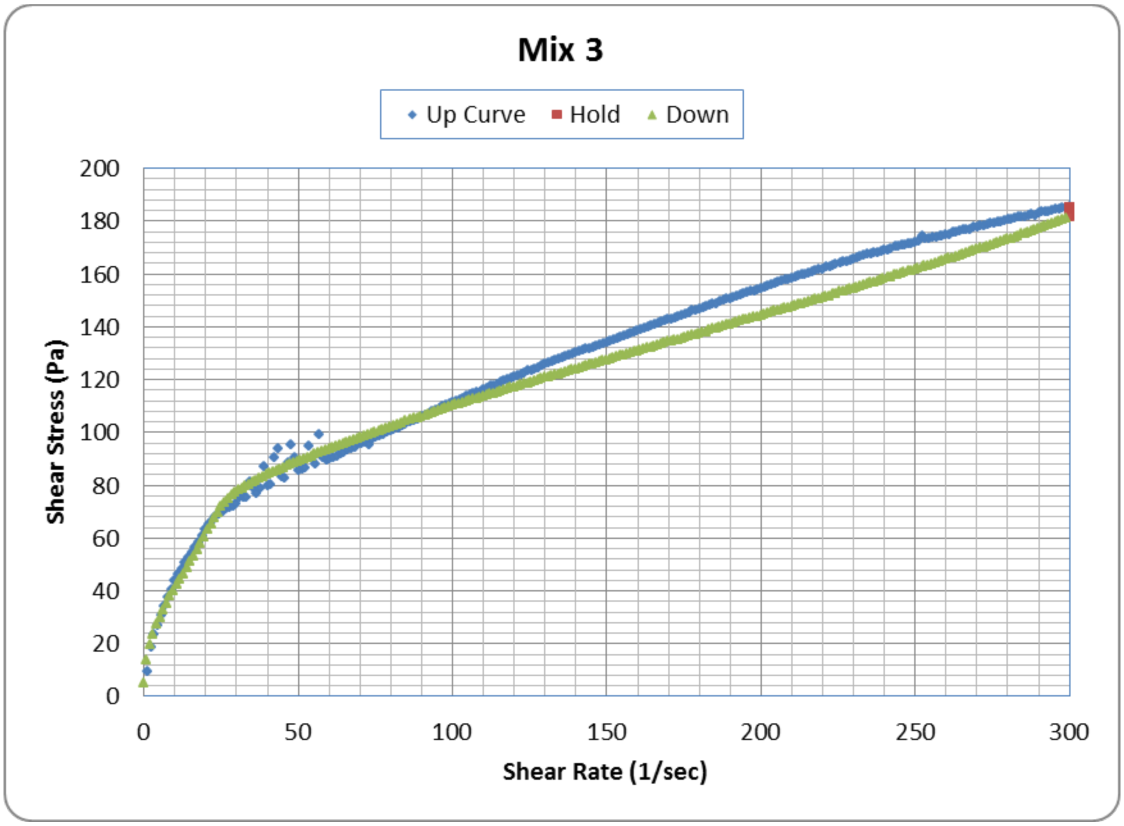
Mix 3
◆ Up Curve
■ Hold
▲ Down
Shear Stress (Pa)
200
180
160
140
120
100
80
60
40
20
0
0
50
100
150
200
250
300
Shear Rate (1/sec)

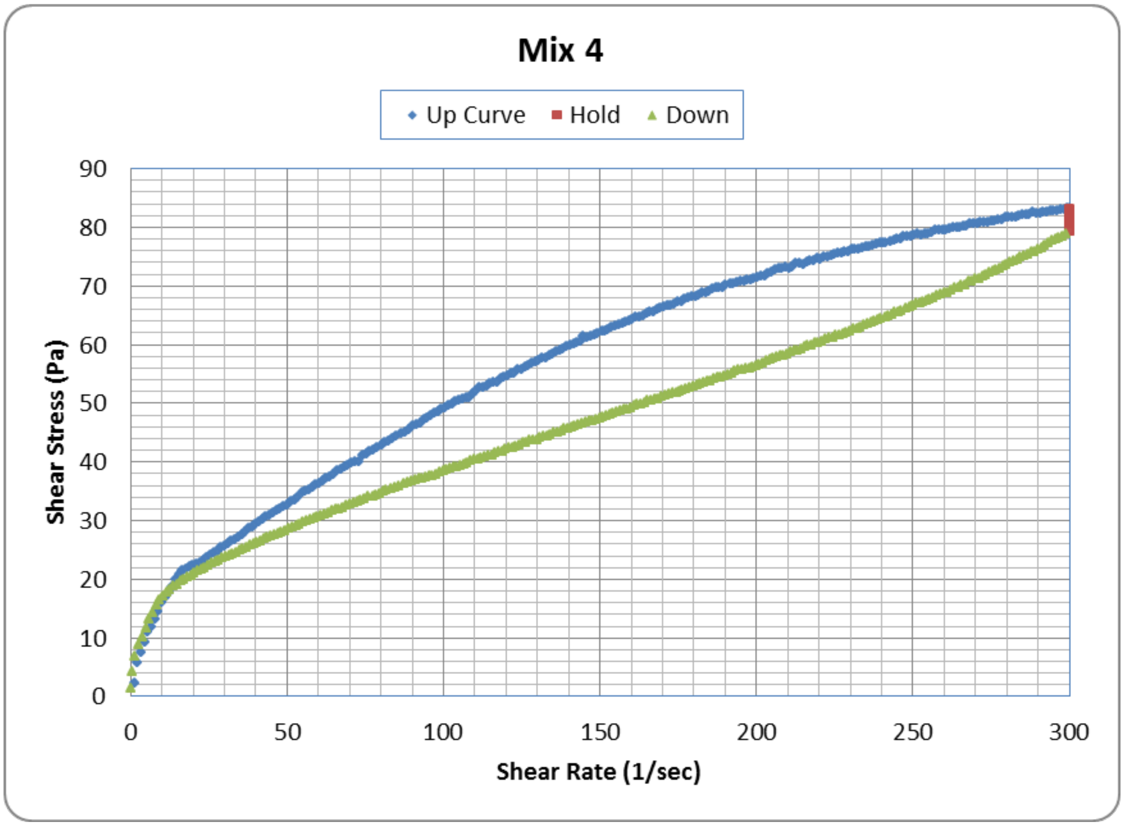
Mix 4
◆ Up Curve
■ Hold
▲ Down
Shear Stress (Pa)
90
80
70
60
50
40
30
20
10
0
0
50
100
150
200
250
300
Shear Rate (1/sec)

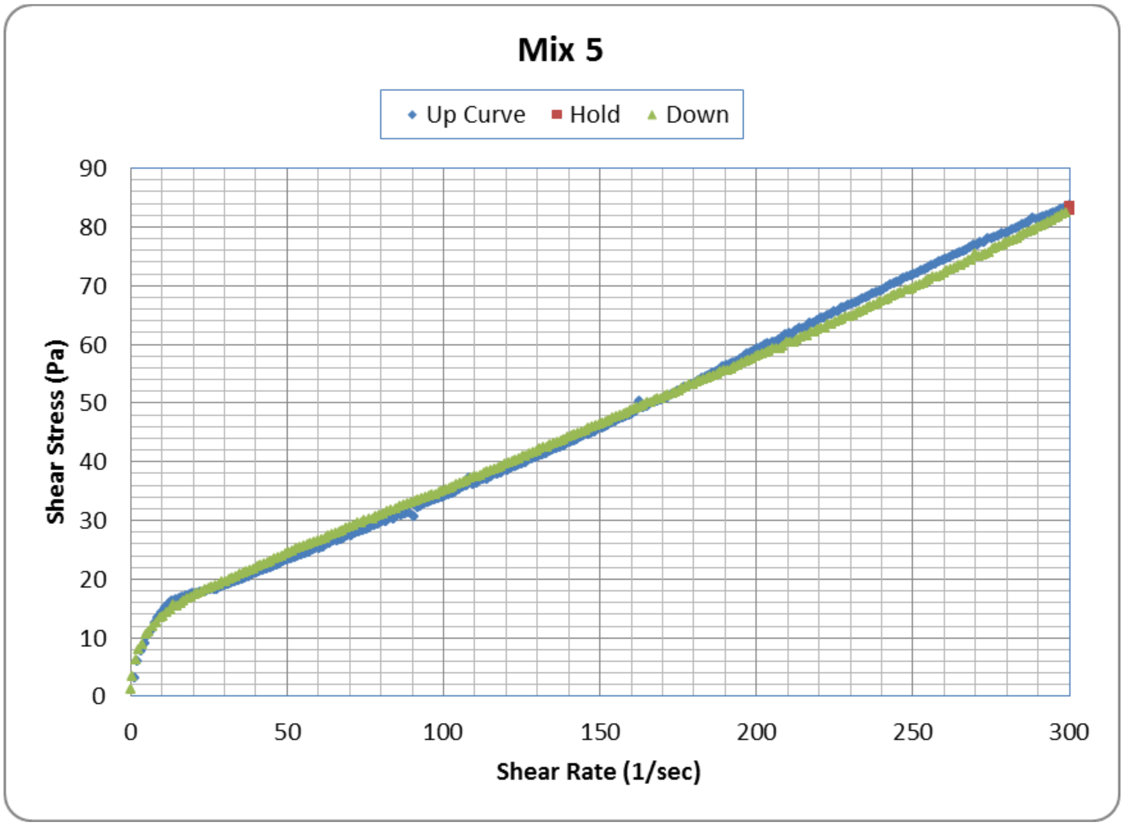
Mix 5
Up Curve
Hold
Down
Shear Stress (Pa)
Shear Rate (1/sec)
0
10
20
30
40
50
60
70
80
90
0
50
100
150
200
250
300

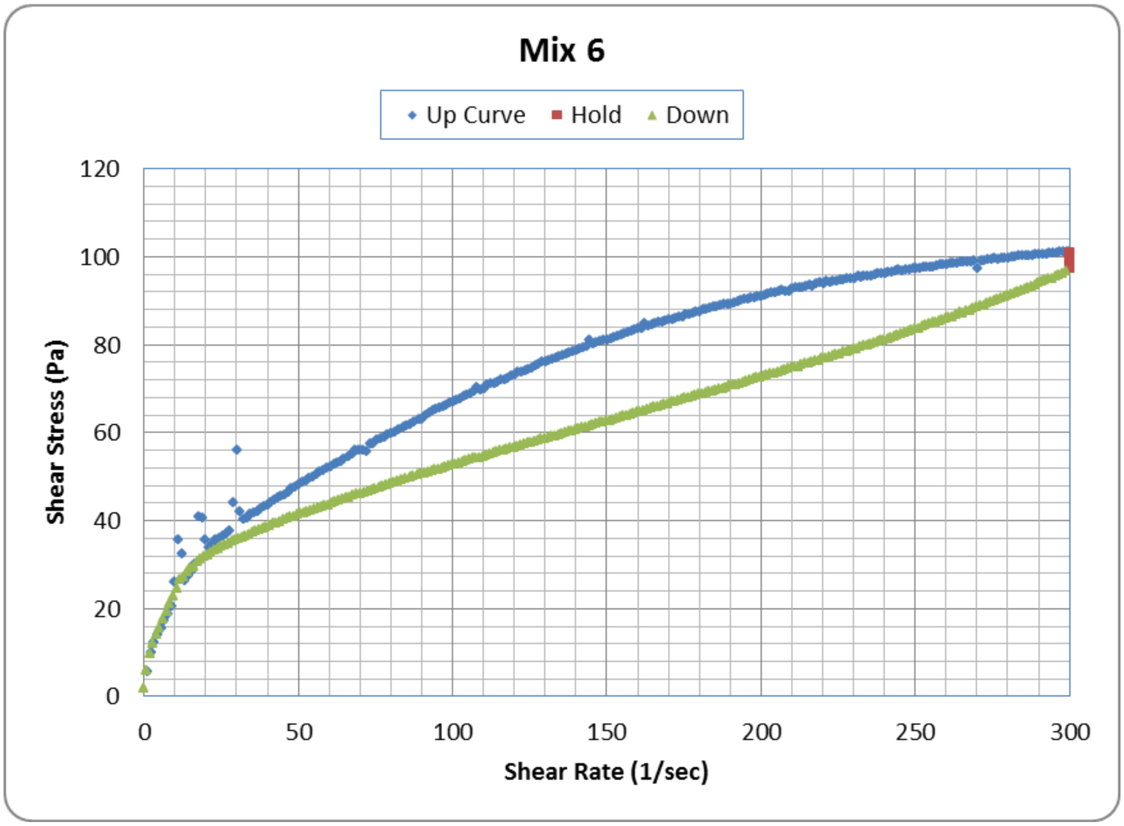
Mix 6
Up Curve
Hold
Down
Shear Stress (Pa)
Shear Rate (1/sec)
0
20
40
60
80
100
120
0
50
100
150
200
250
300

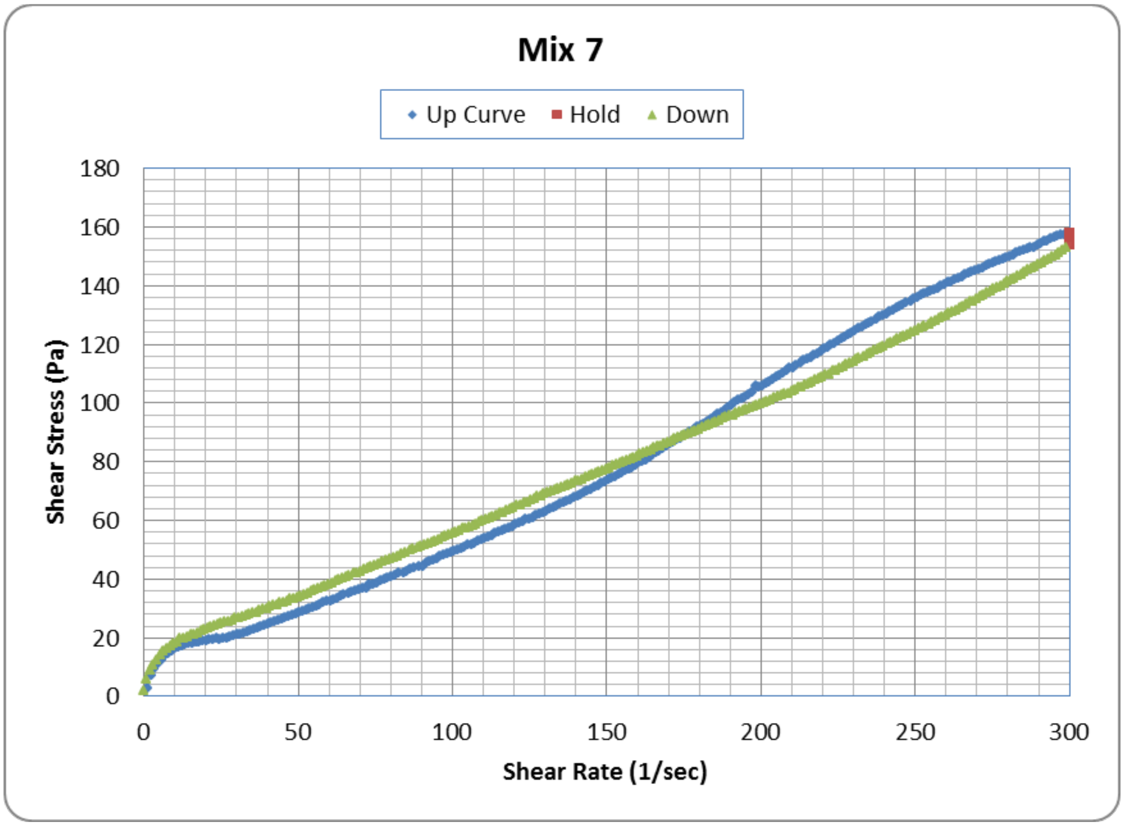
Mix 7
◆ Up Curve
■ Hold
▲ Down
Shear Stress (Pa)
180
160
140
120
100
80
60
40
20
0
0
50
100
150
200
250
300
Shear Rate (1/sec)

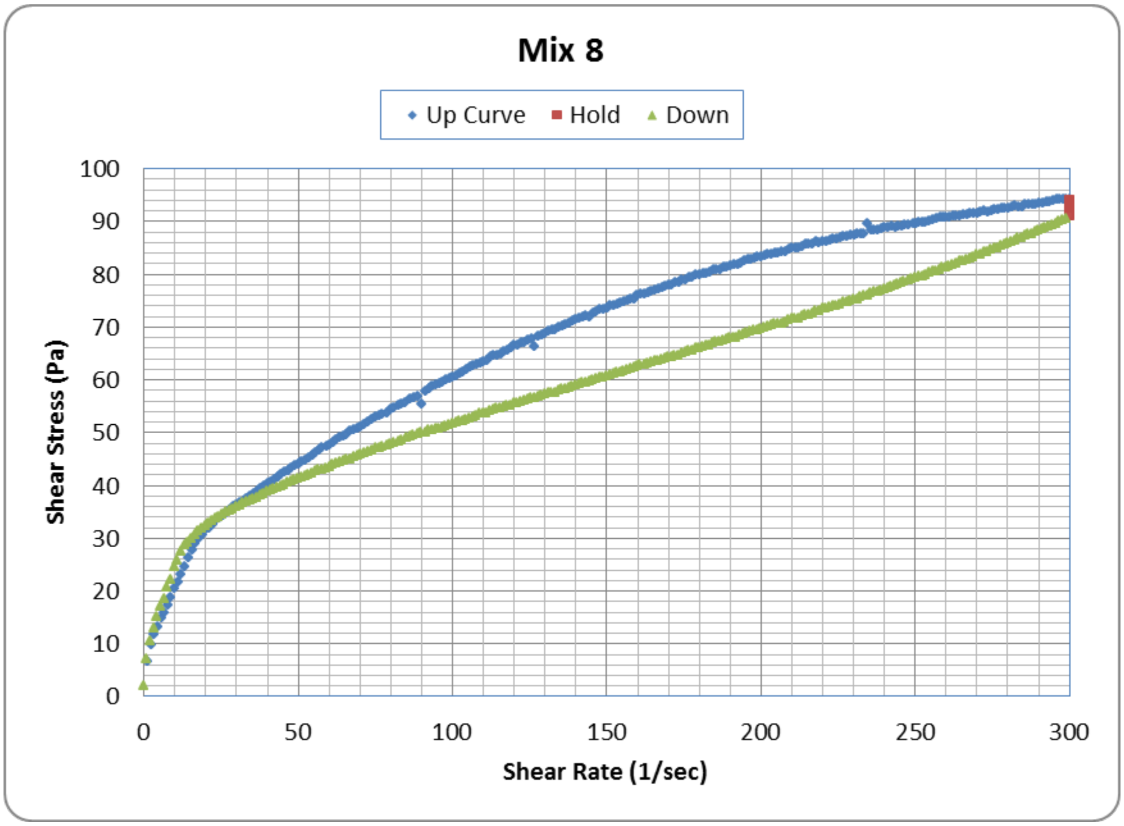
Mix 8
◆ Up Curve
■ Hold
▲ Down
Shear Stress (Pa)
100
90
80
70
60
50
40
30
20
10
0
0
50
100
150
200
250
300
Shear Rate (1/sec)

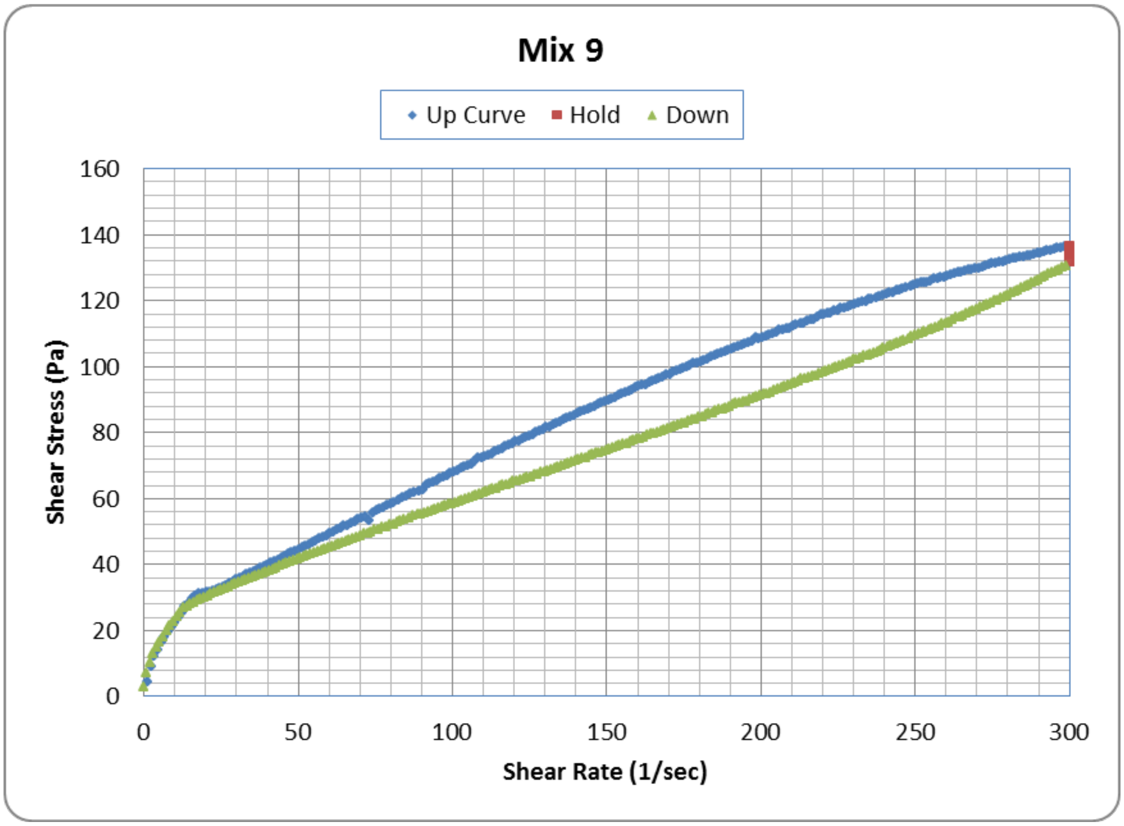
Mix 9
Up Curve
Hold
Down
Shear Stress (Pa)
160
140
120
100
80
60
40
20
0
0
50
100
150
200
250
300
Shear Rate (1/sec)

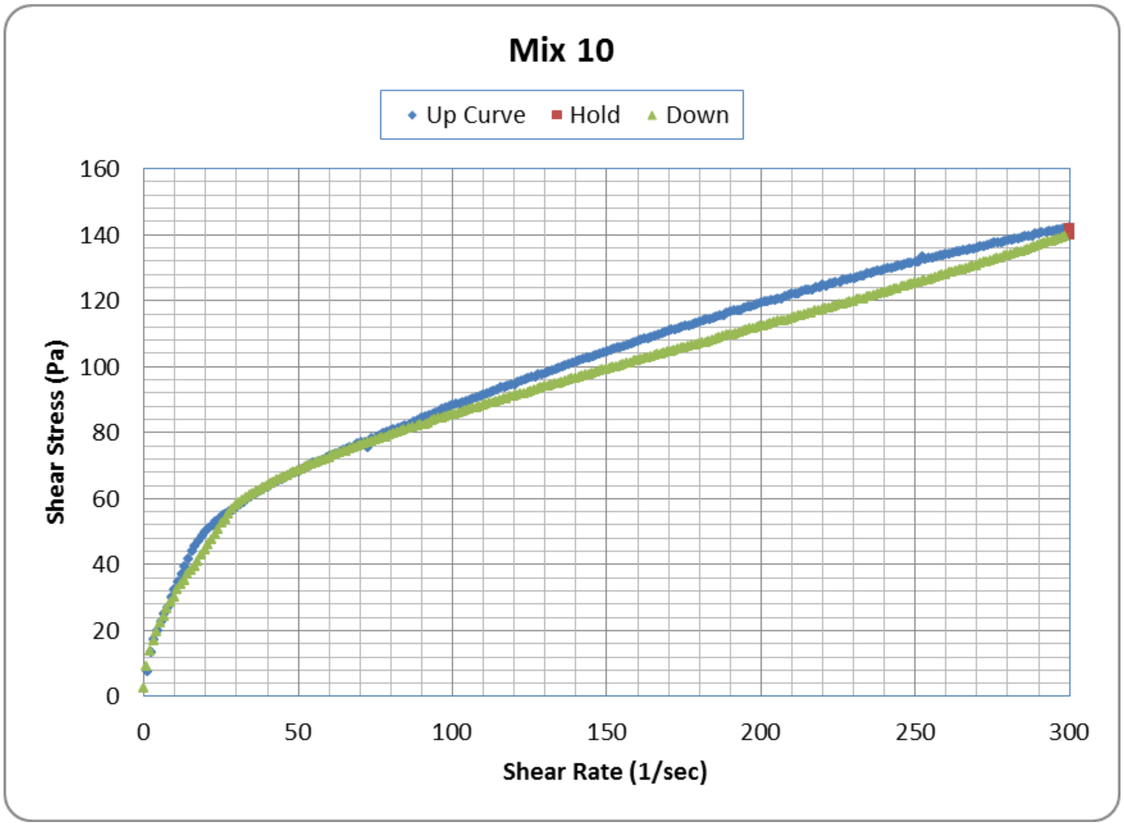
Mix 10
Up Curve
Hold
Down
Shear Stress (Pa)
160
140
120
100
80
60
40
20
0
0
50
100
150
200
250
300
Shear Rate (1/sec)

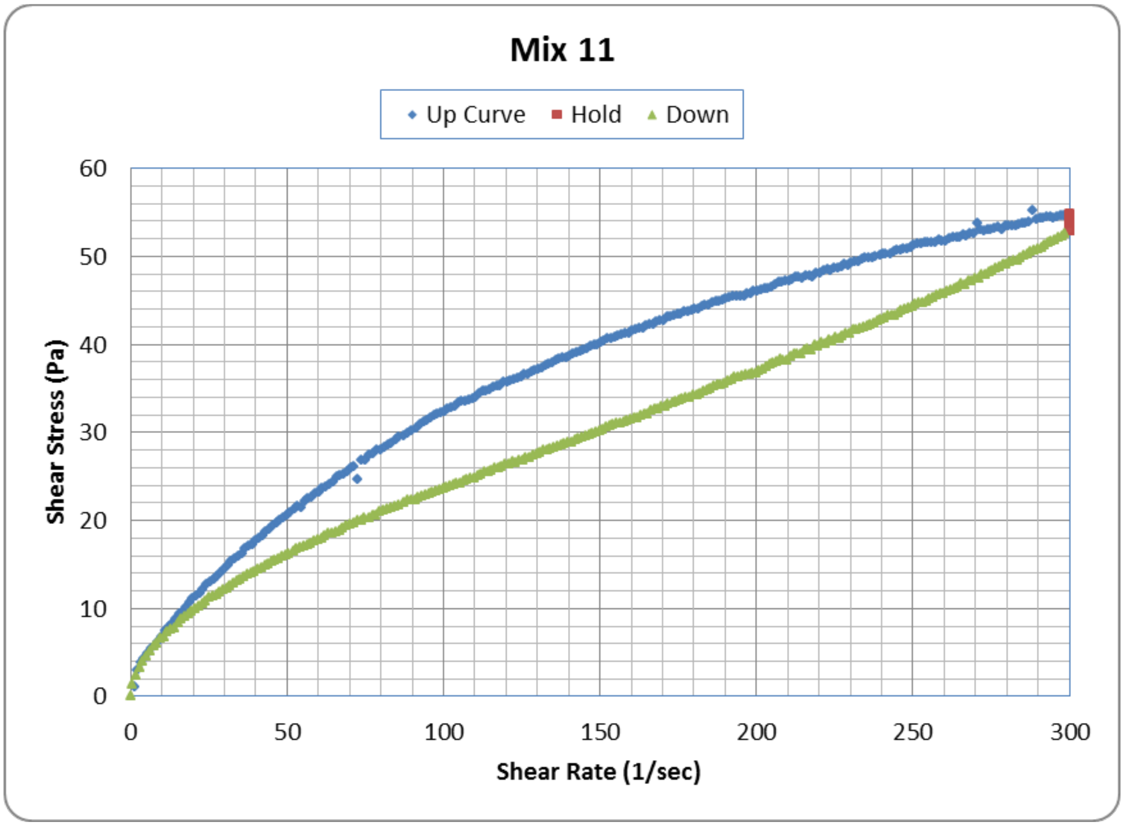
Mix 11
Up Curve
Hold
Down
Shear Stress (Pa)
60
50
40
30
20
10
0
0
50
100
150
200
250
300
Shear Rate (1/sec)

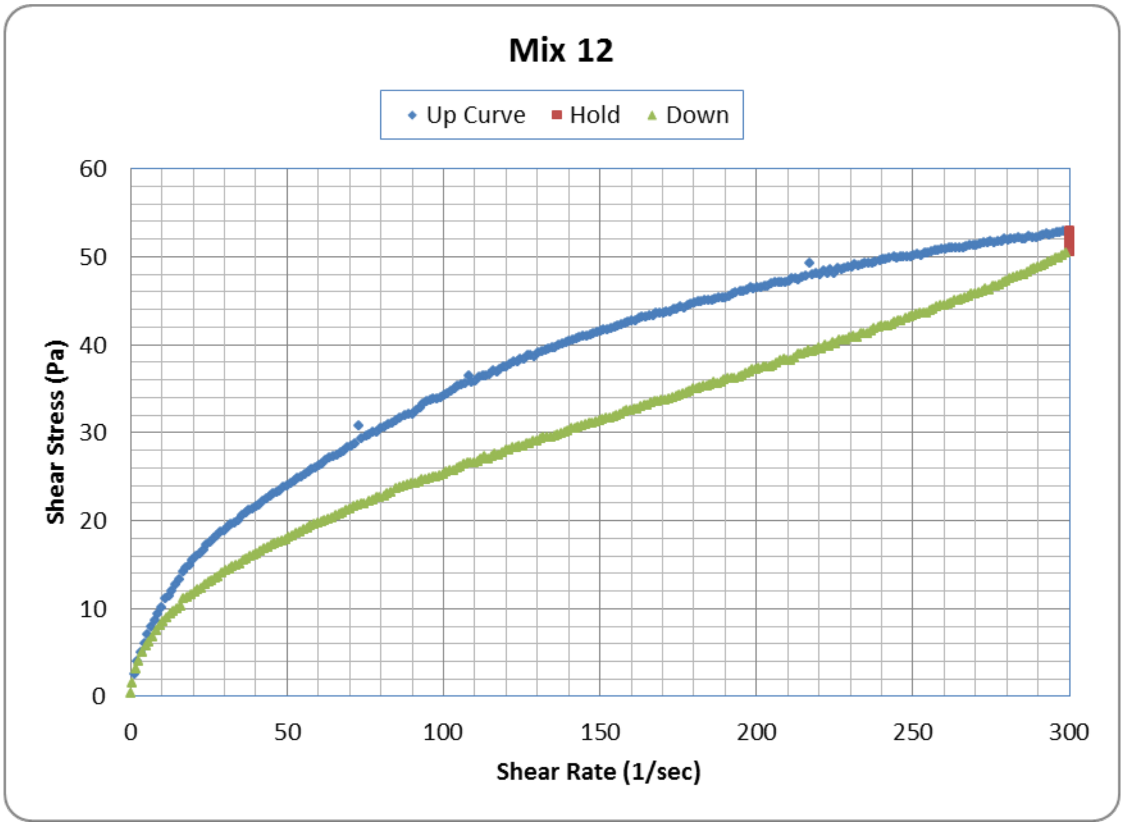
Mix 12
Up Curve
Hold
Down
Shear Stress (Pa)
60
50
40
30
20
10
0
0
50
100
150
200
250
300
Shear Rate (1/sec)

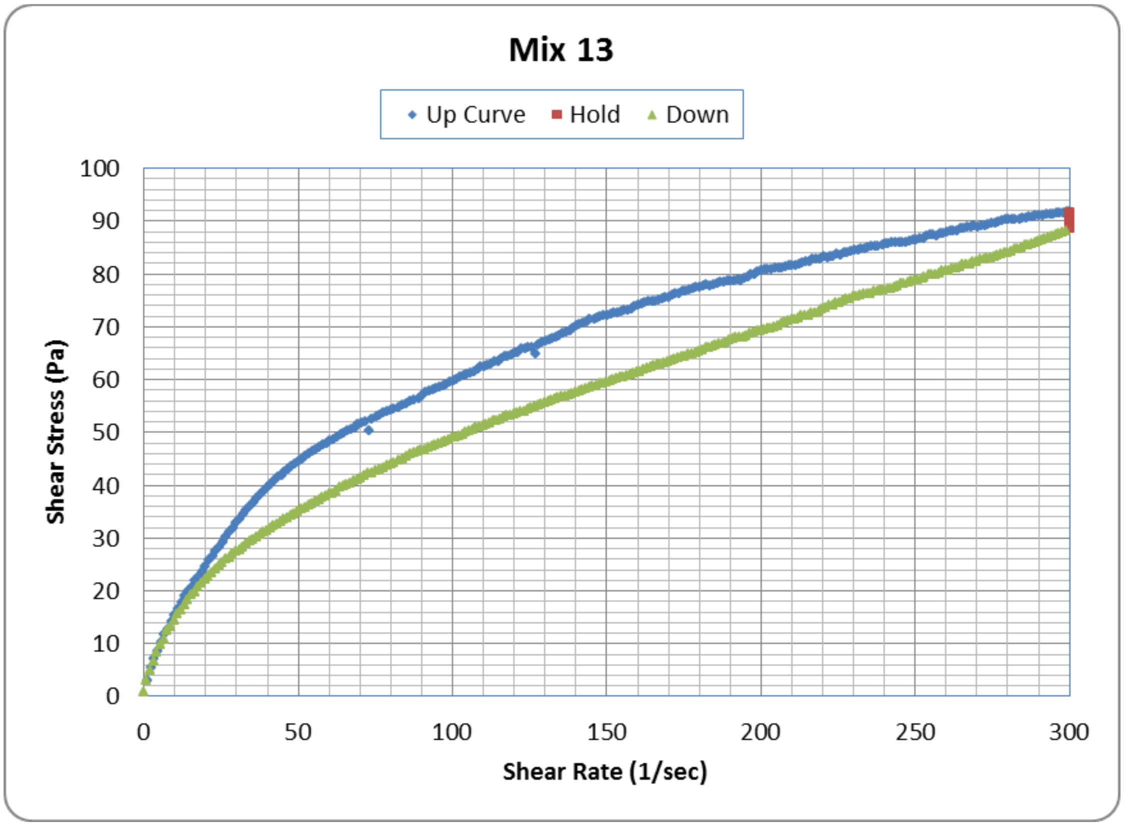
Mix 13
Up Curve
Hold
Down
Shear Stress (Pa)
100
90
80
70
60
50
40
30
20
10
0
0
50
100
150
200
250
300
Shear Rate (1/sec)

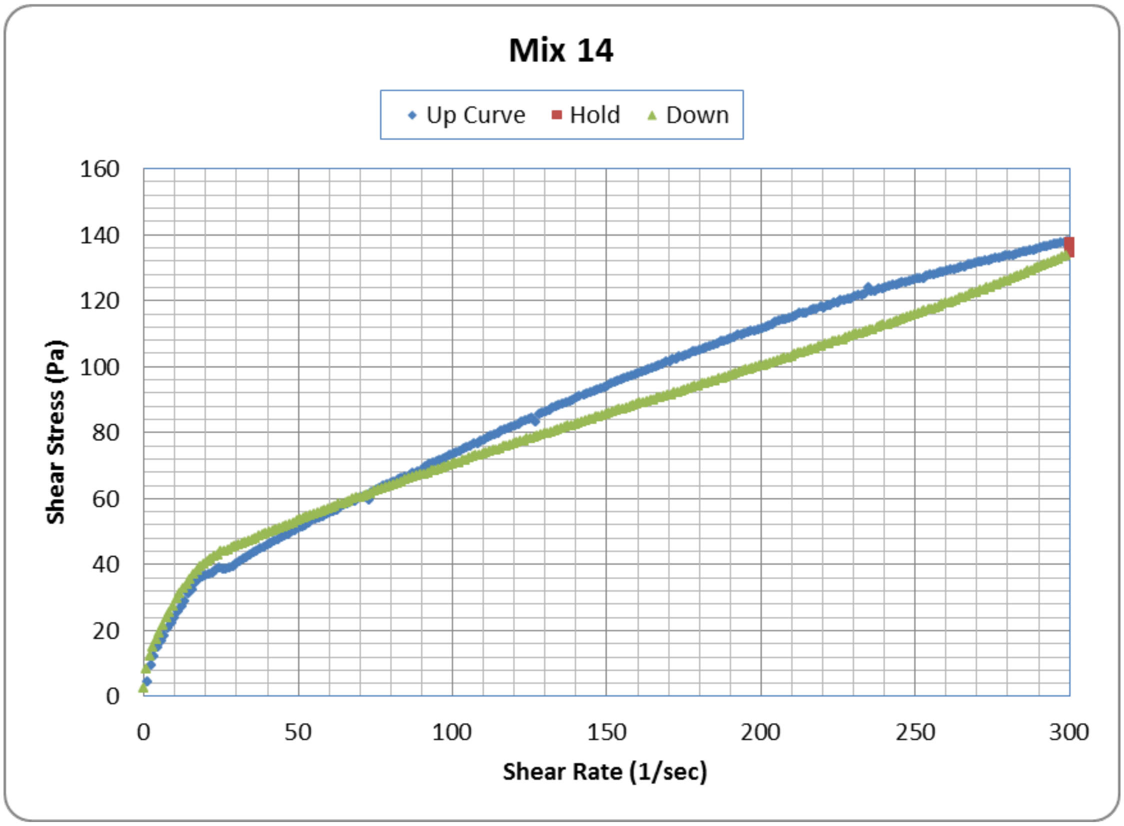
Mix 14
Up Curve
Hold
Down
Shear Stress (Pa)
160
140
120
100
80
60
40
20
0
0
50
100
150
200
250
300
Shear Rate (1/sec)

Appendix E. Moisture Retention Data Measured using a Chilled Mirror Humidity Sensor

Sample ID	Gravimetric Moisture Content (cm^3/cm^3)	Volumetric Moisture Content (cm^3/cm^3)	Saturation (fraction)	Total Potential (bar)	Total Potential (cm H_2O)
6-1-1	0.4518	0.5421	0.96	129.80	132362.8
11-1-1	0.4335	0.5159	0.89	86.63	88343.8
6-2-1	0.4235	0.5082	0.90	149.27	152213.8
11-2-1	0.4216	0.5017	0.87	92.07	93884.5
3-2-1	0.3702	0.4849	0.92	206.40	210475.2
3-1-1	0.3330	0.4362	0.83	315.30	321525.4
6-1-1	0.3631	0.4357	0.77	288.10	293788.3
11-1-1	0.3477	0.4138	0.72	299.50	305413.4
6-2-1	0.3353	0.4023	0.71	329.90	336413.6
3-2-1	0.2851	0.3734	0.71	412.60	420746.5
11-2-1	0.3057	0.3637	0.63	327.40	333864.3
6-1-1	0.2795	0.3354	0.59	513.00	523128.8
3-1-1	0.2486	0.3256	0.62	521.10	531388.7
11-1-1	0.2704	0.3218	0.56	455.40	464391.5
6-2-1	0.2649	0.3179	0.56	506.20	516194.6
11-2-1	0.2587	0.3078	0.53	484.00	493556.2
3-2-1	0.2165	0.2836	0.54	639.50	652126.5
6-1-1	0.2194	0.2632	0.47	796.40	812124.4
6-2-1	0.2111	0.2533	0.45	824.50	840779.2
11-1-1	0.2114	0.2516	0.43	739.10	753693.0
3-1-1	0.1881	0.2464	0.47	885.00	902473.7
11-2-1	0.2046	0.2434	0.42	744.70	759403.6
3-2-1	0.1722	0.2255	0.43	998.80	1018520.6
6-1-1	0.1497	0.1796	0.32	1501.90	1531553.9
6-2-1	0.1471	0.1766	0.31	1444.80	1473326.5
11-1-1	0.1384	0.1647	0.28	1383.40	1410714.2
3-1-1	0.1244	0.1630	0.31	1778.60	1813717.2
11-2-1	0.1364	0.1624	0.28	1352.00	1378694.3
3-2-1	0.1226	0.1606	0.30	1657.00	1689716.3

Exhibit E-1. Moisture Retention Data - Drying

Sample ID	Gravimetric Moisture Content (cm^3/cm^3)	Volumetric Moisture Content (cm^3/cm^3)	Saturation (fraction)	Total Potential (bar)	Total Potential (cm H_2O)
11-1-1	0.4663	0.5549	0.96	42.50	43339.1
11-2-1	0.4652	0.5536	0.96	39.80	40585.8
6-1-1	0.4247	0.5096	0.90	88.00	89737.5
6-2-1	0.3957	0.4749	0.84	98.30	100240.9
3-2-1	0.3499	0.4583	0.87	122.20	124612.8
3-1-1	0.3443	0.4510	0.85	125.20	127672.0
11-2-1	0.3681	0.4380	0.76	79.80	81375.6
11-1-1	0.3675	0.4373	0.76	95.00	96875.7
6-1-1	0.3221	0.3865	0.68	169.90	173254.6
6-2-1	0.2931	0.3517	0.62	223.50	227912.8
3-1-1	0.2550	0.3340	0.63	264.30	269518.4
3-2-1	0.2501	0.3277	0.62	295.50	301334.4
11-1-1	0.2750	0.3272	0.57	199.60	203541.0
11-2-1	0.2692	0.3204	0.55	200.10	204050.8
6-1-1	0.2288	0.2746	0.49	372.10	379446.8
3-1-1	0.1685	0.2207	0.42	569.70	580948.3
6-2-1	0.1807	0.2168	0.38	570.70	581968.1
11-1-1	0.1796	0.2137	0.37	501.40	511299.8
3-2-1	0.1576	0.2064	0.39	635.50	648047.5
11-2-1	0.1699	0.2022	0.35	546.70	557494.2
6-1-1	0.1379	0.1655	0.29	748.20	762972.7

Exhibit E-2. Moisture Retention Data - Wetting

Appendix F. X-Ray Diffractograms for All Mixes Tested

Mix 1

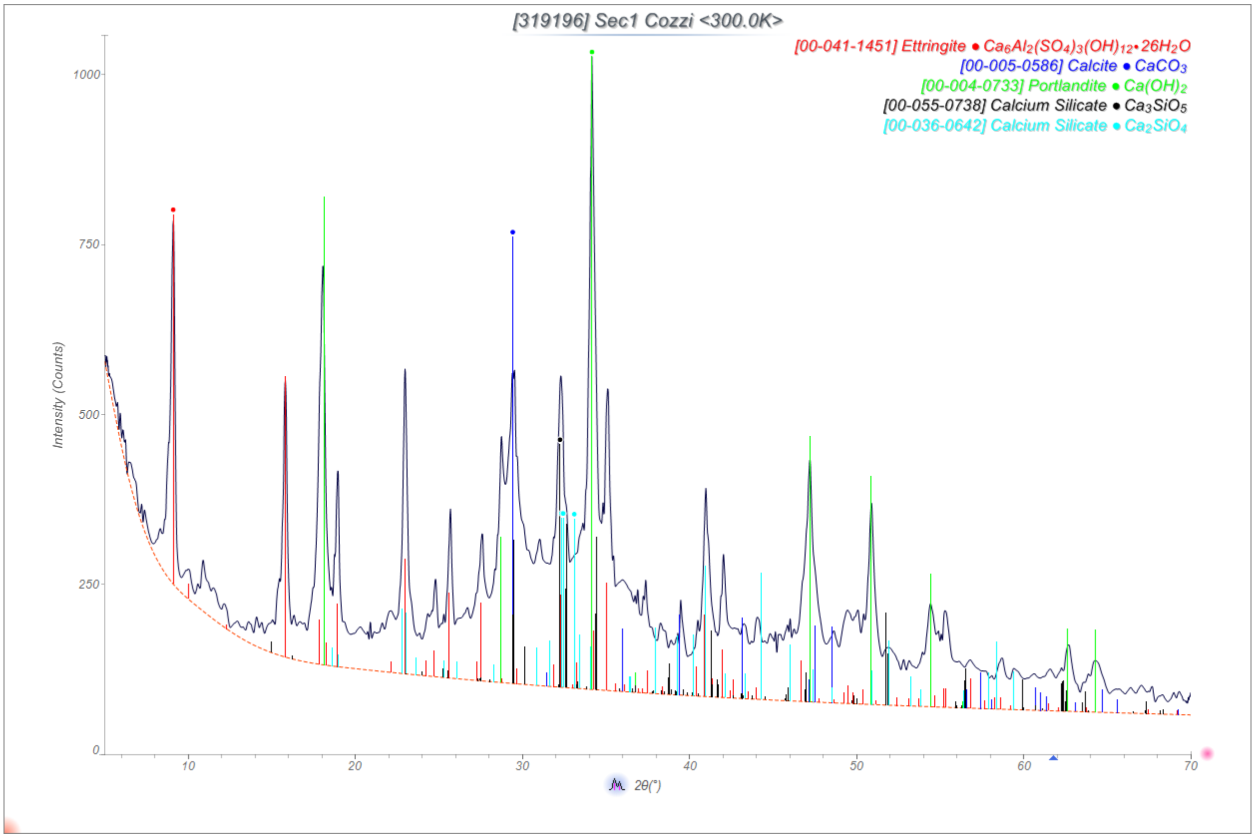
[319196] Sec1 Cozzi <300.0K>
[00-041-1451] Ettringite • $Ca_6Al_2(SO_4)_3(OH)_{12}\cdot 26H_2O$
[00-005-0586] Calcite • $CaCO_3$
[00-004-0733] Portlandite • $Ca(OH)_2$
[00-055-0738] Calcium Silicate • Ca_3SiO_5
[00-036-0642] Calcium Silicate • Ca_2SiO_4
Intensity (Counts)
0
250
500
750
1000
10
20
30
40
50
60
70
2θ(°)

Mix 2

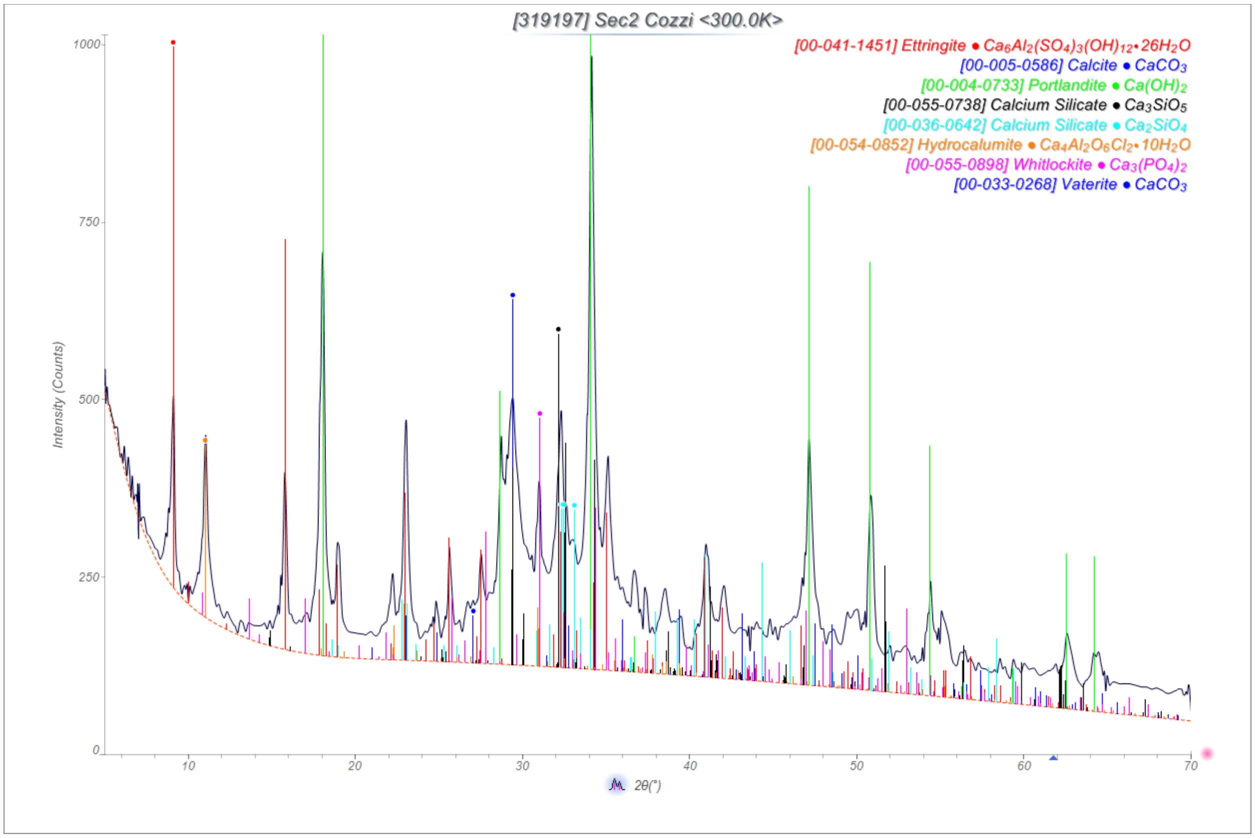
[319197] Sec2 Cozzi <300.0K>
[00-041-1451] Ettringite • $Ca_6Al_2(SO_4)_3(OH)_{12}\cdot 26H_2O$
[00-005-0586] Calcite • $CaCO_3$
[00-004-0733] Portlandite • $Ca(OH)_2$
[00-055-0738] Calcium Silicate • Ca_3SiO_5
[00-036-0642] Calcium Silicate • Ca_2SiO_4
[00-054-0852] Hydrocalumite • $Ca_4Al_2O_6Cl_2\cdot 10H_2O$
[00-055-0898] Whitlockite • $Ca_3(PO_4)_2$
[00-033-0268] Vaterite • $CaCO_3$
Intensity (Counts)
0
250
500
750
1000
10
20
30
40
50
60
70
2θ(°)

Mix 3

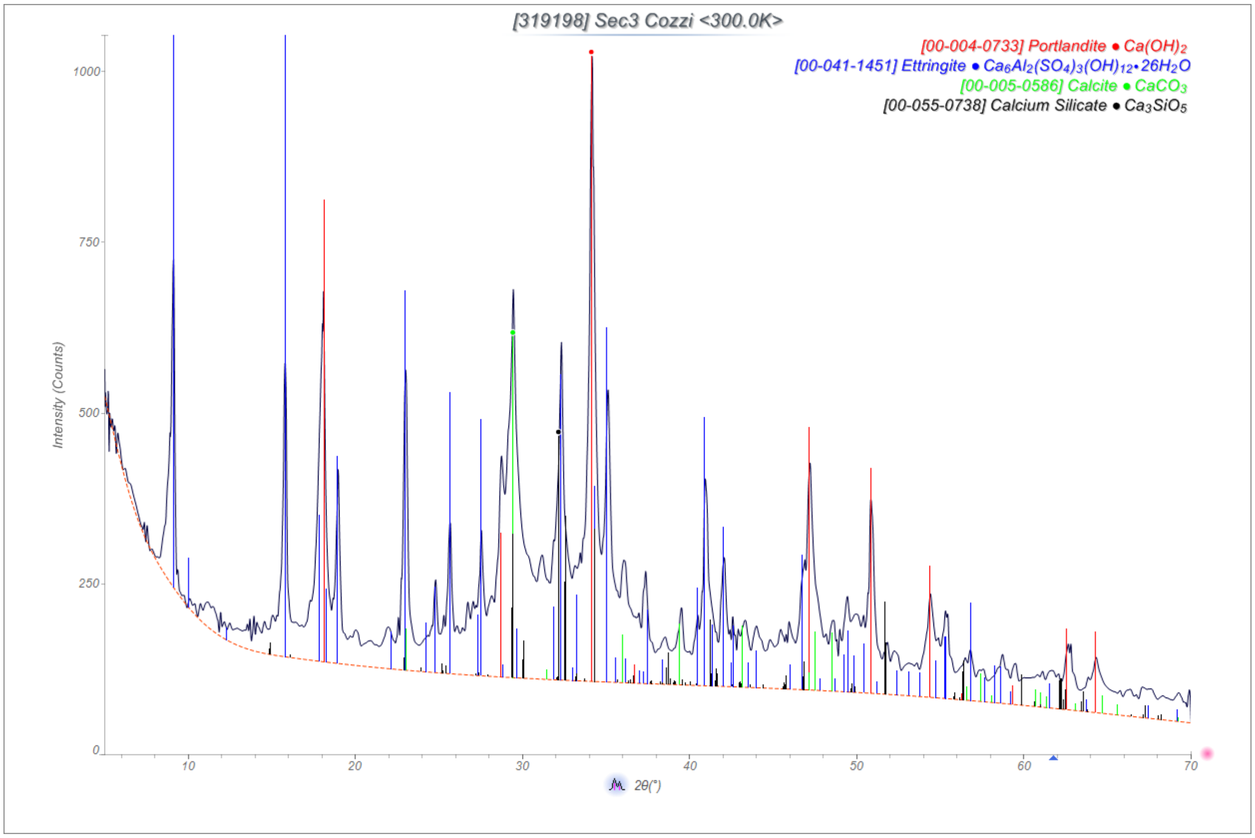
[319198] Sec3 Cozzi <300.0K>
[00-004-0733] Portlandite ● $Ca(OH)_2$
[00-041-1451] Ettringite ● $Ca_6Al_2(SO_4)_3(OH)_{12}•26H_2O$
[00-005-0586] Calcite ● $CaCO_3$
[00-055-0738] Calcium Silicate ● Ca_3SiO_5
Intensity (Counts)
0
250
500
750
1000
10
20
30
40
50
60
70
2θ(°)

Mix 4

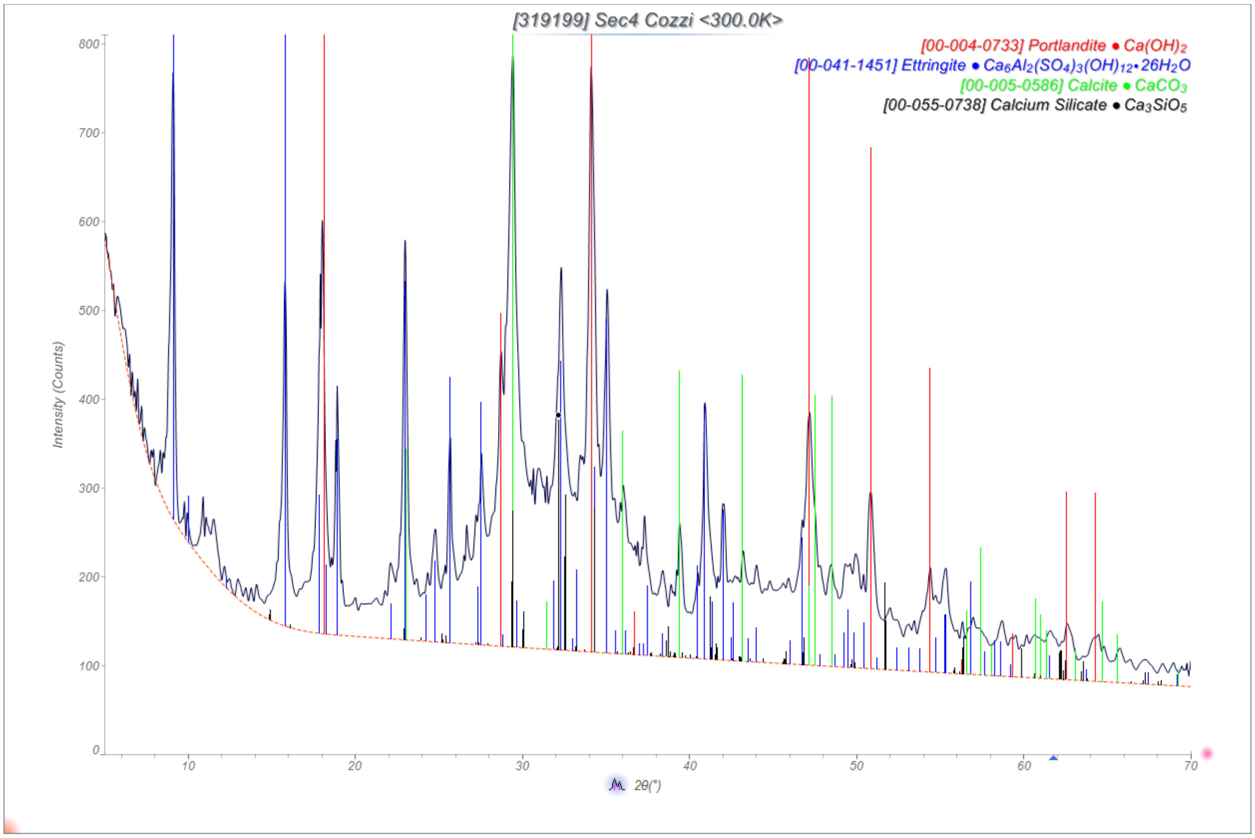
[319199] Sec4 Cozzi <300.0K>
[00-004-0733] Portlandite ● $Ca(OH)_2$
[00-041-1451] Ettringite ● $Ca_6Al_2(SO_4)_3(OH)_{12}•26H_2O$
[00-005-0586] Calcite ● $CaCO_3$
[00-055-0738] Calcium Silicate ● Ca_3SiO_5
Intensity (Counts)
0
100
200
300
400
500
600
700
800
10
20
30
40
50
60
70
2θ(°)

Mix 5

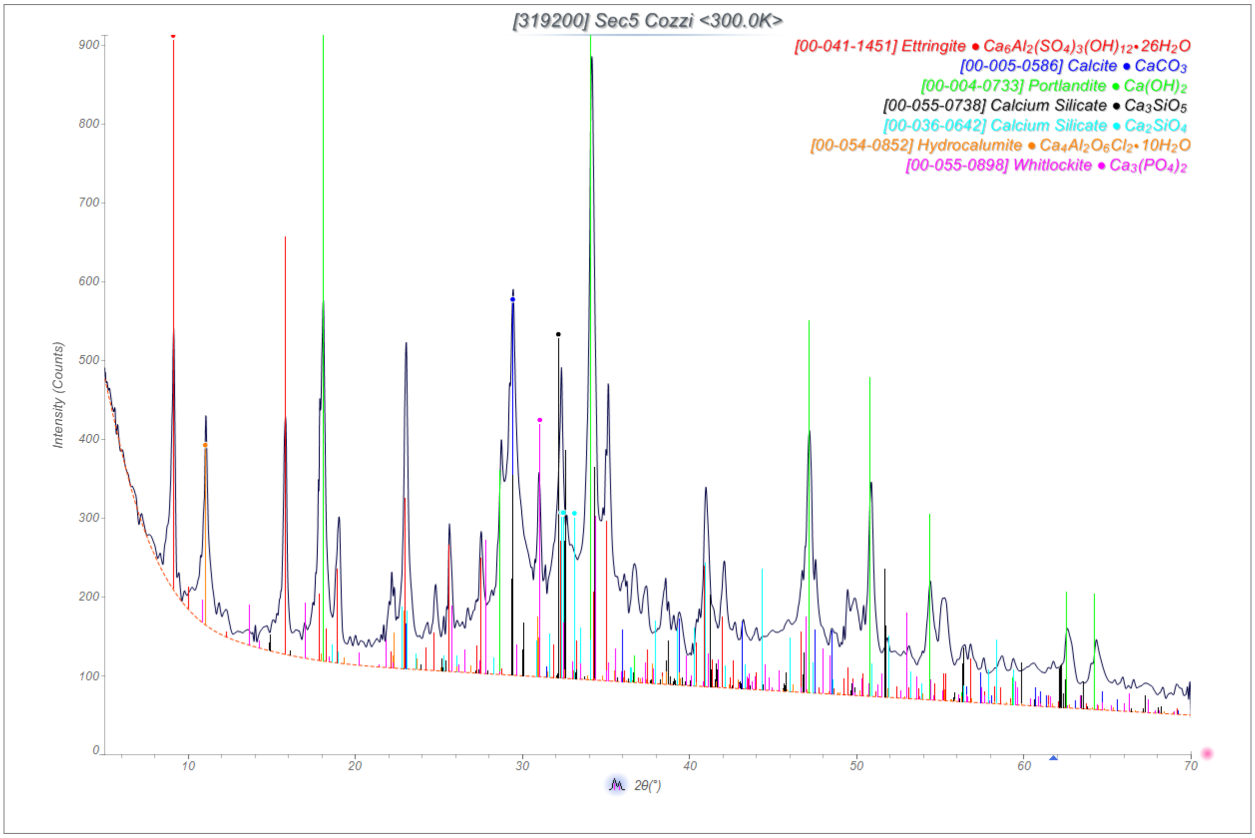
[319200] Sec5 Cozzi <300.0K>
[00-041-1451] Ettringite ● $Ca_6Al_2(SO_4)_3(OH)_{12}•26H_2O$
[00-005-0586] Calcite ● $CaCO_3$
[00-004-0733] Portlandite ● $Ca(OH)_2$
[00-055-0738] Calcium Silicate ● Ca_3SiO_5
[00-036-0642] Calcium Silicate ● Ca_2SiO_4
[00-054-0852] Hydrocalumite ● $Ca_4Al_2O_6Cl_2•10H_2O$
[00-055-0898] Whitlockite ● $Ca_3(PO_4)_2$
Intensity (Counts)
900
800
700
600
500
400
300
200
100
0
10
20
30
40
50
60
70
2θ(°)

Mix 6

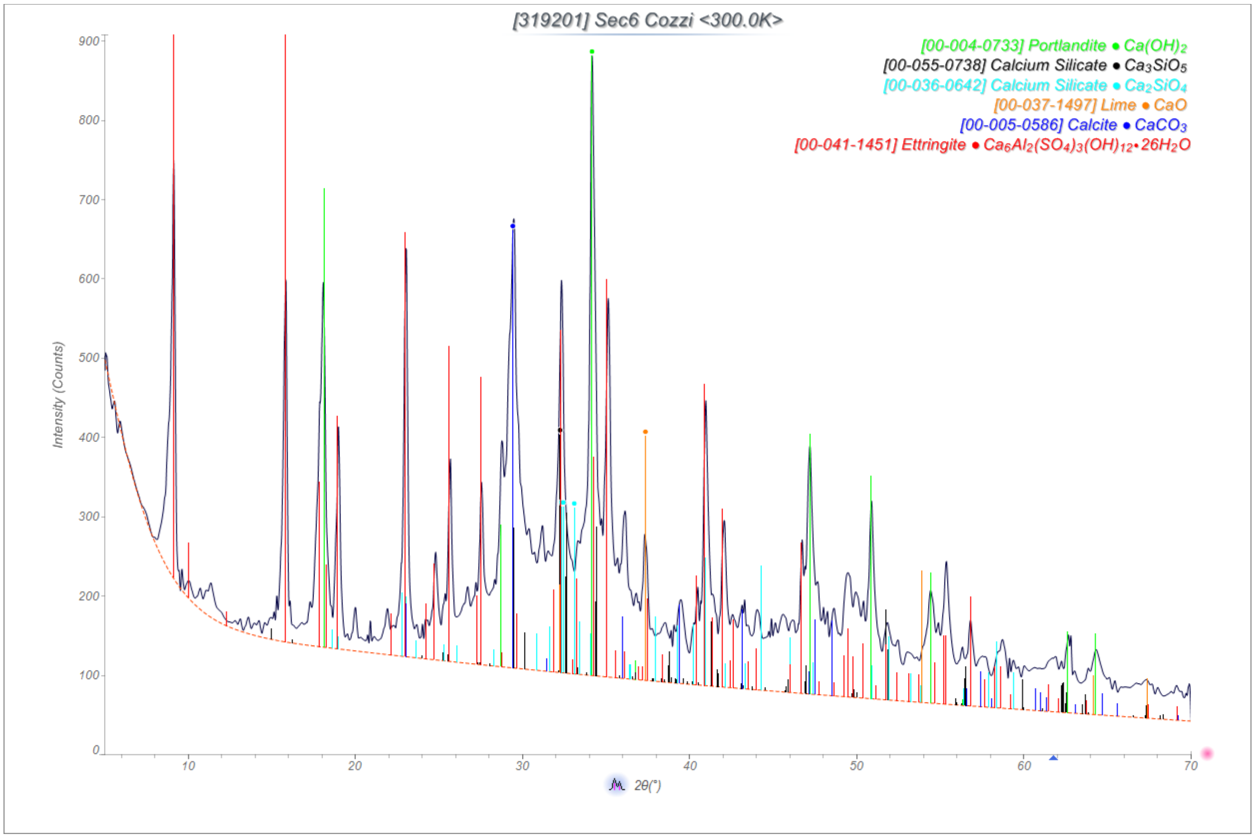
[319201] Sec6 Cozzi <300.0K>
[00-004-0733] Portlandite ● $Ca(OH)_2$
[00-055-0738] Calcium Silicate ● Ca_3SiO_5
[00-036-0642] Calcium Silicate ● Ca_2SiO_4
[00-037-1497] Lime ● CaO
[00-005-0586] Calcite ● $CaCO_3$
[00-041-1451] Ettringite ● $Ca_6Al_2(SO_4)_3(OH)_{12}•26H_2O$
Intensity (Counts)
900
800
700
600
500
400
300
200
100
0
10
20
30
40
50
60
70
2θ(°)

Mix 7

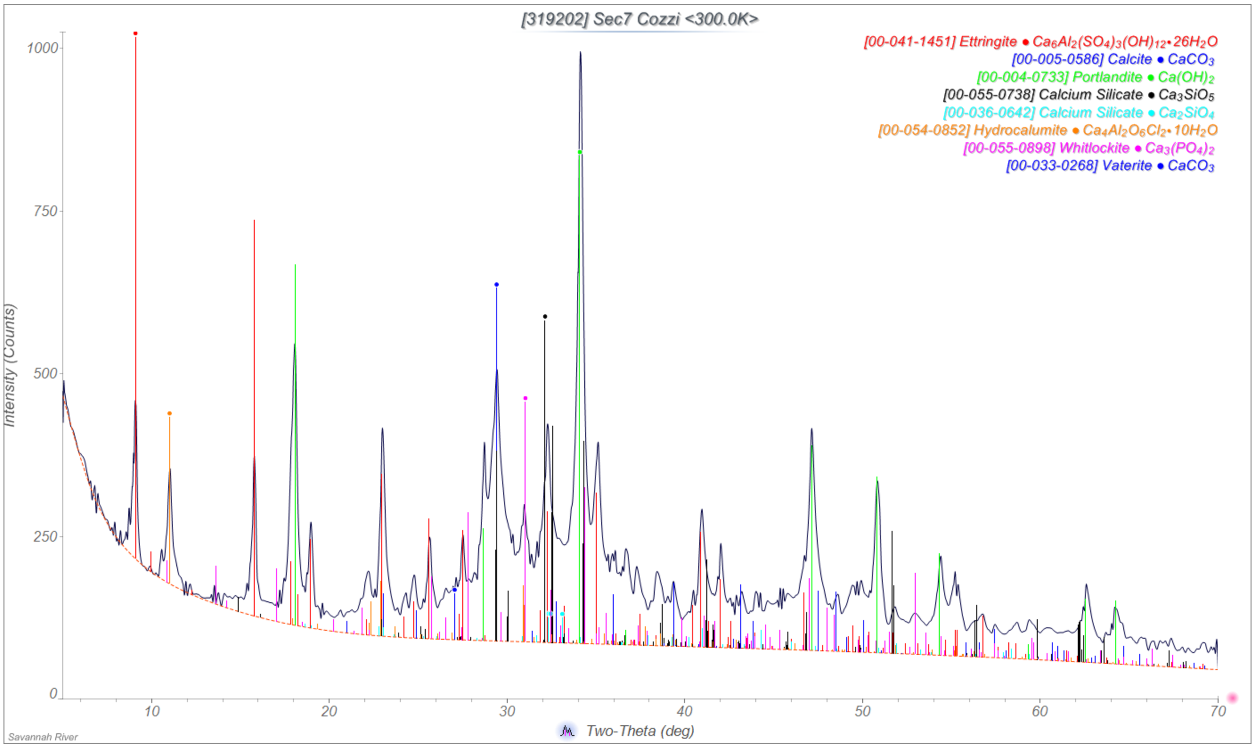
[319202] Sec7 Cozzi <300.0K>
[00-041-1451] Ettringite ● $Ca_6Al_2(SO_4)_3(OH)_{12}\cdot26H_2O$
[00-005-0586] Calcite ● $CaCO_3$
[00-004-0733] Portlandite ● $Ca(OH)_2$
[00-055-0738] Calcium Silicate ● Ca_3SiO_5
[00-036-0642] Calcium Silicate ● Ca_2SiO_4
[00-054-0852] Hydrocalumite ● $Ca_4Al_2O_6Cl_2\cdot10H_2O$
[00-055-0898] Whitlockite ● $Ca_3(PO_4)_2$
[00-033-0268] Vaterite ● $CaCO_3$
Intensity (Counts)
1000
750
500
250
0
10
20
30
40
50
60
70
Two-Theta (deg)
Savannah River

Mix 8

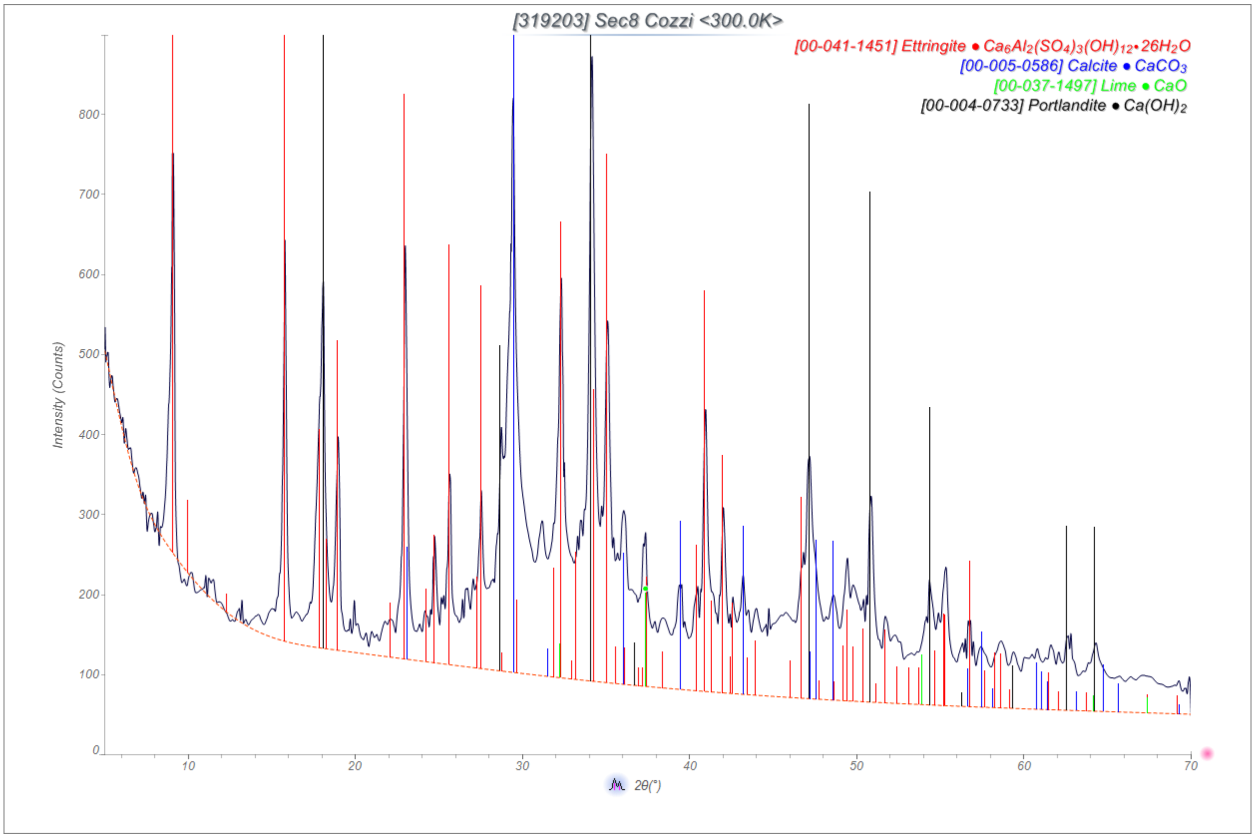
[319203] Sec8 Cozzi <300.0K>
[00-041-1451] Ettringite ● $Ca_6Al_2(SO_4)_3(OH)_{12}\cdot26H_2O$
[00-005-0586] Calcite ● $CaCO_3$
[00-037-1497] Lime ● CaO
[00-004-0733] Portlandite ● $Ca(OH)_2$
Intensity (Counts)
800
700
600
500
400
300
200
100
0
10
20
30
40
50
60
70
2θ(°)

Mix 9

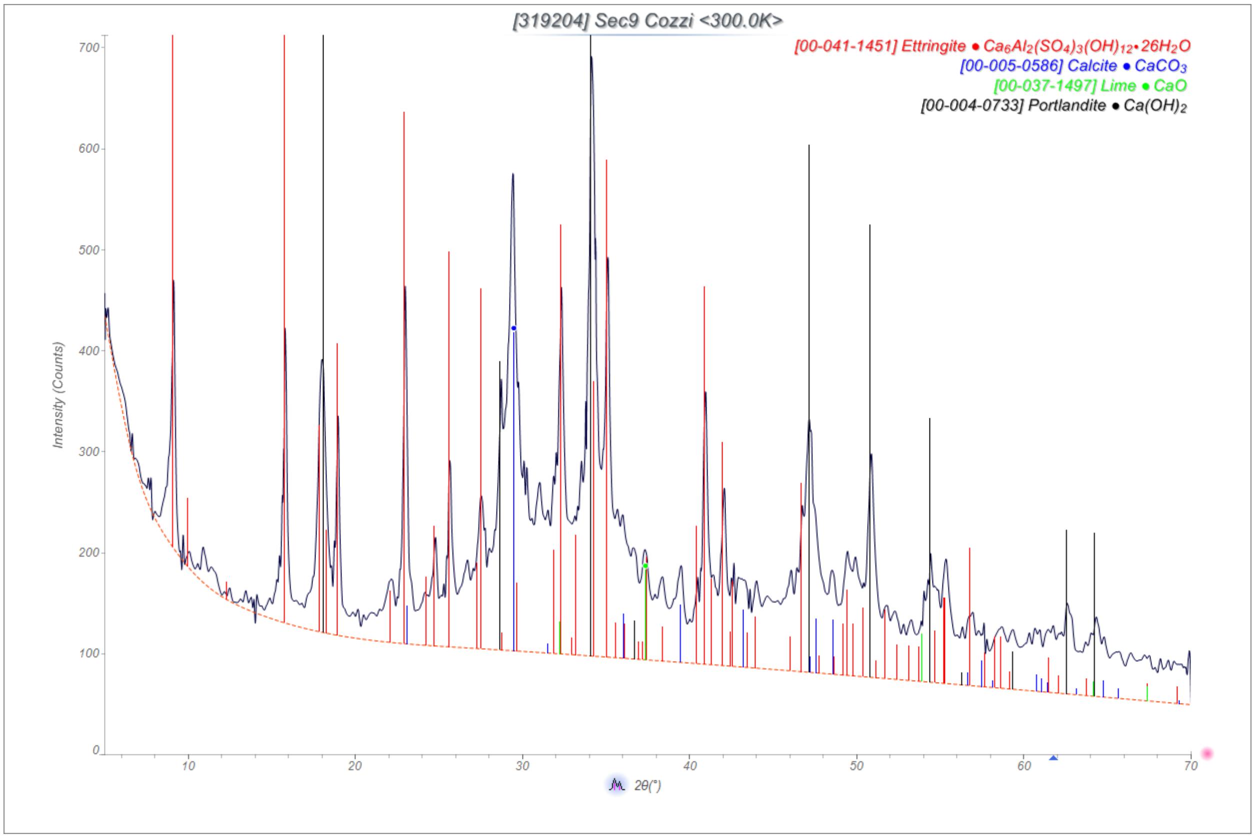
[319204] Sec9 Cozzi <300.0K>
[00-041-1451] Ettringite ● $Ca_6Al_2(SO_4)_3(OH)_{12}•26H_2O$
[00-005-0586] Calcite ● $CaCO_3$
[00-037-1497] Lime ● CaO
[00-004-0733] Portlandite ● $Ca(OH)_2$
Intensity (Counts)
0
100
200
300
400
500
600
700
10
20
30
40
50
60
70
2θ(°)

Mix 10

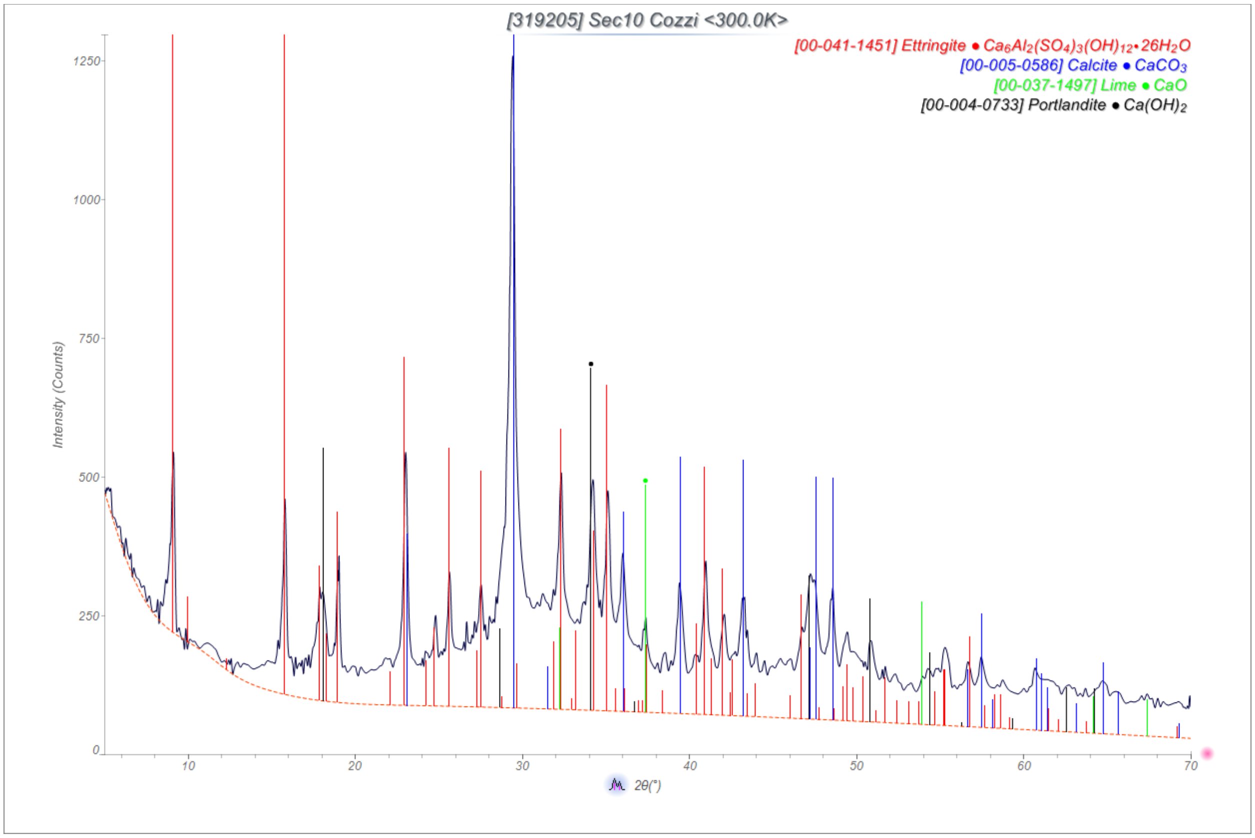
[319205] Sec10 Cozzi <300.0K>
[00-041-1451] Ettringite ● $Ca_6Al_2(SO_4)_3(OH)_{12}•26H_2O$
[00-005-0586] Calcite ● $CaCO_3$
[00-037-1497] Lime ● CaO
[00-004-0733] Portlandite ● $Ca(OH)_2$
Intensity (Counts)
0
250
500
750
1000
1250
10
20
30
40
50
60
70
2θ(°)

Mix 11

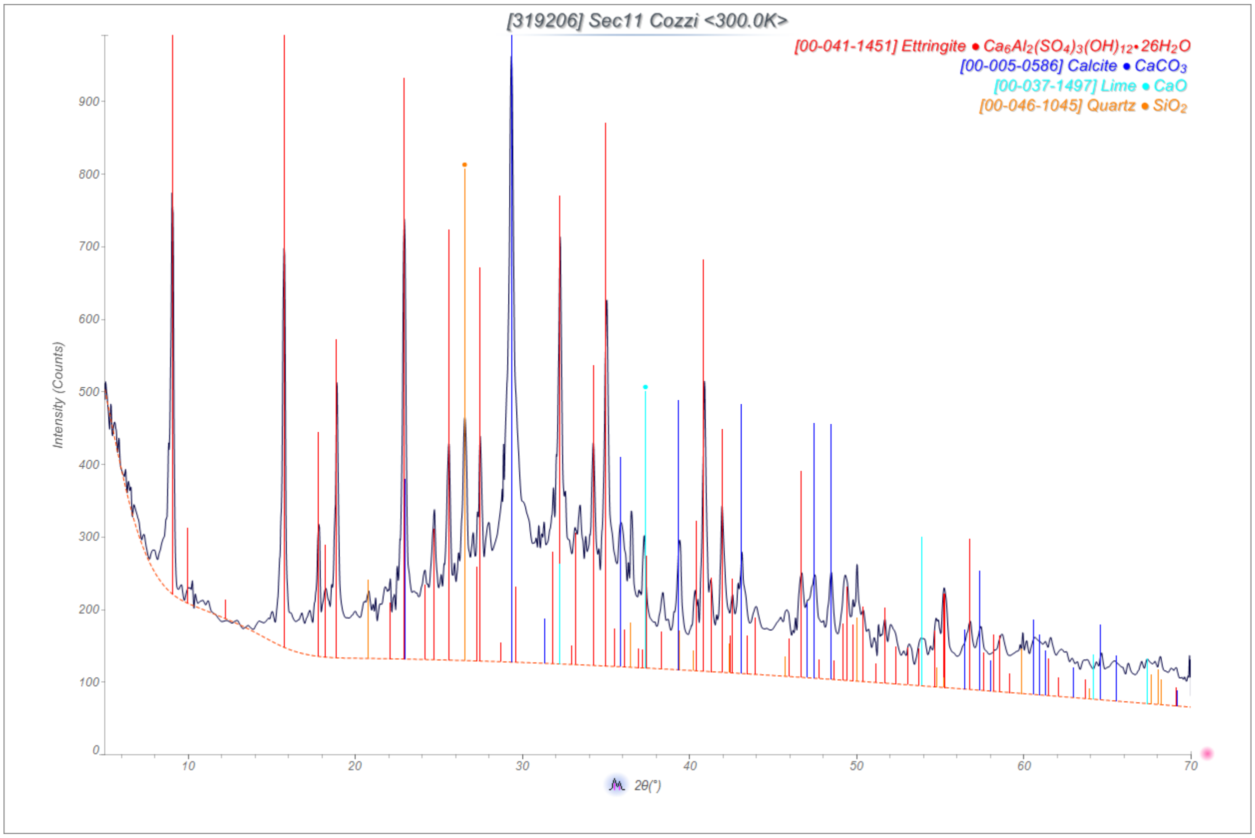
[319206] Sec11 Cozzi <300.0K>
[00-041-1451] Ettringite ● $Ca_6Al_2(SO_4)_3(OH)_{12}\cdot 26H_2O$
[00-005-0586] Calcite ● $CaCO_3$
[00-037-1497] Lime ● CaO
[00-046-1045] Quartz ● SiO_2
Intensity (Counts)
0
100
200
300
400
500
600
700
800
900
10
20
30
40
50
60
70
2θ(°)

Mix 12

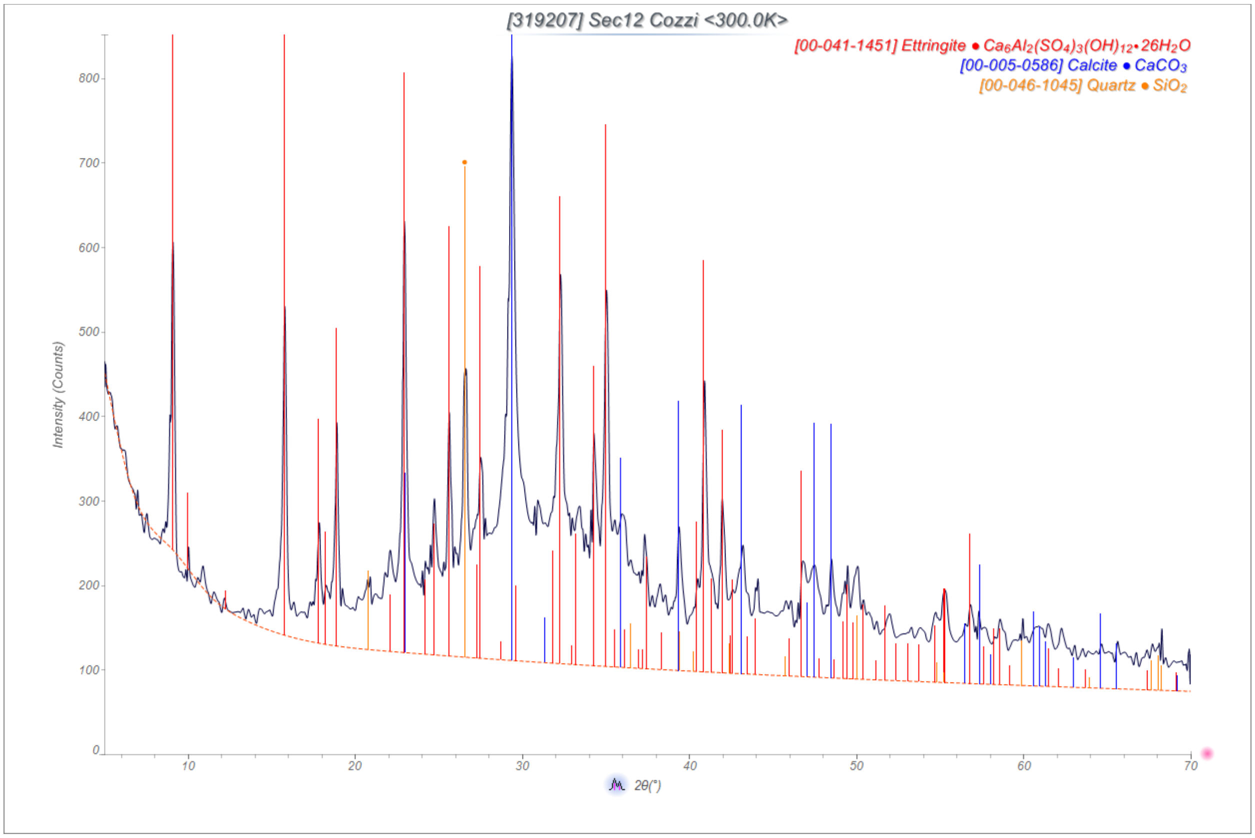
[319207] Sec12 Cozzi <300.0K>
[00-041-1451] Ettringite ● $Ca_6Al_2(SO_4)_3(OH)_{12}\cdot 26H_2O$
[00-005-0586] Calcite ● $CaCO_3$
[00-046-1045] Quartz ● SiO_2
Intensity (Counts)
0
100
200
300
400
500
600
700
800
10
20
30
40
50
60
70
2θ(°)

Mix 13

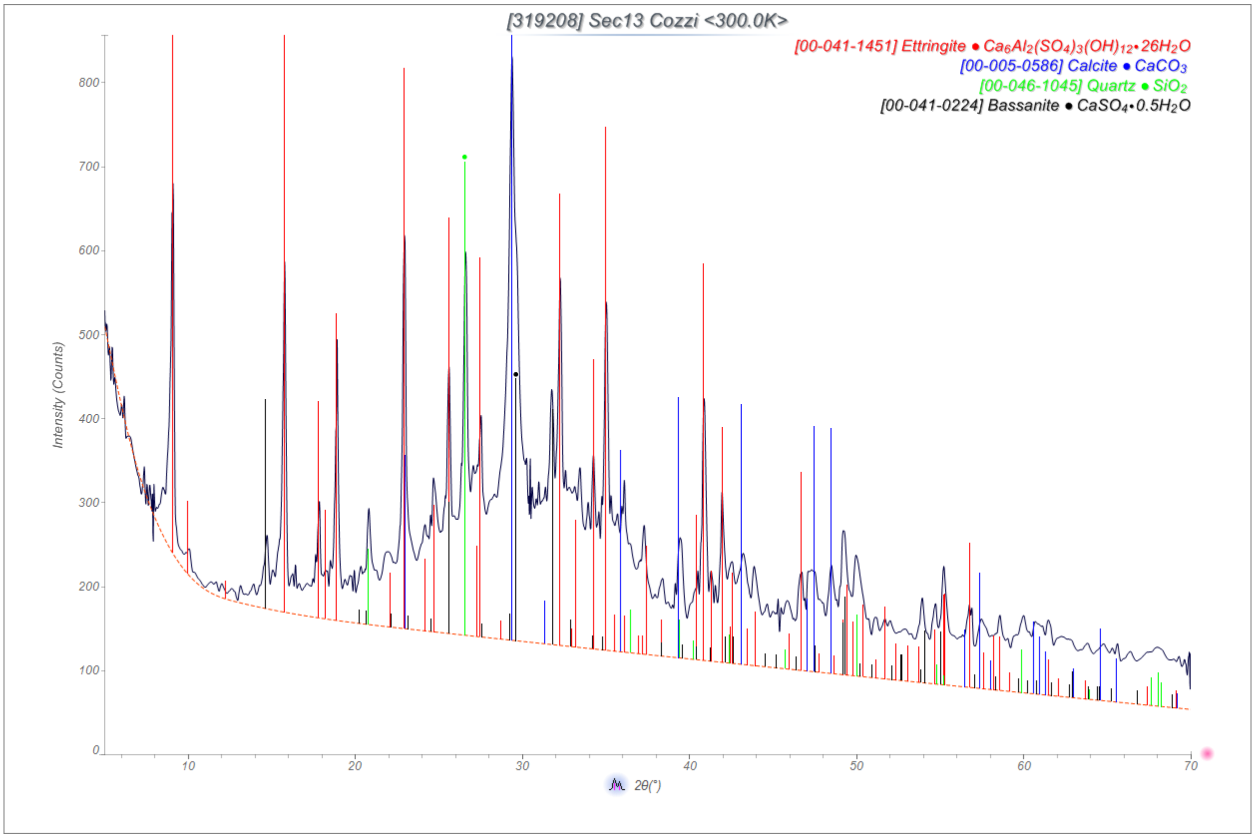
[319208] Sec13 Cozzi <300.0K>
[00-041-1451] Ettringite ● $Ca_6Al_2(SO_4)_3(OH)_{12}\cdot 26H_2O$
[00-005-0586] Calcite ● $CaCO_3$
[00-046-1045] Quartz ● SiO_2
[00-041-0224] Bassanite ● $CaSO_4\cdot 0.5H_2O$
Intensity (Counts)
0
100
200
300
400
500
600
700
800
10
20
30
40
50
60
70
2θ(°)

Mix 14

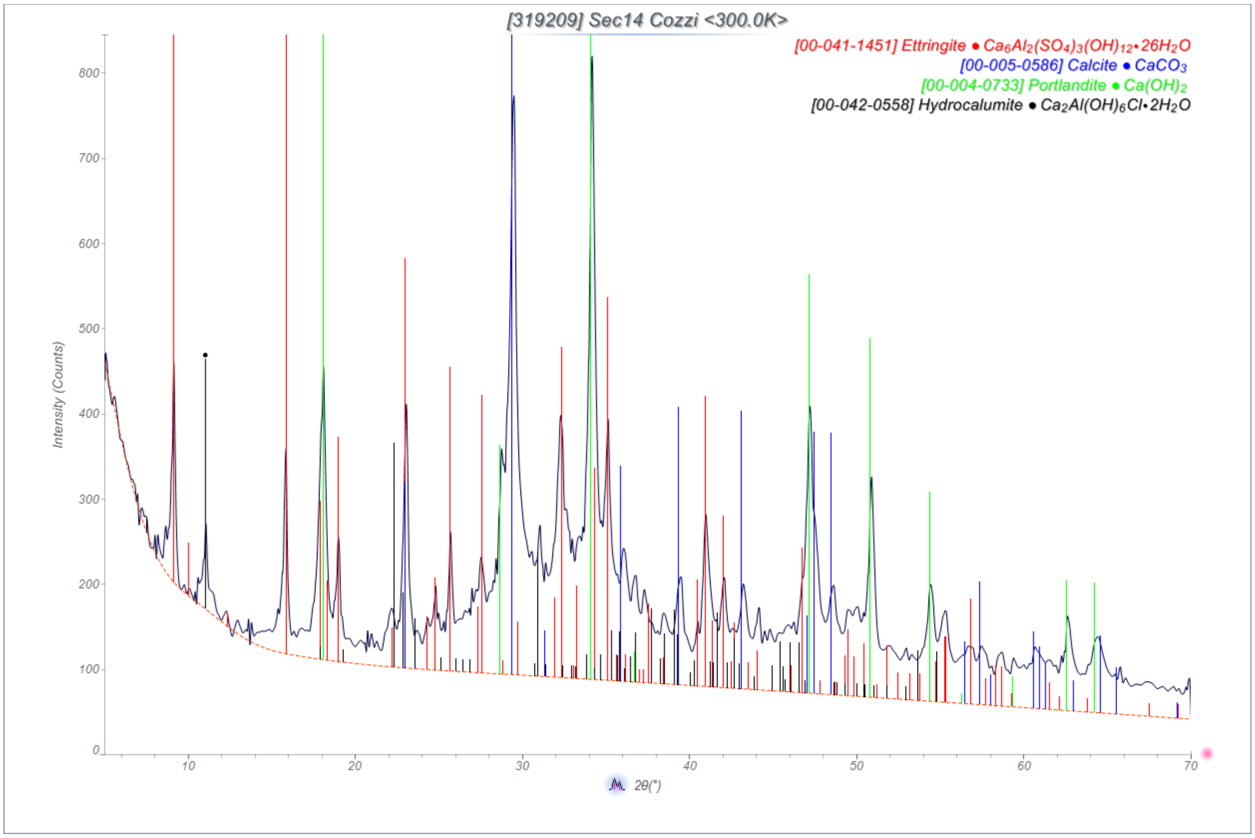
[319209] Sec14 Cozzi <300.0K>
[00-041-1451] Ettringite ● $Ca_6Al_2(SO_4)_3(OH)_{12}\cdot 26H_2O$
[00-005-0586] Calcite ● $CaCO_3$
[00-004-0733] Portlandite ● $Ca(OH)_2$
[00-042-0558] Hydrocalumite ● $Ca_2Al(OH)_6Cl\cdot 2H_2O$
Intensity (Counts)
0
100
200
300
400
500
600
700
800
10
20
30
40
50
60
70
2θ(°)

Distribution:

SRNL
T. B. Brown, 773-A
M. E. Cercy, 773-42A
D. A. Crowley, 773-43A
D. E. Dooley, 999-W
A. P. Fellinger, 773-42A
S. D. Fink, 773-A
C. C. Herman, 773-A
D. T. Hobbs, 773-A
E. N. Hoffman, 999-W
J. E. Hyatt, 773-A
K. M. Kostelnik, 773-42A
B. B. Looney, 773-42A
D. A. McGuire, 773-42A
T. O. Oliver, 773-42A
F. M. Pennebaker, 773-42A
G. N. Smoland, 773-42A
B. J. Wiedenman, 773-42A
W. R. Wilmarth, 773-A
Records Administration (EDWS)

WRPS
K.H. Subramanian, Karthik_Subramanian@rl.govP.A. Cavanah, Paul_A_Cavanah@rl.govM.G. Thien, Michael_G_Thien@rl.govA.A. Ramsey, Amy_A_Ramsey@rl.gov
D.J. Swanberg, David_J_Swanberg@rl.gov
R.B. Mabrouki, Ridha_B_Mabrouki@rl.gov
K.P. Lee, Kearn_P_Lee@rl.gov
N.R. Davis, Neil_R_Davis@rl.gov
E.E. Brown, Elvie_Brown@rl.gov